TOHOKU UNIVERSITY

Graduate School of Information Sciences

# Haptic Modulation of High-frequency Vibration based on Human Perceptual Similarity

（ヒトの高周波振動知覚の類似特性に基づく触覚変調）

A dissertation submitted for the degree of Doctor of Philosophy
(Information Science)

Department of Applied Information Sciences

by

Nan CAO

January 29，2019

# Haptic Modulation of High-frequency Vibration Based on Human Perceptual Similarity

Nan Cao

Abstract

This study aims to investigate the human perception of high-frequency vibrations via the haptic modulation method. Haptic modulation is the modulation of the waveform of high-frequency vibrations while maintaining a similar tactile sensation to preserve the original tactile information. There are several issues caused by high-frequency vibrations. First, the available actuators used for generating the vibrations have a limited range of acceleration along the frequency; this means the available actuators may not be able to generate the necessary range of amplitude.. Second, the sounds of the vibration increases with frequency, and the sounds of high-frequency vibrations are loud. Haptic modulation could be a suitable solution for these issues. The purpose of this type of modulation is to maintain a similar envelope sensation while adjusting the carrier frequency to the appropriate frequency range. Tactile sensation shouldbe retained after the modulation. An example of application of haptic modulation is the teleoperation of construction robots. . However, envelop discrimination ability, envelop detection range, and the perceptual model of envelop sensation are some of the concepts of human perception that scientists do not fully understand.

With respect to continuous high-frequency vibrations, the perceptual characteristics of envelope and amplitude-modulated (AM) vibrations have been investigated by several researchers. The intensity of high-frequency vibrations (i.e., vibrations $>$ 100 Hz), which is defined as the integral of the intensity of stimulus over time or the sum of the spectral power across all frequencies, has been identified as a primary cue with which to convey vibrotactile information as per the Pacinian system. However, the intensity is insufficient when interpreting the perception of an envelope of high-frequency vibration. Together, the intensity and envelope affect the ability of humans to discriminate high-frequency vibrations. In this study, we focus on investigating the perception of high-frequency vibration, especially the effects of envelope, intensity, and other factors on the perceptual similarity of collision vibration and amplitude-modulated vibrations. This study can contribute to the high-frequency perceptual characteristics and act as a guide for high-frequency vibration design in terms of the perceptual similarity.

Firstly, we investigate envelope perception for one impulse vibration such as collision vibration. The experimental results of this investigation suggest that humans can perceive the envelope of vibration for a single pulse vibration such as collision vibration. Our results indicate that the discrimination of the envelope of collision vibration, the upper just-noticeable difference (JND) of time constant, increases marginally with an increase in frequency from 250 Hz to 1,000 Hz, and JND of time constant tends to increase for a smaller time constant. With respect to the discrimination of continuous amplitude-modulated vibration, our results indicated that a higher carrier frequency of periodic AM vibration shows a higher discrimination ability. These results contradict our assumption that a lower carrier frequency, which has a lower threshold, is more sensitive. In general, our investigation results suggested that humans can perceive the envelope for both single-impulse and continuous high-frequency vibrations. The ability of an envelope to discriminate a collision has not been investigated. We believe these results will contribute to the understanding of hardness discrimination by tapping and will help to find a suitable carrier frequency that enhances envelope perception.

Secondly, we introduce a time-domain segment to the intensity-based perception model. In particular, we investigate the discrimination ability of the reproduced, time-segmented waveform, which has the same intensity as that of the original vibration in each segment, to investigate the suitable segment size for the intensity-based modulation. The results suggest that the time-segmented intensity-based model can reproduce perceptually similar vibrations for the AM vibrations, as opposed to the conventional intensity-based model. Furthermore, we found that a small segment number of the envelope period ($r_s = 1/4$) could reproduce similar perception of the AM vibration in the experiment. This will contribute to the

transmission of high-frequency vibrations, especially AM vibrations.

Thirdly, we investigate the perceptual property of an envelope and the intensity that affects a persons ability to discriminate high-frequency vibrations, as well as the effects of carrier frequency on this ability. For the envelope frequency of an AM vibration ranging from 12–50 Hz, a higher degree of discrimination was observed compared to the sinusoidal vibration, while the intensity did not have a significant effect on the discrimination ability in this range. When the envelope frequency of an AM vibration is 125 Hz, a lower degree of discrimination occurred compared to the sinusoidal vibration. The boundary for the perception of an envelope is based on the envelope frequency (80–125 Hz). The intensity model works well in the higher envelope frequency ranging up to 125 Hz. However, when the intensity is the same, it is difficult to discriminate the vibration. We also found that the carrier frequency has little effect on discrimination of a vibration.

Finally, we developed a methodology for modulating noisy, high-frequency vibrotactile signals to noise-free, perceptually similar collision vibrations in the frequency range of 300–1,012 Hz. The results of this investigation suggest that the new modulation method can reduce the decibels of the collision vibration while preserving the perceptual quality. Additionally, the perceptual similarity stimuli occurred over broad ranges of amplitude and frequency.

This dissertation makes four majors contributions to the literature on high-frequency perceptual characteristics. First, our results reveal that humans can perceive both periodic and non-periodic, high-frequency vibration envelopes. Second, it introduces a time-domain segment to the intensity-based perception model and reproduced perceptually similar vibrations for the AM vibrations in contrast to the conventional intensity-based model. Third, it finds that the perceptual discrimination of the vibration has an envelope frequency dependence; the discrimination ability decreases as the envelope frequency increases. Fourth, it develops a methodology for modulating noisy and high-frequency vibrotactile signals to create noise-free, perceptually similar collision.

# Contents

# List of Figures

# List of Tables

# Chapter 1

# Introduction

## 1.1 Background

Haptic technology aims to emulate or enhance the tactile experience of manipulating or perceiving real or virtual contact stimuli through mechatronic devices and computer controls. Conventional human–machine interactions are visual and auditory. Recently, many researchers have noted the importance of haptics in the interaction between humans and robots [7, 8, 9, 10], as well as humans and virtual reality (VR) environments [11, 12, 13, 14, 15]. Haptic technologies combine the sense of touch to help the users to have a more realistic, immersive experience while remotely interacting with machines and virtual environments and help them work more efficiently. Teleoperated robots are beneficial in that they can reach treacherous and/or narrow spaces while being controlled by an operator from a remote location. The use of teleoperation for robots dates back to nuclear research the 1930s and 1950s [16] wherein Goertz et al. created systems with robots that could be operated by human operators to handle radioactive material from behind the shielding walls of a reactor. However, because of the lack of stimuli, these operations took longer and felt inconvenient. Later, Goertz et al. built a master–slave robotic systems to help operators employ more natural hand gestures. The systems transmitted forces and contact vibrations to the operator to reduce the difficulties during teleoperation. The application of haptic technologies for teleoperation to other fields such as space, medicine, and underwater projects began in the 1980s and 1990s. In the early 1990s, a dual-arm, force reflecting, telerobotic system was built by Bejczy et al. [17] at National Aeronautics and Space Administration (NASA)s Jet Propulsion Laboratory (JPL) for space applications. Kuchenbecker et al., [18] measured the tactile vibrations induced by the contact between the tools and objects and found that the haptic devices immediately recreate the vibration on the master handles for the surgeon to perceive. Their augmentation method enables surgeons to perceive the rough texture feelings of the contact surfaces and the start and the end of the contact, as well as other tactile events, when using the system to manipulate objects.

High-frequency vibrations play an essential role in producing tactile sensation. Haptic sensation marks contact activities between the human body and the object, or the tool-mediated activities with the kinesthetic information (e.g., low-frequency forces) and vibrotactile information (e.g., high-frequency vibrations). In [19], Kuchenbecker et al. suggested that high-frequency vibration feedback could improve the realism in touch sensations on haptically rendered surfaces. They demonstrated this by considering the tapping on a wood surface holding a pen-shape tool, each collides during the tapping event creating sudden transient acceleration signal with a frequency of up to several hundreds of Hertz. The sudden high-frequency vibration signal was overlaid with traditional force feedback for its short duration. When compared to the conventional force feedback, the new feedback only needed to be fed with high-frequency vibrations to increase realism in touch response. These high-frequency contact vibrations provide richer information on the material properties of the contact object, such as hardness of the contact surface [20].

This study focuses on the haptic modulation of high-frequency vibrations and considers haptic modulation as the modulation of the waveform of a high-frequency wave while maintaining similar tactile sensation to preserve the original tactile information. There are several issues with modulating high-frequency vibrations using conventional methods. First, the available actuators used for generating the vibrations have a limited range of acceleration along the frequency, i.e., a large amplitude of the high-frequency vibration cannot be generated by using available actuators. Second, sound increases with frequency, and the sound from a high-frequency vibration is loud. Haptic modulation can be a suitable solution for these issues. Modulation of high-frequency vibration is achieved by maintaining the similarity of envelope sensation while adjusting the carrier frequency to the suitable frequency range. The tactile sensation should be maintained after the modulation. An example of the application of haptic modulation methods was the teleoperation of a construction machine [21]. Because a construction machine is accompanied with several haptic interactions, such as digging holes and handling heavy loads, the lack of tactile output is a serious disadvantage for teleoperation. The stiffness of a robots chassis may be high, and the frequencies of the contact vibration are often higher than the perceivable somatosensory range of the human body. If the haptic system transmits the contact vibration directly to the operators, the operators cannot perceive the contact sensation. The purpose of the modulation was to maintain the envelope signal while shifting the imperceptible high-frequency carrier to the human bodys perceivable frequency range. The results demonstrated that the modulated waves perceived upon contacting different materials are distinguishable and suggested that the envelope contains the necessary tactile contact information. However, the understanding of human perception of high-frequency vibrations are still under investigation. The study in this thesis aims to investigate human perception for supporting the rendition of high-frequency vibrations.

## 1.2 Human tactile sensation

### 1.2.1 Human skin and receptors

The skin on different parts of the human body have different sensitivities. Figure 1.1 shows the two-point touch and the point localization thresholds for different parts of the body. The two-point touch threshold representing the smallest spatial separation can be detected between two different stimuli applied on the skin. For example, the threshold of the fingertip is 2–4 mm, while it exceeds 40 mm for the back. When evaluating the point-localization threshold, a stimulus is applied to the skin of humans subjects and a second stimulus may or may not be applied at the same point in succession. The subjects answer whether they feel the two stimuli at the same location. In general, the point-localization thresholds are lower than the two-point touch thresholds (e.g., 1–2 mm on the fingertip).

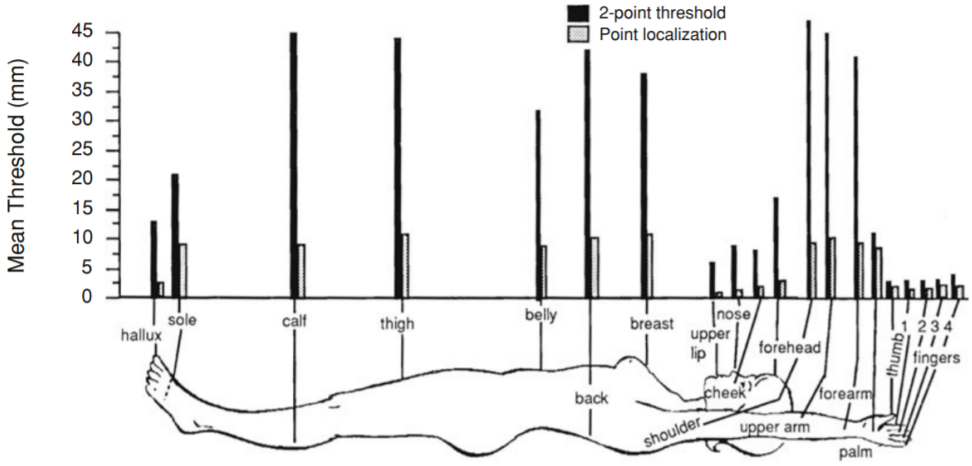


Figure 1.1: Two-point touch and point localization thresholds are shown for various body sites.[1]

Generally, there are two types of human skin: hairy skin and glabrous skin (also called no-hair skin). Glabrous skin is found on the palm of the hand, as well as the fingertips and foot soles. Both types of surfaces have a layered structure. Figure 1.2 (a) shows the cross-section view of the smooth, glabrous skin of the fingertip of humans. Tactile receptors are located from the border of the epidermis and the dermis to the subcutaneous tissue. There are four types of mechanoreceptors: slowly adapting type 1 (SA1), or Merkel's disks; slowly adapting type 2 (SA2), or Ruffini corpuscles; rapidly adapting type 1 (RA1), or Meissner corpuscles; and rapidly adapting type 2 (RA2), or Pacinian corpuscles. Their classifications (types, adaption rate, spatial acuity, threshold, frequency range, conduction velocity, effective stimuli, and sensory function) are described in Figure 1.2(a).

When the skin is stimulated, a series of complex mechanical, perceptual, and cognitive phenomena will occur. As shown in Figure 1.2(b), the related information is transmitted to the central nervous system (CNS) for higher-level processing and interpretation, majorly via two pathways: spinothalamic and dorsal-column-medial lemniscus (DCML).

The spinothalamic pathway carries temperature and pain-related information. DCML, on the other hand, conveys pressure/vibration-related information to the brain and helps to compare the spatial and temporal information on stimuli. Figure 1.2(c) showed a sequence of events during tactile transmission.

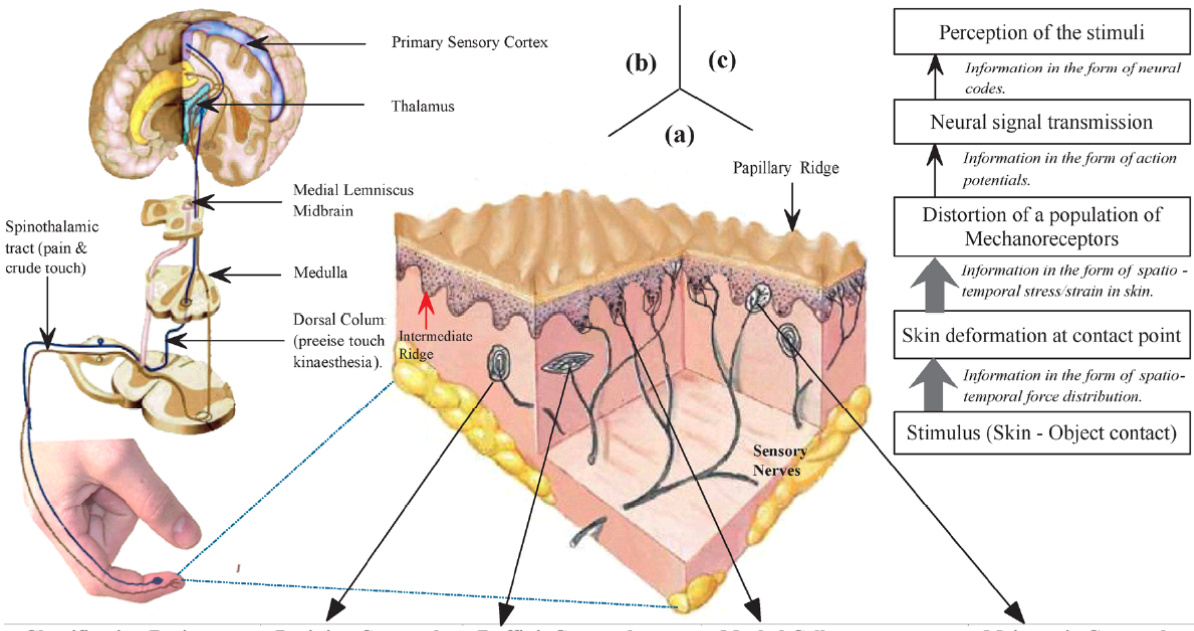


| Classification Basis | | Pacinian Corpuscle | Ruffini Corpuscle | Merkel Cells | Meissner's Corpuscle |
|---|---|---|---|---|---|
| Type | | FA II | SA II | SA I | FA I |
| Adaptation Rate | | Fast | Slow | Slow | Fast |
| Spatial Acuity (mm) | | 10+ | 7+ | 0.5 | 3-4 |
| Vibration/rapid indent. threshold | Best(μm) | 0.01 | 40 | 8 | 2 |
| | Mean(μm) | 0.08 | 300 | 30 | 6 |
| Stimuli Frequency (Hz) | | 40-500+ | 100-500+ | 0.4-3 | 3-40 |
| Conduction Velocity (m/s) | | 35-70 | 35-70 | 40-65 | 35-70 |
| Effective Stimuli | | Temporal changes in the skin deformation | Sustained downward Pressure; Lateral skin stretch; Skin slip. | Spatial deformation; Sustained pressure; Curvature, edge, corners. | Temporal changes in skin deformation |
| Sensory Function | | High frequency vibration detection; Tool use. | Finger position; Stable grasp; Tangential Force; Motion direction | Pattern/form detection; texture perception; Tactile flow perception. | Low frequency vibration & motion detection; Grip control; Tactile flow perception. |

Figure 1.2: (a) Section of glabrous skin showing the physical location and classification of various mechanoreceptors. (b) Tactile signal transmission from fingertips to somatosensory area of brain. (c) Functional events during tactile signal transmission from contact point to brain. Image is adopted from [2].

### 1.2.2 Exploration procedure

Human tactile sensory information is derived from the mechanoreceptors and thermoreceptors across the surface of the body. Lederman and Klatzky classified six EPs as lateral motion EP, pressure EP, static contact EP, unsupported holding EP, enclosure EP (global shape), and contour EP (exact shape), while some other researchers also mentioned tapping or collide EP in [22, 23, 20]. In these seven basic EPs, lateral motion EP and tapping or collide EP induce high-frequency vibrations on the contact areas of a human body or a robot. These EPs are as follows:

1. The lateral motion EP is the lateral movement between the skin and an objects surface, i.e., rubbing or scratching. Typically, the fingers rub back and forth across an area

on the surface. During the stick-slip transition [24], continuous high-frequency vibrations with the envelope are generated.

2. The tapping or collide EP is that a finger or the hand moves up and down contacting a surface of the object. Typically, tapping occurs when the finger or the hand contacts the surface of the object. Tapping can sense the hardness of the contacted surface. During the tapping motion, single-impulse collision vibrations with a damping envelope are generated.

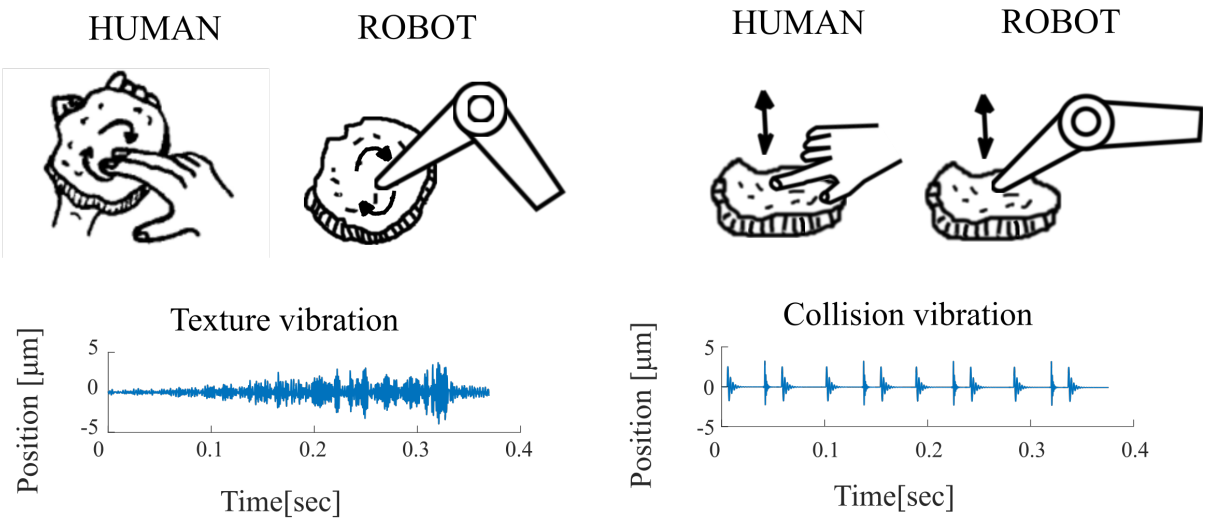


(a) Lateral motion EP with texture vibrations (b) Tapping or collide EP with collision vibrations

Figure 1.3: Lateral motion EP and tapping or collide EP with their corresponding high-frequency vibrations on the contact areas of human body or robot

## 1.3 Psychophysics of high-frequency vibration

In this study, we aim to understand the perceptual characteristics of high-frequency vibration in the haptic modulation method. Psychophysical investigations are connecting human sensation to the physical parameters of the stimuli. It mainly focuses on the detection and discrimination of the vibration and contributes to its modeling. These investigations help determine the parameters suitable for generating the vibration.

### 1.3.1 Basic psychophysical measurements of high-frequency vibration

Psychophysical measurements are an essential source for defining the requirements of sensors and actuators. A considerable number of stimuli for the sense of vibration are still under investigation. For high-frequency vibration, parameters such as amplitude, frequency, and duration of stimuli play a significant role in creating the sensation. There are two essential parameters of the necessary psychophysical measurements: threshold, which decides whether a stimulus can be perceived, and just-noticeable difference (JND),

which measures whether the differences between stimuli can be perceived.

One of the basic measurements of human perception, the amplitude threshold (AT), is defined as the minimum amplitude of the stimulus barely perceivable to a human being. Previous studies have shown that the human detection threshold curve for sinusoidal vibrations and the thresholds depend on the frequency related to the activities of the receptors. The measurements of ATs are shown in Figure 1.4.

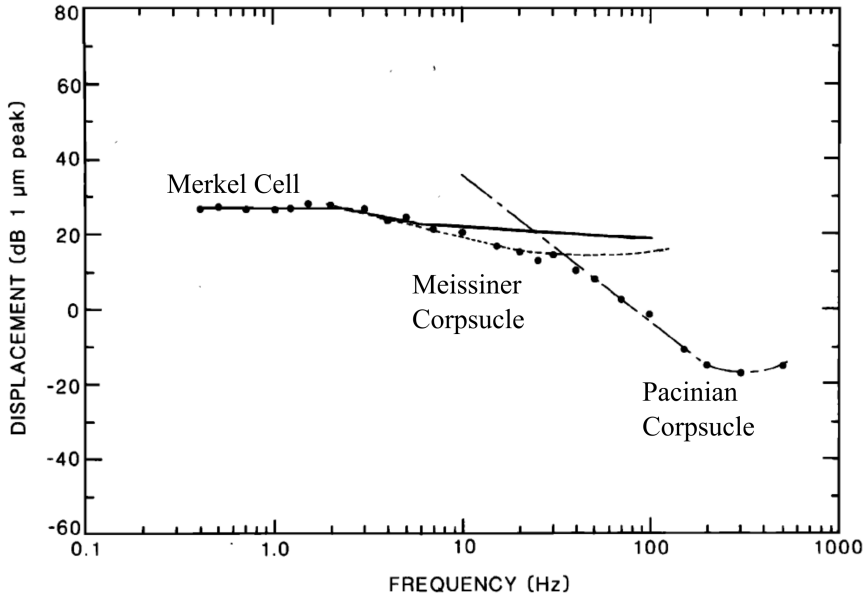


Figure 1.4: Threshold frequency characteristics of vibration showing the directed measured threshold: • • • and of the various channels: — Merkel Cells; - - - Meissner Corpuscle; – - – Pacinian Corpuscle [3].

The JND is a measuring of the minimum difference between two stimuli, which could be necessary for a human being to reliably perceive. JND is conventionally measured for the force feedback. In the early 19th century, Weber et al. measured JNDs of roughly 10 % in experiments involving the active lifting of 2-oz weights by the hand and arm [25]. Hatzfeld et al., measured the JNDs of vibrotactile force amplitudes in a bandwidth of 5-1,000 Hz. The measuring of the AT and JNDs can contribute to the designing of haptic vibrations, such as data reduction through signal sampling [26, 27].

### 1.3.2 Psychophysical modeling

Many researchers are working on modeling the intensity of high-frequency vibrations($> 100$ Hz), which is generally regarded as the integral of stimulus intensity over time or the spectral power summed across all frequencies. This intensity has been considered to be a primary cue in conveying vibrotactile information perceived by the Pacinian system [28, 29, 30, 4]. Makous et al. [28] modeled the intensity as a function of spectral power divided by the corresponding threshold power related to the frequency of the wave. Bensmaia et al. enhanced the ability of the intensity model as a spectral model to in-

terpret the perceptual similarity of stimuli with spectral characteristics based on the psychophysical and neurophysiological findings [30]. Bensmaia et al. also improved the intensity model based on the spectral model to infer the perceptual dissimilarity of the finely textured stimuli [4], as shown in Figure 1.5.

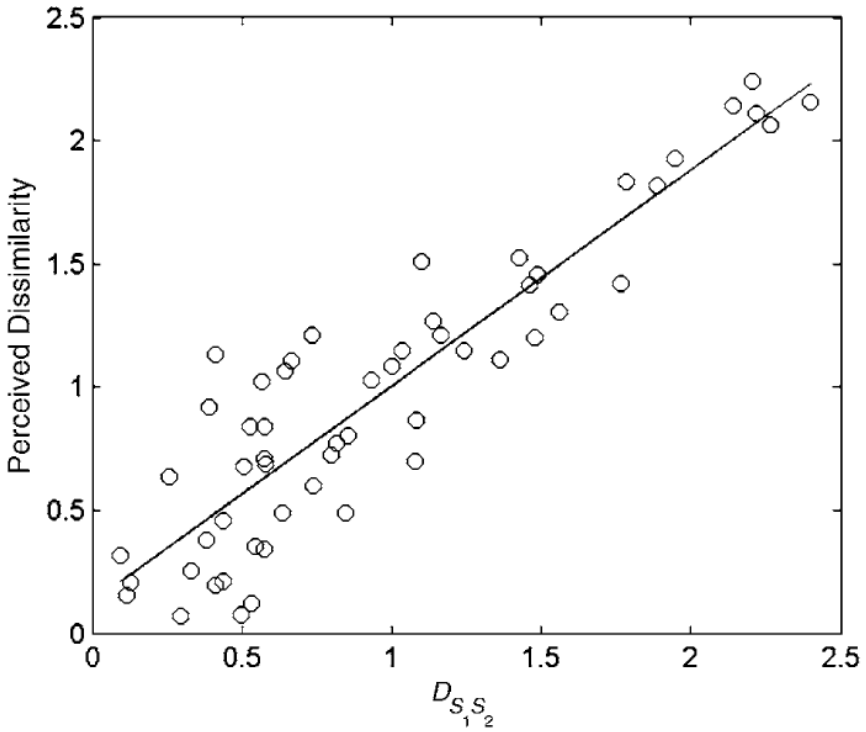


Figure 1.5: Relationship between perceived dissimilarity of fine texture-induced vibrations and intensity dissimilarity $D_{S_1S_2}$ by spectral intensity model is approximately linear. $D_{S_1S_2}$ accounts for 81.6 % of the variance in perceived dissimilarity [4].

### 1.3.3 Envelope perception in previous studies

In [31, 32], researchers found that a human being can perceive the low-frequency envelope of an amplitude-modulated (AM) vibration even when the carrier frequency is above the perceivable frequency range. In addition, Lim et al. [5] found that humans can perceive beats for the envelope frequencies from 2.5–10 Hz, and the ratio of beats detection threshold $AT_B(f)$ to amplitude thresholds $AT(f)$ decreases from 20 to 1.25 as carrier frequency increases from 63.1 Hz to 398 Hz. Figure 1.6 shows the beats detection threshold was measured on the finger pad. They also found that when $f_c$ is increased, the beats can be perceived for very low envelope frequencies and closer to the $AT$ of sinusoidal vibration. These results suggest that humans can perceive the envelope of high-frequency vibrations.

There are many applications that the envelope plays an important role in that require the forming of sensation of modulated vibrations and vibration patterns, which are used to generate the textures of message or tactile messages. Decaying sinusoidal waves applied

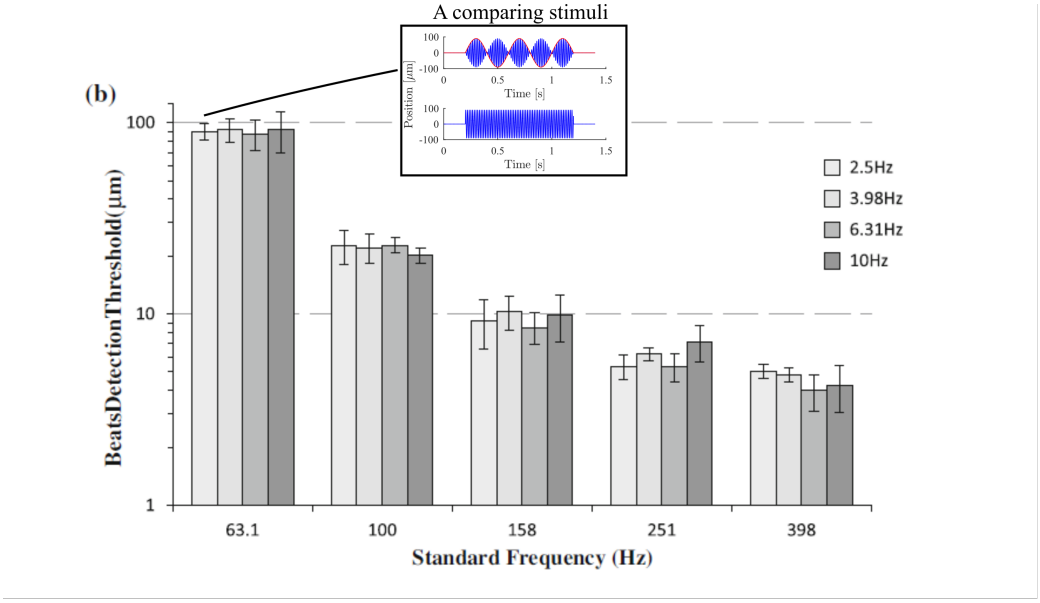


Figure 1.6: Detection threshold of 75 % correct performance was measured on the finger pad [5].

to the skin have been used to indict the roughness or collisions in a virtual environment [24, 33]. In [34], Ahmaniemi et al. applied modulated vibrations to render the texture of a contact surface. Image-based tactile vibration are used modulated vibrations to render different contact surfaces in a flat tablet [35]. Vibration patterns are widely used for tactile generation in VR environments [34] for supporting the teleoperation of robots [36, 37]. Takenouchi et al., [21] extracted the envelope of a high-frequency vibration for which the carrier frequency was above the range of human perception.

Currently, psychophysical measurements are primarily on the threshold and JND of amplitude or frequency of a sinusoidal wave. Detection and discrimination for envelope perception have not been fully investigated yet. The current psychophysical intensity models focusing on the intensity or spectral intensity information have not been successful in interpreting the perception of the envelope of high-frequency vibrations either. The range of intensity models that can predict the perceptual discrimination may be affected by the envelope. Therefore, The understanding of the effect of an envelope on human perception is needed for further investigation of the intensity models.

## 1.4 Current issues concerning haptic modulation

This study aims is to investigate the human perception of high-frequency vibration through the haptic modulation method for the high-frequency vibrations. Humans can perceive the vibration envelope, which contains information on contact characteristics such as material properties. The proposed method modulates the envelope of an original vibrotactile signal to enhance the perceptual feeling of the transmitted vibration applied in [21]. The original wave is shown in Figure 1.7 and the envelope extraction is shown in

Figure 1.8. However, the previous studies could gather little knowledge of the perceptual characteristics of the envelope of high-frequency vibrations. Therefore, this study is to bridge this knowledge gap and focus on investigating the perceptual characteristics of the envelope. To the best of our knowledge, these investigations can improve our modulation method for the design of teleoperation of a construction machine and devices in other applications that use the high-frequency vibration feedback.

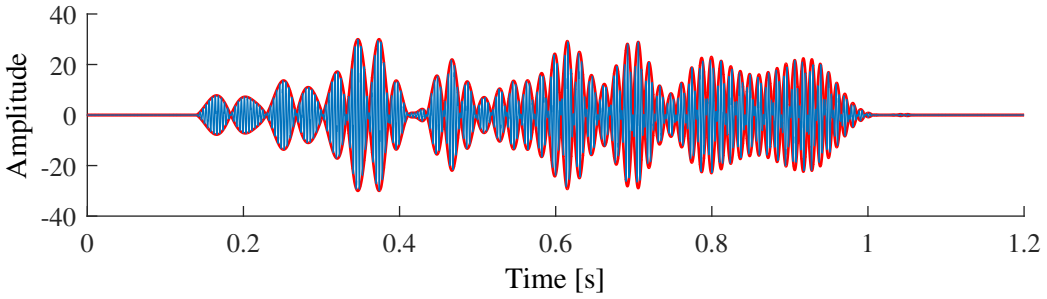


Figure 1.7: Original wave of high-frequency vibration. The red curve showed the envelope signal detected by the peaks the wave.

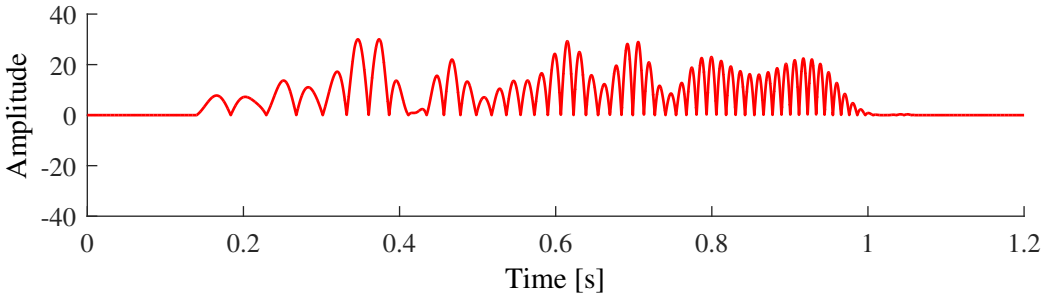


Figure 1.8: Envelope signal extracted by all the peaks of the original wave.

### 1.4.1 Envelope discrimination of high-frequency vibrations

Several researchers have found that humans can perceive the envelope of high-frequency vibration. This thesis examines the perceptual discrimination ability of high-frequency vibrations and the effect of carrier frequency on a humans ability to discriminate a vibration envelope. One of the high-frequency vibrations with an envelope is the single-impulse collision vibration. In [38], Okamura found that amplitude, frequency, and time constant $\tau$ work together to emulate the hardness of tapping. The time constant $\tau$ is a parameter that decides the envelope shape of collision vibration, as shown in Figure 1.9. The discrimination ability of the envelope of collision has not been examined yet. By knowing the discrimination ability and carrier frequency effect of the collision vibration, collision vibration can be modulated for various applications, e.g., sound reduction.

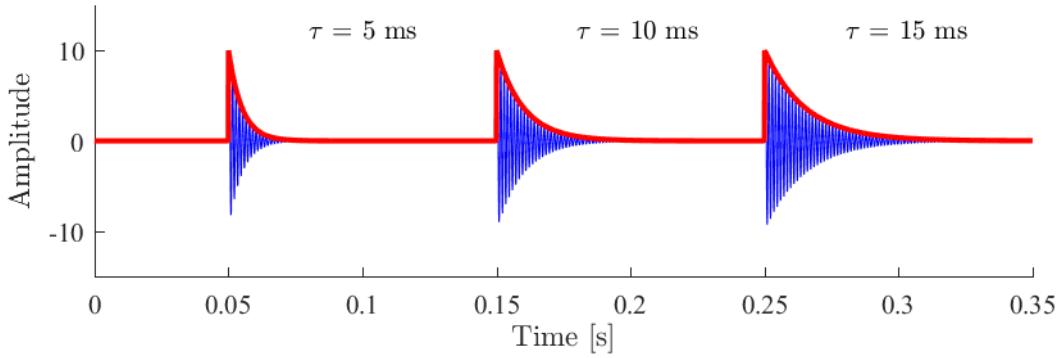


Figure 1.9: Changes in the envelope of the collision vibration by the time constant $\tau$.

### 1.4.2 Sensitivity of periodical high-frequency vibrations

For the transmission of high-frequency vibrations, the proposed method preserves the envelope of the original vibrotactile signal to enhance the perceptual feeling of the transmitted vibration. The carrier frequency is modulated for enhancing the perception and the carrier frequency range that is sensitive enough for human perception is estimated. This will contribute to finding the carrier frequency suitable for envelope perception enhancement.

### 1.4.3 Envelope perceptual boundary of the high-frequency vibrations

The intensity of high-frequency vibrations (i.e., vibrations $>$ 100 Hz) has been identified as a primary cue with which to convey the vibrotactile information as per the Pacinian system. However, the intensity itself is insufficient when interpreting the perception of a high-frequency vibration envelope. The intensity and envelope together affect the ability of humans to discriminate high-frequency vibrations. Park et al.[39] found that AM vibrations at a very high frequency envelope are similar to sinusoidal vibrations ($f_e = 0$), which suggests that when the envelope frequency is high, the beats cannot be perceived and the waveform is therefore perceptually similar to vibrations without an envelope frequency. For the teleoperation of a construction machine, one of the modulation procedures is to extract the envelope. However, it is not known which envelope frequency range is suitable for maintaining. By investigating the boundary where the envelope has a strong impact on vibration discrimination, the extraction of envelope signal of modulation in the teleoperation system can be guided. By knowing the perceivable envelope frequency range, the envelope of frequency lower than the boundary can be preserved and a relatively lower carrier could be used for the modulation. We can improve the envelope extraction as executed in the example shown in Figure 1.10, which compares the extraction of all the envelope signals shown in Figure 1.8. After improving the envelope extraction, a lower frequency carrier can be used to preserve the envelope sensation, as shown in Figure

1.11. It may contribute toward reducing the difficulties in generating the high-frequency vibration and the sound of the vibration.

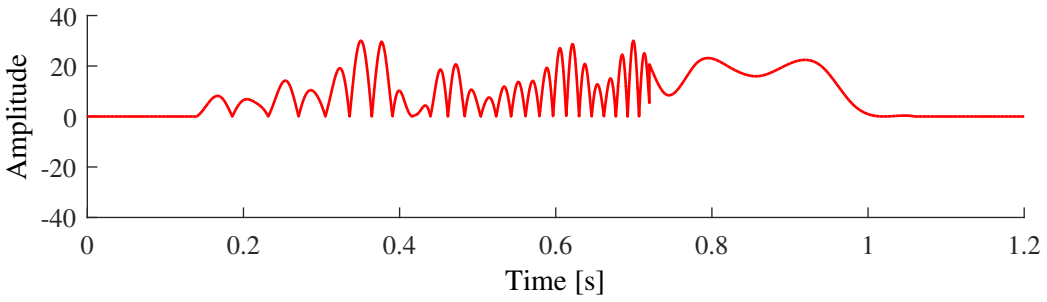


Figure 1.10: Imperceptible high-frequency envelope components could not be maintained. The red curve represents the envelope signal.

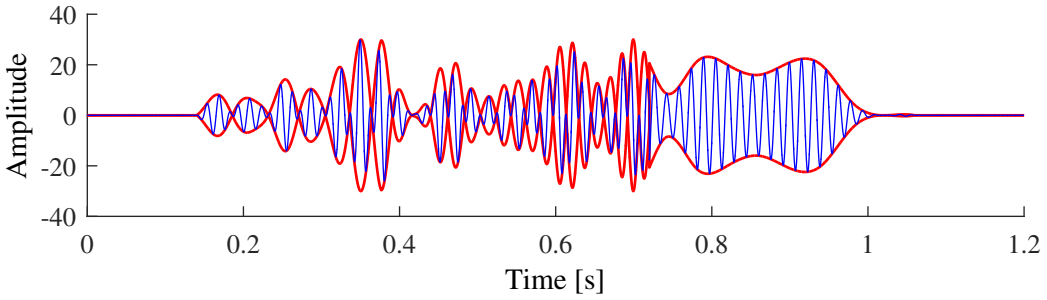


Figure 1.11: Improving the envelope extraction, a lower frequency carrier can be used to preserve the envelope sensation. The red curve represents the envelope signal.

### 1.4.4 Transmission of the high-frequency vibrations

The intensity of high-frequency vibration can help predict the perceptual differences of fine texture vibrations. However, if the vibration has a low-frequency envelope, the intensity itself cannot interpret the perceptual similarity. The intensity change (caused by the envelope modulation) in the time domain may also affect the human perception. The high-frequency vibration is transmitted in packets. We want to investigate how the perceptual characteristic of a vibration can be affected by these packets. We introduce the segment in the time domain to analyze the psychophysical characterization of AM vibration using its intensity and frequency information. As shown in Figure 1.12, the wave is modulated from the wave of Figure 1.11 in the segments of the time domain. It will contribute to the transmission of high frequencies, especially the AM vibrations with the envelope sensation.

### 1.4.5 Sound of the high-frequency vibrations

The high-frequency vibrations introduce noise in the audible range. For example, a loud sound generated by the haptic feedback system will occur in the teleoperation of a construction machine, when a high-frequency vibration is generated[21]. The sound

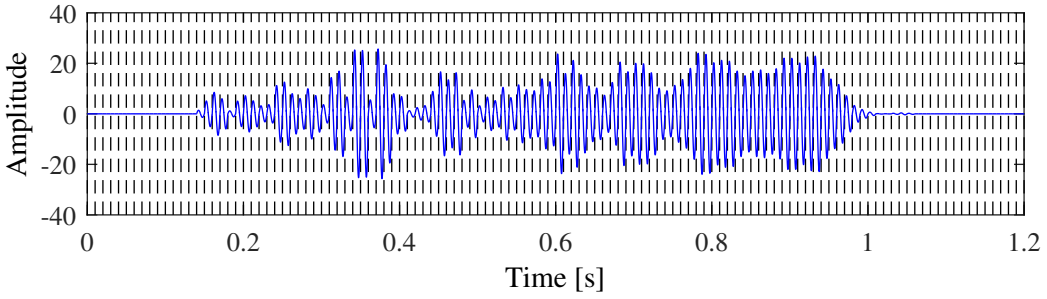


Figure 1.12: Time segments used to modulate the wave. The dashed lines are the boundaries of the segments.

level of the vibrations increases with frequency when the amplitude is constant [40]. It is necessary to establish a modulation method that can reduce the sound while preserving perception.

## 1.5 Research objectives and approaches

### 1.5.1 Objectives

The broader objectives of this thesis are to investigate the human perceptual characteristics of the high-frequency vibration concerning the haptic modulation method And the relationships between the intensity, the envelope, and the perceptual discrimination of high-frequency vibrations.

To achieve these objectives, we set the following specific objectives:

- We investigate the human envelope detection ability of the impulse envelope of a high-frequency collision vibration and periodic high-frequency AM vibration.
- We introduce the time segment to the intensity model for reproducing the perceptually similar vibration from the original high-frequency AM vibration, which has a low-frequency envelope.
- Measuring the boundary where the envelope has a strong impact on vibration discrimination. In addition, the effects of the carrier frequency and intensity on the discrimination was also investigated.
- Investigating the envelope modulation of high-frequency vibrations to the perceptually sound reduction of high-frequency collision vibrations for the users in the teleoperating system and VR environment.

### 1.5.2 Approaches to fulfill objectives

The general research methodology of the thesis is divided into four parts. Specific techniques employed in each section are detailed as follows.

**1) Investigating the envelope discrimination ability of the high-frequency vibration**

In this study, we investigated the discrimination ability of the envelope perception of single-impulse, high-frequency collision vibrations by measuring the JNDs of time constant. Here, JNDs are frequently measured to evaluate the discrimination ability of the differences of the target parameters. Several studies have measured the JNDs of the amplitude (e.g. [41, 42] ) and frequency (e.g. [43, 44]) of sinusoidal vibrations. The relationships between hardness perception and mechanical parameters, including the time constant, have been investigated; however, perceptual resolutions for the time constant are yet to be investigated. We investigated the JND of time constant at several different frequencies. Generally, the most sensitive frequencies for human beings are in the range 200–300 Hz; hence, for the time constant, the highest perceptual resolution (lowest JND) range may also be in the range of 200–300 Hz. High frequencies like 1,000 Hz are not perceived by humans, and the JNDs of time constants in high-frequency waves are expected to be high. By investigating JND of time constants, we can find how it will change with frequency, for example, in which frequency range the JND of time constant will be the lowest or highest, whether the JND of time constant was linearly changed by frequency and if not in which frequency range the JND of time constant changed most rapidly.

**2) Investigating the time unit of integrating the intensity for the high-frequency vibration of a time-variant envelope.**

We introduce a time-domain segment to the intensity-based perception model and investigate the discrimination ability of the reproduced, time-segmented waveform that has the same intensity as the original vibration on each segment, as a pilot study to determine the suitable segment size for the intensity-based modulation. This study targets the AM high-frequency vibrations (carrier frequency $f_c = 300$ or 600 Hz) that have relatively low envelope frequencies ($f_e$ =15, 30, or 45 Hz). To simplify the experimental conditions, we incorporated several assumptions:

1. The original and reproduced vibrations have identical carrier frequency.

2. The stimulus energy is the general integral power of vibration displacement in the time domain.

We aim to verify whether the segmented intensity model can reproduce similar perceptual vibrations and what could be the proper segment size for the model.

**3) Measuring the boundary where the envelope has a strong effect on discriminating vibrations and the effects of carrier frequency and intensity**

The intensity of high-frequency vibrations (i.e., vibrations > 100 Hz), which is generally defined as the integral of the intensity of stimulus over time or the spectral power summed across all frequencies, has been identified as a primary cue that helps convey

vibrotactile information as per the Pacinian system. However, the intensity model is insufficient when interpreting the perception of a high-frequency vibration envelope. The intensity and envelope together affect the ability of humans to discriminate high-frequency vibrations.

We ran an experiment to assess the discrimination ability of subjects exposed to sinusoidal and AM vibrations of different envelope frequencies, carrier frequencies, and intensity levels using the intensity model developed in previous studies. This allowed us to investigate the effect of intensity and envelope on a human beings ability to discriminate high-frequency vibrations. Our results revealed the envelope frequency dependence of perceptual discrimination of the tested stimuli, where the ability to discriminate increased with the envelope frequency.

**4) Apply the modulation of high-frequency vibration to realize the perceptual sound reduction**

For perceptually reducing the sound, we focus on modulating the high-frequency collision vibration that occurs when we tap on the surface of the object by hands or tools. In [33], Okamura et al. found that the perception of collision vibration can be modeled by using three parameters (amplitude A, frequency f, and time constant t) of their decaying sinusoidal model. It can generate the perception of tapping different materials such as wood, metal, and rubber. Our modulation method aims to use perceptually similar low-frequency collision vibrations to represent high-frequency collision vibrations, which is assumed to reduce the sound. We conducted a psychophysical experiment to adjust the amplitude of low-frequency test collision vibrations to produce a sensation as close to that provided by the reference high-frequency collision vibrations as possible.

## 1.6 Structure of the thesis

The thesis is composed of six chapters. To the best of the authors knowledge, these are original contributions in envelope sensation of the high-frequency vibrations.

In Chapter 1, the background and the objective of this study are presented. The needs of haptic feedback and an introduction to haptics was described at Section 1.1. The exploration procedure that induces tactile vibration, the function of mechanoreceptors in human skin, and the sensation of high-frequency vibrations were described in Section 1.2. Basic psychophysics measurements and modeling for high-frequency vibrations were described in Section 1.3. The research objectives and approach are described in Section 1.4.

In Chapter 2, by investigating the JND of time constant, we could find the degree of sensitivity of the envelope for human beings and whether this degree would be changed by frequency. In addition, we also conduct the preliminary experiment to investigate the envelope and carrier discrimination of the AM vibration. The AM vibrations have different carrier frequencies with frequency less than 1 kHz, which is supposed to be in

the somatosensory range of frequency for human beings and frequencies higher than 1 kHz, which are beyond this range.

In Chapter 3, we find the boundary for the perception of the envelope and investigate the intensity and carrier effect on human beings ability to discriminate high-frequency vibrations. We conduct a psychophysical experiment using the amplitude-modulated vibration of different envelope frequency and intensity. By comparing the AM vibration with the sinusoidal vibration at different intensity conditions, we intend to find how the similarity between the two vibrations varies. By comparing the vibrations of different envelopes and vibrations of the same envelope, we aim to examine the effect of envelope on perception. By comparing the stimuli at different intensities, we aim to investigate the effect of intensity on perception. In addition, we also verify the effect of carrier frequency on discrimination.

In Chapter 4, we introduce a time-domain segment to the intensity-based perception model. In particular, we explore the discrimination ability of a reproduced time-segmented waveform that has the same intensity as that of the original vibration on each segment, as a pilot study to determine the suitable segment size for the intensity-based modulation. This study targets the AM high-frequency vibrations (carrier frequency $f_c = 300$ or 600 Hz) that have relatively low envelope frequencies ($f_e = 15$, 30, or 45 Hz). We found that a small segment number of the envelope period ($r_s = 1/4$) could emulate the perception of the AM vibration in the experiment.

In Chapter 5, we develop a methodology for modulating noisy and high-frequency vibrotactile signals to noise-free, perceptually similar collision vibrations in the frequency range of 300 Hz–1,012 Hz. Firstly, we conduct a psychophysical experiment to adjust the amplitude of low-frequency test collision vibrations to produce a sensation as close to that provided by the reference high-frequency collision vibrations as possible. Secondly, we verify whether a human could perceive the difference between the perceptually similar collision vibrations obtained. Thirdly, we measure the sound pressure level of the experimental collision vibrations at different frequencies. besides reducing the sound level, we can also reduce the frequency of collision vibrations to maintain a similar sensation.

Finally, Chapter 6 concludes this thesis.

# Chapter 2

# Investigating the envelope discrimination ability of a high-frequency vibration

## 2.1 Introduction

Humans can perceive the frequency of AM) vibrations even when the carrier frequency is higher than their perceivable somatosensory frequency range [31, 32]. These findings reveal that humans can perceive the envelope of continuous AM sinusoidal vibrations. Regarding the continuous high-frequency vibrations, the perceptual characteristics of an envelope and a carrier of vibrations have been investigated in earlier studies [31, 32]; however, those characteristics for one-impulse high-frequency vibrations such as a collision vibration have not yet been investigated.

The high-frequency collision vibrations occur when we tap a surface and its waveform helps us to perceive the different characteristics of the contact materials. The perceptual characteristics of collision vibrations, which contribute to the discrimination of tapped surfaces, have been investigated [38] to virtually represent collision sensation by simulating transient collision vibrations. Okamura et. al [38] parametrically modeled collision vibrations in which the amplitude, the frequency, and the time constant (which present the shape of the envelope) partially reflect the materials. Okamura et al. used the model to present the collision vibrations by the frequencies that differ from the measured frequencies of vibrations. These frequencies enabled people to distinguish materials [33]. This collision vibration model, which is combined with kinesthetic force displays, has been used to represent hardness sensations that are stronger than the limited levels of hardness in the force devices [19]. In the transient collision vibration, the role of frequency has been investigated. These studies found that higher frequencies in the model led to the perception of a greater level of hardness.

However, the effects of the envelope, which is presented as the time constant in the

model, have not yet been thoroughly investigated.

Our study in this chapter is to investigate the degree of sensitivity of the human beings discrimination ability, and the effect of varying carrier frequencies on this ability. The investigation is conducted by measuring the JND of time constant. Here, JND is frequently used to evaluate the perceptual resolutions for target parameters, as several studies found for the amplitude (e.g. [45]) and frequency (e.g. [44]) of periodic vibrations. The relationships between hardness perception, and mechanical parameters including time constant have been investigated [46, 22]; however, the perceptual resolutions for the time constant have been investigated.

To efficiently generate the collision vibrations induced by tapping, we need to investigate the perceptual resolutions for the parameters of the models. For example, we can produce the perceptually different collision vibrations by using two perceptually different time constants from the generated model based on its perceptual resolutions.

We investigated the JND of time constant at several different frequencies. Generally, the most perceived frequencies for humans lie in the 200–300 Hz range; hence, for the time constant, the highest perceptual resolution (lowest JND) range may also be in the 200–300 Hz range. High frequencies like 1,000 Hz are not perceivable to humans and the JNDs of time constant are expected to be high. By investigating the JND of time constant, we can find how it will be affected by frequency; for example, in which frequency range the JND of time constant will be the lowest or highest, whether the JND of time constant was linearly changed by frequency, and if not, in which frequency range the JND changes most rapidly.

In addition, a human being can perceive the frequency of AM sinusoidal vibration even when the carrier frequency is higher than the perceivable frequency range [31, 32]. It suggests that humans can perceive the envelope of high-frequency vibration. In this chapter, we also conduct the preliminary experiment to investigate the envelope and carrier discrimination of the AM) vibration. The AM vibration has a different carrier frequency less than 1 kHz, which is in the perceivable frequency range, and a frequency higher than 1 kHz, which is beyond the range. We aim to know whether there is a possibility that these two types of carrier frequencies will induce a different discrimination ability of human. The work in this chapter was published in [47, 48].

## 2.2 Objectives of the chapter

As mentioned earlier, several studies have found that humans can perceive the envelope of high-frequency vibration. However, this perceptual ability to discriminate high-frequency vibration envelope are not quantified. This ability plays an important role in generating tactile vibrations especially for virtual texture or collision vibration rendering. We investigated the ability to detect an envelope of the one-pulse high-frequency collision vibration and continuous high-frequency AM vibration.

The objectives of this chapter are:

- To investigate how much is the discrimination ability of the envelope of the vibration especially for the one pulse vibration such as collision vibration.

- To find whether the carrier frequency range will affect the ability to discriminate the envelope difference.

## 2.3 Significance of the Study

By understanding the ability of a human being to discriminate an envelope, we can find whether the envelope can be considered for designing the artificial tactile vibration or understanding the perception of tactile vibration. Primarily, we aim to know whether the envelope of the tactile vibration could help humans to discriminate a short, one-impulse vibration such as collision vibration. This can help us to design a short-duration collision on a human–tactile interface that supports VR experience or teleoperation. The high-frequency vibration can be regarded as both carrier signal and envelope signal. If the carrier can affect envelope discrimination, we can find the suitable carrier frequency that helps accurately discriminate the envelope difference by the modulation. If the carrier does not affect the envelope discrimination, we can shift the carrier frequency but still preserve the envelope sensation by modulation. A lower carrier frequency could reduce the difficulties of generating high-frequency vibration and reduce its sound.

## 2.4 Study of envelope effect on collision vibration perception through investigating just noticeable difference of time constant

### 2.4.1 Specific objective

By measuring the JNDs of time constant, we can find whether collision vibration will be affected by the carrier frequency. For example, in which frequency range the JND of time constant will be the lowest or highest, whether the JND of time constant was linearly altered by frequency, and if not, in which frequency range the JND of time constant changed most rapidly.

### 2.4.2 Methods

#### 2.4.2.1 Materials

- Decaying sinusoidal vibration

  The collision vibration feedback model developed from the measured data is a decaying sinusoidal waveform[38], where $Q(t)$ is the vibration produced by contact, $A$ is the attack amplitude, $\tau$ is the time constant, and $f$ is the frequency.

$$Q(t) = Ae^{-\frac{t}{\tau}}\sin(2\pi ft) \tag{1}$$

Assuming the observed amplitude changes with a change in time constant, a dynamic amplitude was applied to keep the maximum value of the waveform a constant. This process eliminated the possible perception difference caused by the amplitude.

When $Q'(t_0) = 0$ and $t_0 = \tan^{-1}(2\pi f\tau)/2\pi f$, $Q(t_0) = Q_0$ is the maximum value of the waveform. The maximum value $Q_0$ is set to a constant value. Finally, the collision vibration model after amplitude is

$$P(t) = \frac{Q_0}{e^{-\frac{t_0}{\tau}}\sin(2\pi ft_0)}e^{-\frac{t}{\tau}}\sin(2\pi ft) \tag{2}$$

In addition, the generated vibrations cannot reflect the vibratory input profiles of signals because of the frequency characteristics of a voice coil actuator apparatus. Therefore, we preliminarily analyzed the frequency characteristics of the actuator and then modified the input signals using the frequency characteristics to generate the desired output. The frequency characteristics of the actuator was measured and its result are shown in Figure 2.1.

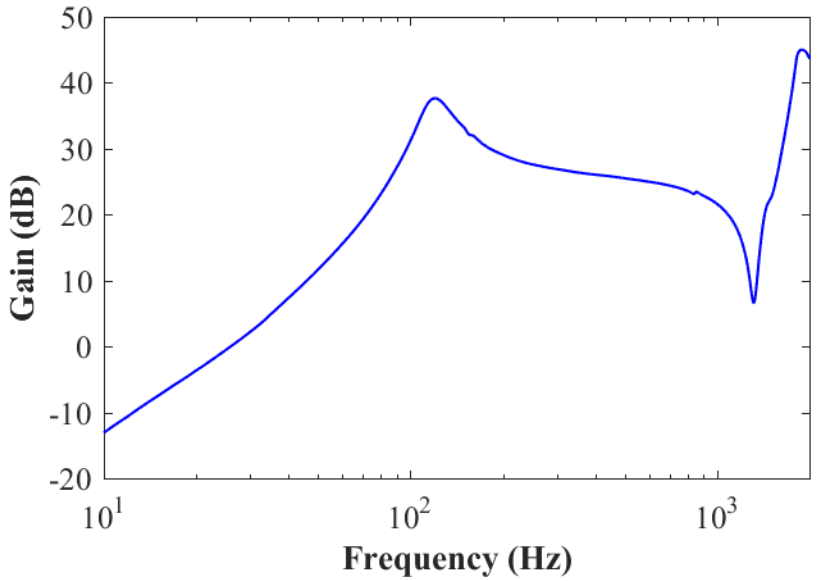


Figure 2.1: Frequency characteristics of the vibrator from 10 Hz to 2,000 Hz

- Time Constant

  The time constants of the vibrations were measured by the output signal from a piezo sensor rather than by the input signal. As shown in Figure 2.2, function $y = A * e^{-\frac{t}{\tau}}$ was found by a least-square fit to all the positive and negative peaks in the waves of the vibrations. The absolute maximum amplitude value of the

Table 2.1: Stable range of time constant

| Frequency (Hz) | Lower boundary (ms) |
|---|---|
| 150 | 10.8 |
| 250 | 5.6 |
| 500 | 5 |
| 800 | 2.4 |
| 1000 | 8 |

waveform was set as the starting point for fitting the function. Figure 2.2 shows that time constant $\tau$ reflected the envelope shape of the stimuli (matching the peak values). When $\tau$ is longer, the envelope shape of stimuli is smoother, and when $\tau$ is smaller, the envelope shape is steeper.

The input time constant $\tau_i$ and output time constant $\tau_o$ were measured in five iterations and the standard errors of five times $\tau_o$ were calculated. The test time constants were used only when the standard errors were less than 5% of the average value. The input values were tested several times. These measured values linearly interpolated other time constants. In addition, the lower boundaries of the time constant at different frequencies are shown in Table. 2.1.

To obtain the JNDs at all the test frequencies, a relatively high time constant of 50 ms was used based on the preliminary experiments. The lower reference of time constants was not chosen in this experiment because some of the subjects were unable to distinguish the time constants at certain frequencies, and an example of this is shown in the test range in Table. 2.1. One of the results obtained using the experimental procedures in this research is shown in Figure 2.3. While the reference time constant was 30 ms and the frequency of vibration was 800 Hz, the possible distinguished time constant could not be derived owing to the limited low boundary of the time constant 2.4 ms.

- Just Noticeable Difference of time constant

  This psychophysical parameter is defined by Webers Law as the detectable difference between a reference stimuli and test stimuli. JND of time constant in this research was calculated as following,

$$JND = \frac{|\tau_t - \tau_o|}{\tau_o} \times 100 \tag{3}$$

  Where the $\tau_t$ is a time constant of the test stimuli and $\tau_o$ is a time constant of the reference stimuli. Both sides of the JNDs were investigated in this research. When the test time constant is lower than the reference time constant, the calculated JND is called lower JND. When the test time constant is higher than the reference time

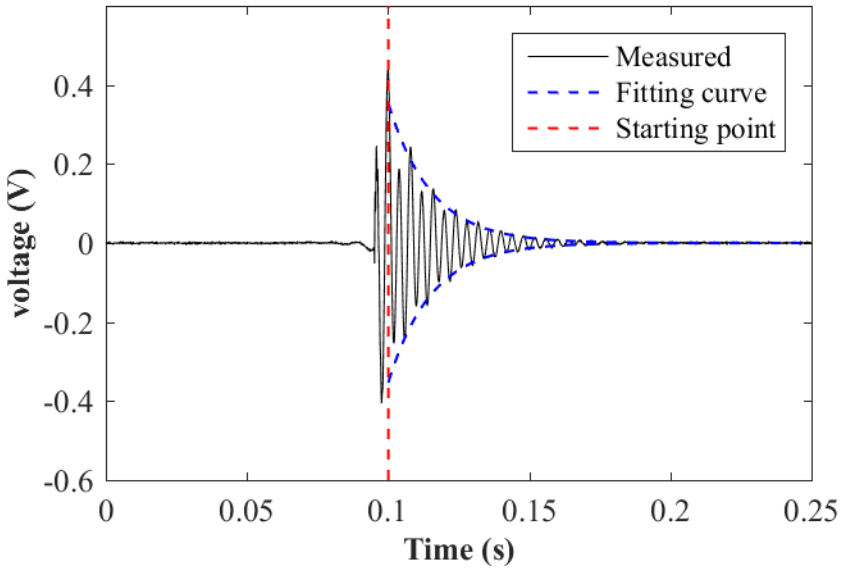


Figure 2.2: Time constant measured by piezo signal

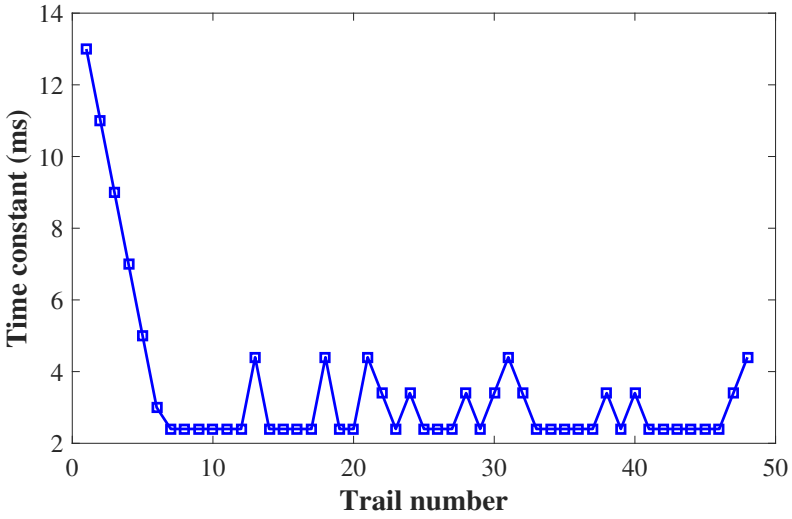


Figure 2.3: Distinguished time constant outside of the test range for the reference stimulus frequency, 800 Hz, and the time constant, $\tau_o$, is 30 ms.

constant, the calculated JND is called upper JND.

#### 2.4.2.2 Apparatus

As shown in Figure 2.4, a subject gripped the actuator between the thumb and index finger to perceive collision vibrations while the gripped normal force was being measured. The test apparatus comprised an actuator (Vp210, ACOUVE LABORATORY, INC., JAPAN), an amplifier, and a computer. The actuator was suspended in air by a sewing thread. A force sensing resistor was attached to the center of the actuator to measure the force by which the subjects gripped the actuator.

The generated waves of the actuator were measured by a piezoelectric vibration sensor

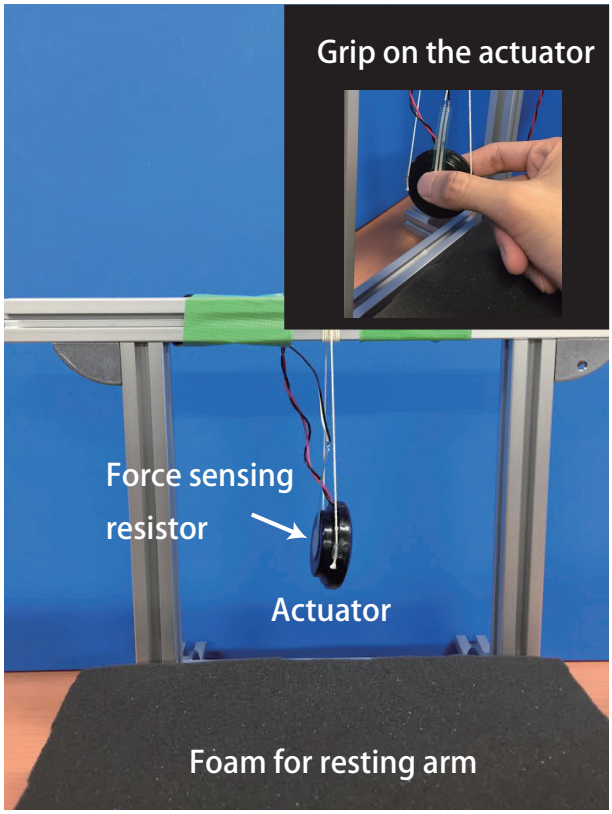


Figure 2.4: Experimental apparatus. Actuator is suspended in air, and a subject gripped the actuator between the thumb and the index finger.

(VS-BV02, NEC TOKIN, JAPAN).

#### 2.4.2.3 Subjects

Seven subjects (age group 21–28, six males, one female, all right-handed) took part in the experiment. Subjects had no motor or sensory limitations as their self-report.

#### 2.4.2.4 Tasks and procedures

The subjects sat comfortably on a chair in front of computers and gripped the actuators slightly with their thumbs and index fingers. The subjects rested their forearm on a big foam. According to the values from the force sensing resistor, the subjects gripped the actuators with a constant force (approximately 0.25 N) during the experiment. After they reached the required force, each subject completed a short test run to familiarize with the procedures. The order of stimuli was randomized for each subject.

Five test frequencies (150, 250, 500, 800, and 1,000 Hz) were chosen in the experiment. Frequencies of 250 Hz and 1,000 Hz were selected because, in general, the most sensitive frequency is in the range of 200–300 Hz while 1,000 Hz is the highest frequency in human haptic perceptual range. A frequency of 500 Hz was also essential because many haptic actuators generate a vibration frequency of up to 500 Hz. The frequencies of 150 Hz (lower than the sensitive range) and 800 Hz (higher than 500 Hz but may only occur during collision contacts by tapping hard materials) were selected to better analyze the

frequency effect within the perceptual frequency range of humans.

The JNDs were obtained using an adaptive staircase method with a 1down-1up progression rule combined with a three-interval, forced-choice answer paradigm (3IFC) [49]. In this process, the JNDs obtained corresponded to 50 % point on the psychometric function [49]. In each trial, the subject was presented with three stimuli. There was a 1.5-s-long interval between each stimulus. One of the three stimuli was the test stimuli while the other two stimuli were the same reference stimulus. The task was to identify the test stimulus out of the three stimuli by pressing the corresponding keys (1, 2, 3) on the keyboard. The subjects were not instructed on the difference between the test and reference stimuli. Instead, the initial test stimuli were initially set to be easily distinguishable, and the subjects were able to identify the differences between the reference and test stimuli by themselves in the first several trials.

Owing to the long duration of the experiment (approximately 2 h), the subjects could lose their concentration eventually; thus, they could repeat the same three stimulus by pressing the key (space), while the orders of the stimuli would be changed through repetition. The subject was instructed to choose their answers as quickly as possible.

Both sides of the JNDs (upper and lower) were tested when the reference of time constant was 50 ms. Besides, while only the upper JNDs were tested at the time constant of 10.8 ms. For all the tests, the first six step sizes were set to be 5 ms (for fast converge) and the last 12 step sizes were set to be 1 ms (for finer resolution). The test series was terminated after 18 reversals.

Each measurement run lasted approximately 6 to 10 min, and the subjects had a 3-minutes break between two runs. The entire experiment took approximately 2 hours.

### 2.4.3 Results

Five subjects took the tests of reference 50 ms and another five subjects (who also took the tests in reference 50 ms) took the tests of reference 10.8 ms. For each subject and each frequency, the JND was calculated by the mean of the last 12 reversals of the staircase.

For the reference 50 ms of the time constant, the average upper JNDs of all subjects and standard errors are shown in Figure 2.5, while the average lower JNDs and standard errors are shown in Figure 2.6. For reference 10.8 ms of the time constant, the average upper JNDs and standard errors are shown in Figure 2.7.

Two-way analysis of variance (ANOVA) with frequency and subject as independent variables was calculated separately for upper JNDs of reference 50 ms, lower JNDs of reference 50 ms, and upper JNDs of reference 10.8 ms.

For upper JNDs of reference 50 ms, frequency ($F(4, 24) = 1.88, p = 0.1625$) and subjects ($F(4, 24) = 2.59, p = 0.0762$) did not have any significant influence. This means the JNDs of time constant were similar for the frequencies.

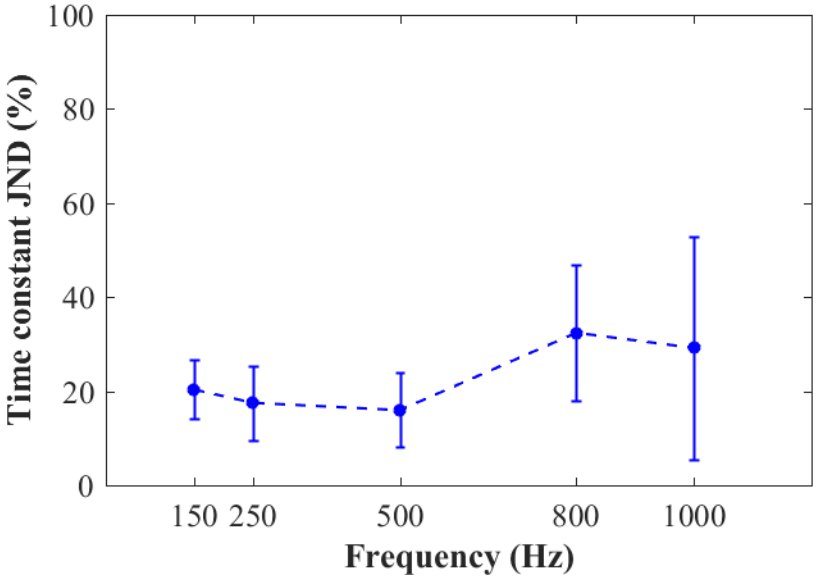


Figure 2.5: Reference 50 ms: average upper JND and standard error of time constant

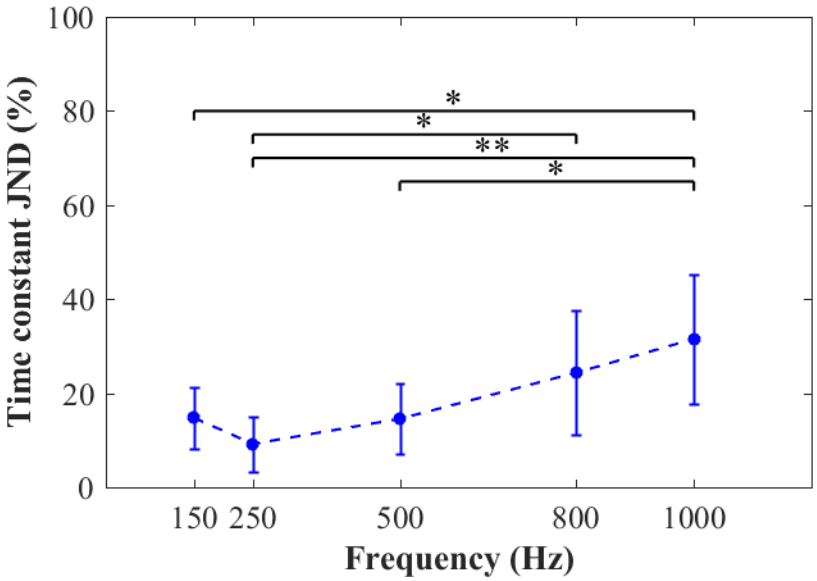


Figure 2.6: Reference 50 ms: average lower JND and standard error of time constant. * $p < 0.05$, ** $p < 0.01$

For lower JNDs of reference 50 ms, both the frequency ($F(4, 24) = 7.85, p = 0.0011$) and the subject ($F(4, 24) = 5.85, p = 0.0043$) had significant influence. Multiple comparison tests were performed by using the Bonferroni method to verify whether the difference of the carrier frequency had a significant effect on the JNDs of the time constant. The results are shown in Table. 2.2. The first two columns of Table. 2.2 show the frequencies that were compared. The third column shows the mean differences among the JNDs of the compared frequencies. The fourth column shows the p-values for the compared frequencies. It demonstrated the occurrence of small p-values in the compared frequencies

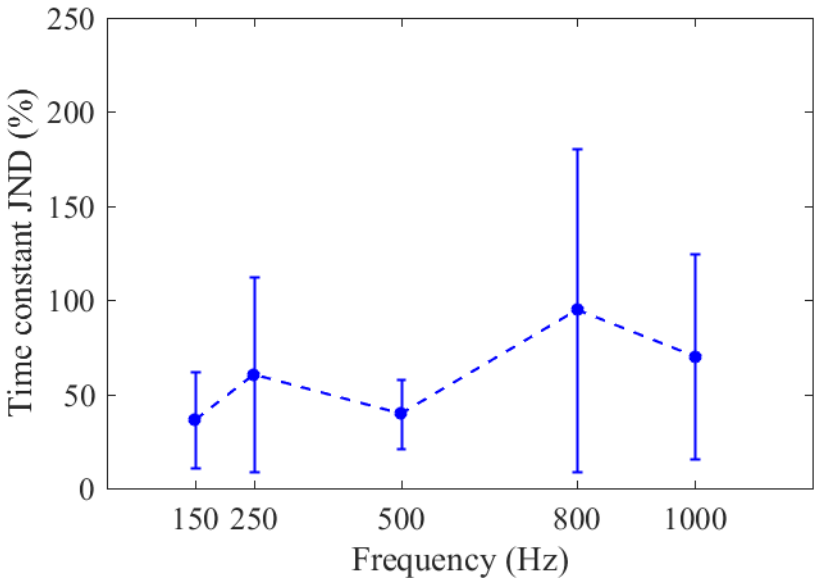


Figure 2.7: Reference 10.8 ms: average upper JND and standard error of time constant

Table 2.2: Lower JND of reference 50 ms: Result of a multiple-comparison test performed using the Bonferroni method

| Frequency 1 | Frequency 2 | Mean difference | P-value |
|---|---|---|---|
| 150 | 250 | 5.55 | 1.00 |
| 150 | 500 | 0.22 | 1.00 |
| 150 | 800 | -9.60 | 0.49 |
| 150 | 1000 | -16.77 | 0.02 |
| 250 | 500 | -5.33 | 1.00 |
| 250 | 800 | -15.15 | 0.04 |
| 250 | 1000 | -22.32 | 0.00 |
| 500 | 800 | -9.82 | 0.45 |
| 500 | 1000 | -16.98 | 0.02 |
| 800 | 1000 | -7.17 | 1.00 |

between 1,000 and 150, 1,000 and 250, 1,000 and 500, and 800 and 250 Hz (significantly different).

For upper JNDs of reference 10.8 ms, frequency ($F(4, 24) = 2.26, p = 0.1076$) and subjects ($F(4, 24) = 7.1, p = 0.0017$) had no significant influences.

Figure 2.8 shows the JNDs compared between the upper JNDs of reference 50 ms, the lower JNDs of reference 50 ms, and the upper JND of reference 10.8 ms. We found that there were significant differences between the upper JNDs of reference 50 ms and upper JNDs of reference 10.8 ms as well as lower JNDs of reference 50 ms and upper JNDs of reference 10.8 ms at 500 Hz. The p-values are 0.0313 and 0.0224, respectively.

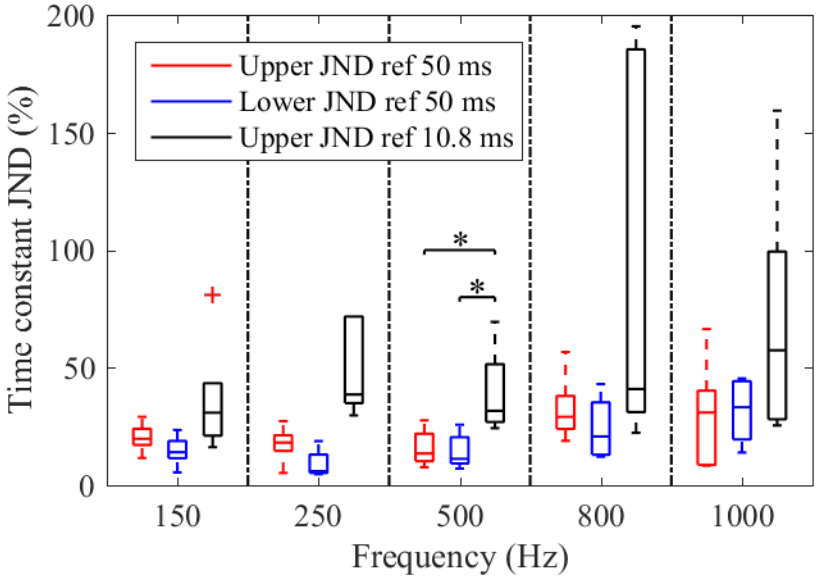


Figure 2.8: Comparison between upper JND of reference 50 ms, lower JND of reference 50 ms, and upper JND of reference 10.8 ms. $^*p < 0.05$

### 2.4.4 Discussions

The experiment in this thesis investigated the JNDs of time constant based on the collision vibration model. To the best of the authors knowledge, the perceptual resolution of collision vibration parameters has not been investigated yet. Our research aims to understand the perceptual resolution of time constant, which is a parameter in the collision vibration model.

#### 2.4.4.1 Sensitive frequency of time constant

Three types of JNDs of time constant (upper JND of reference 50 ms, lower JND of reference 50 ms, and upper JND of reference 10.8 ms) were tested in our experiment. Results of the two-way ANOVA revealed significant differences among frequencies only occurring for lower JND of reference 50 ms.

For lower JNDs of reference 50 ms, Figure 2.6 showed that the shape of the average JNDs had two parts, two slopes occurred at the frequency range (-0.138 %/Hz lower than 250 Hz and 0.085 %/Hz higher than 250 Hz), and the lowest JND occurred at 250 Hz. The results of two multiple comparison tests showed that 1,000 Hz was significantly different from 150, 250, and 500 Hz while 250 Hz was distinct from 800 Hz. The average JNDs of 800 and 1,000 Hz were higher than JNDs of 150, 250, and 500 Hz. Therefore, the JNDs of the time constant may have been lower when the frequency was less than 500 Hz (sensitive, average JND was 12.8 %) and the JNDs were higher when the frequency was higher than 800 Hz (not sensitive, average JND was 27.9 %).

For upper JNDs of reference 50 ms, Figure 2.5 shows that the curve of average upper JNDs had a stage shape and at frequencies 150, 250 and 500 Hz, JNDs were similar

(average 17.9 %) while at frequencies 800 and 1,000 HZ they were similar (average 30.8 %). Average JNDs of 800 and 1,000 Hz were also higher than the average JNDs of 150, 250, and 500 Hz. However, the result of the two-way ANOVA revealed no significant effect of frequency. This may mean that the JNDs of time constant did not have obvious differences in the frequency range. The average JND of all frequencies was 23 %.

For upper JNDs of reference 10.8 ms, Figure 2.7 showed that the curve of the average upper JND also had a stage shape. At frequencies 150, 250, and 500 Hz, the JNDs were similar (average 52.8 %) and at frequencies 800 and 1000 HZ, JNDS were similar (average 66 %). Average JND of 800 and 1,000 Hz were also higher than JND of 150, 250, and 500 Hz. However, the result of the two-way ANOVA revealed no significant effect of frequency. This may mean that the JNDs of the time constant does not have obvious differences in the frequency range. The average JND of all frequencies was 65 %.

In conclusion, the sensitive frequency of the time constant was approximately 250 Hz (150 to 500 Hz, average JND was 12.8 %) and it was not sensitive at high frequencies (800 to 1,000 Hz, average JND was 27.9 %) for the lower JNDs of reference 50 ms. The JNDs of time constant did not have obvious differences in the upper JNDs of reference 50 ms (average JND was 23 %) and upper JNDs of reference 10.8 ms (average JND was 65 %).

#### 2.4.4.2 Time constant range effects on JNDs

The average upper JNDs of the lower reference, 10.8 ms, were bigger than the JNDs of the reference, 50 ms, and relatively higher standard errors occurred. In the research [50], Hatzfled et al. investigated the JND of force near the absolute threshold, and each of the subject was tested by using the individual thresholds at frequencies tested in [51]. They found that the JNDs were much larger than the reference used well above the threshold. In our research, we investigated the JNDs of the time constant and not the force. However, reference values may also affect the JNDs.

For example, at lower reference 10.8 ms, subjects had significant effects on JNDs of time constant. The reason for subject effects on JNDs may be their threshold for the time constant. In some frequencies, the reference time constant, 10.8 ms, may be near their threshold, so higher JNDs and big differences between subjects occur. In this research, we did not investigate the threshold of time constant because it may be negligible. In our tests, the smallest time constant as shown in Table. 2.1 was easily perceived by the subjects. However, the JNDs (perception resolution) of time constant may be largely affected near the individual threshold.

Before we conducted these experiments, we assumed that the frequency would affect the JND of time constant. Considering the test range of time constant based on JNDs, the time constant range (considering the differences among subjects) was approximately 50 ms–80 ms for the upper JNDs of reference 50 ms, 30–50 ms for the lower JNDs of reference 50 ms, and 10.8–30 ms for the upper JNDs of reference 10.8 ms. In view of

the time constant range, the results showed that there were no significant effects (subject and frequency) at the test range of 50–80 ms, significant effect (frequency and subject) at the test range 30–0 ms and significant effects (subject) at the test range 10.8–30 ms. Therefore, for the high time constant range (e.g., 50–80 ms), JNDs may be similar in the frequency range. For the low time-constant range (e.g., 10–30 ms), JNDs may be largely affected by the individual thresholds. While in the middle range of the time constant (e.g., 30–50 ms), the JNDs of time constant may be significantly affected by frequency. The perceptual threshold of time constant and the effect of time constant range on perception resolution must be investigated in future studies.

However, some results of the experiment, such as the different tendencies between the upper and lower JNDs, may be owing to the limited number of subjects. Further investigation is required in the future.

## 2.5 Frequency discrimination of amplitude-modulated vibration

### 2.5.1 Specific Objective

To investigate whether humans can discriminate stimuli based on the difference in envelope frequency and the difference in carrier frequency.

### 2.5.2 Methods

#### 2.5.2.1 Materials

In this experiment, we use the AM vibration to investigate the effects of intensity and envelope on human perception. M vibrations were used to present the texture vibration, which reflects the roughness of the contact surface. The AM vibration is given as,

$$q(t) = \text{env}(t) \times \cos(2\pi f_c t), \tag{2.1}$$

where $env(t)$ is an envelope waveform and $f_c$ is the carrier frequency.

Another type of AM vibration is,

$$q(t) = A\left(0.5 + 0.5\sin(2\pi f_e t - \frac{\pi}{2})\right)\sin(2\pi f_c t) \tag{2.2}$$

where $A$ is the amplitude, $f_e$ is the envelope frequency, and $f_c$ is the carrier frequency.

#### 2.5.2.2 Apparatus

The experimental setup is shown in Figure 2.10(a). Vibrotactile stimulation was delivered to the right hand palm by a vibration generator (EMIC CORPORATION, 511-A).

The displacement of vibrotactile stimulation was measured by a laser Doppler displacement meter (KEYENCE CORPORATION, LK-H025) while activating without grip. One

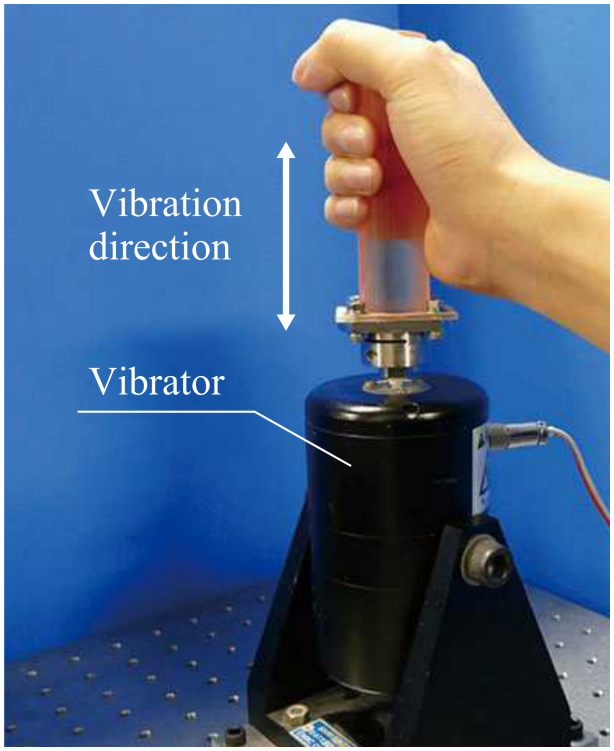


Figure 2.9: (a) Participant perceiving vibrotactile stimulation generated by a vibrator

example of measured displacement is shown in Figure 2.10(b). The amplitude of vibrotactile stimuli is higher than the perceptual thresholds in the frequency range of 40–800 Hz [3].

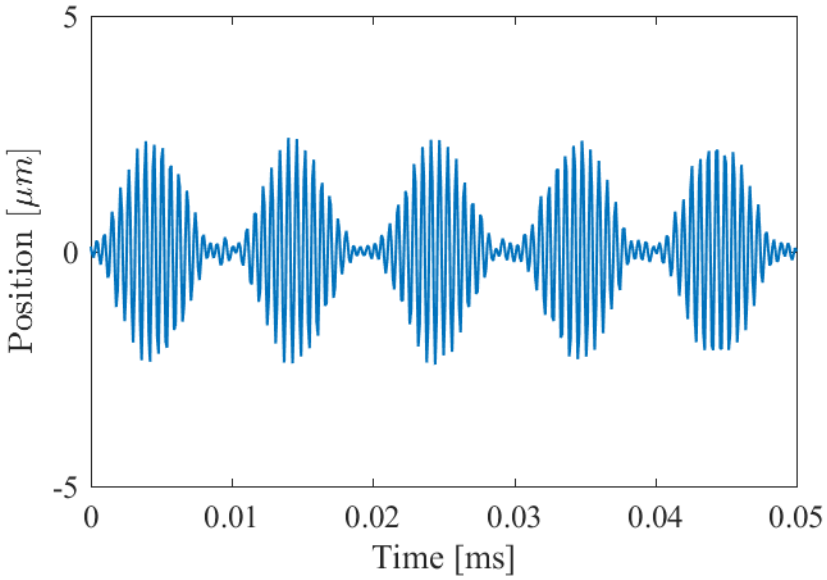


Figure 2.10: Vibrotactile stimulation represented by the combination of envelope and carrier frequencies

Table 2.3: Stimulus sets

| | Parameters of vibrotactile stimuli (envelope freq., carrier freq.) [Hz] | | |
|---|---|---|---|
| Stimulus set 1 | (**80**, 1680) | (**100**, 1680) | (**120**, 1680) |
| Stimulus set 2 | (**80**, 500) | (**100**, 500) | (**120**, 500) |
| Stimulus set 3 | (100, **1120**) | (100, **1400**) | (100, **1680**) |
| Stimulus set 4 | (100, **400**) | (100, **500**) | (100, **600**) |

#### 2.5.2.3 Subjects

Six volunteers (five males and one female, age groups 22 to 29, all right-handed, no history of deficits in tactile processing) participated in the experiments. They were not aware of the purpose of the experiments.

The participants did not receive any special instructions regarding the gripping force as it did not affect the vibration detection threshold in a previous report [52].

#### 2.5.2.4 Tasks and procedures

The participants sat on the chairs and rested their forearms on the armrests during the experiments. To mask the sound generated by the vibrator, they were made to hear pink noise through headphones and use earplugs.

In one trial, four vibrotactile stimuli (1 s) with a 0.5-s interval is provided to a participant. The first stimuli are the test stimuli and the subsequent three stimuli are the three references in the same set shown in Table 2.3. The participant selects one of the three references that they feel is the same as the test stimuli. They can repeat the stimulus as many times as they want, but they are recommended to repeat it less than three times (including the first time). For each iteration, the test stimuli are the same while the order of three references is random.

The orders of stimulus sets and the test stimuli in each stimulus set are randomized for each participant. In the beginning, the first set is conducted in ten trails as training, to help the participant familiarize with the experimental procedure and restart as the actual trials. The training results are not recorded. Each stimulus in the same set is presented ten times as the test stimuli. Thirty trails in total are conducted for each set, 130 trials are conducted for each participant. The participants took a two-minutes break between every set for one stimulus set. The entire experiment took approximately 40 minutes.

### 2.5.3 Results

Tables 2.4 and 2.5 show the answer ratios for stimulus sets 1 and 2, respectively, where the envelope frequencies are different and the carrier frequency has a constant value. The mean value and standard deviations calculated among the participants are shown in the tables. The experimental data for each stimulus is collected from a normal distribution by the Kolmogorov–Smirnov test; a parametric statistical approach is used

Table 2.4: Answer ratio for stimulus set 1. $**$:$p < 0.01$.

| | | Answered stimulus (envelope freq., carrier freq.) [Hz] | | |
|---|---|---|---|---|
| | | (80, 1680) | (100, 1680) | (120, 1680) |
| Actual | (80, 1680) | 0.60±0.14** | 0.37±0.12 | 0.03±0.05 |
| | (100, 1680) | 0.13±0.15 | 0.70±0.15** | 0.17±0.16 |
| | (120, 1680) | 0.03±0.05 | 0.18±0.15 | 0.78±0.17** |

Table 2.5: Answer ratio for stimulus set 2. $*$:$p < 0.05$.

| | | Answered stimulus (envelope freq., carrier freq.) [Hz] | | |
|---|---|---|---|---|
| | | (80, 500) | (100, 500) | (120, 500) |
| Actual | (80, 500) | 0.65±0.21* | 0.32±0.24 | 0.03±0.05 |
| | (100, 500) | 0.15±0.10 | 0.60±0.23* | 0.25±0.16 |
| | (120, 500) | 0.05±0.08 | 0.35±0.24 | 0.60±0.23* |

Table 2.6: Answer ratio for stimulus set 3. $***$:$p < 0.001$, $**$:$p < 0.01$.

| | | Answered stimulus (envelope freq., carrier freq.) [Hz] | | |
|---|---|---|---|---|
| | | (100, 1120) | (100, 1400) | (100, 1680) |
| Actual | (100, 1120) | 0.67±0.10*** | 0.32±0.14 | 0.02±0.04 |
| | (100, 1400) | 0.48±0.28 | 0.48±0.25 | 0.03±0.18 |
| | (100, 1680) | 0.05±0.05 | 0.12±0.16 | 0.83±0.20** |

Table 2.7: Answer ratio for stimulus set 4. $*$:$p < 0.05$.

| | | Answered stimulus (envelope freq., carrier freq.) [Hz] | | |
|---|---|---|---|---|
| | | (100, 400) | (100, 500) | (100, 600) |
| Actual | (100, 400) | 0.55±0.23 | 0.33±0.18 | 0.12±0.08 |
| | (100, 500) | 0.30±0.24 | 0.43±0.24 | 0.27±0.18 |
| | (100, 600) | 0.15±0.12 | 0.23±0.14 | 0.62±0.19* |

for analyzing data. The collect answer ratios with grey cells were higher than the chance level (0.33) of the answer ratios. For example, the answer rate for stimulus whose envelope and carrier frequencies were 100 and 1680 Hz, respectively, is significantly higher than 0.33 ($t(5) = 5.8$, $p = 0.0022$). All six conditions yield significant differences between the answer ratios and the chance level. These results support hypothesis 1, which states that humans can distinguish vibrotactile signals based on the difference in envelope frequency even at a constant carrier frequency.

Tables 2.6 and 2.7 show the answer ratios for stimulus sets 3 and 4, respectively, where the envelope frequency is constant and the carrier frequencies are different. The collect answer ratios with grey cell were higher than the chance level (0.33) of the answer ratios.

For example, the answer rate for the stimulus whose envelope and carrier frequencies were 100 and 1120 Hz, respectively, is significantly higher than 0.33 ($t(5) = 7.9$, $p = 5.3 \times 10^{-4}$). Three conditions show the significant differences between the answer ratios and the chance level. These results support hypothesis 2, which states that humans can distinguish vibrotactile signals based on the difference in carrier frequency even at a constant envelope frequency.

### 2.5.4 Discussion

The results showed that when the difference in envelope frequency is tested in the stimuli sets 1 and 2, subjects can detect 20 % of the change in envelope frequency on both carrier frequencies, 1,680 Hz and 500 Hz. The general assumption that humans cannot perceive the vibration of a frequency higher than 1,000 Hz is, hence, falsified. In [53], Wyse et al. found that humans can still perceive vibrations over 1 kHz or even 2 kHz. Generally, vibrations over 1 kHz are not investigated in [3, 45] because it is difficult to generate enough amplitude by the shaker or the actuator. However, this does not mean that it cannot be perceived. In our experiment, the amplitude of the stimuli was set to be the same at approximately 2 $\mu m$. Furthermore, AM vibrations can also be perceived at over 1 kHz. Our results support the hypothesis that humans can perceive vibrations of over 1 kHz. Our results also show that when the carrier frequency difference (20%) are tested in the stimulus sets 3 and 4, subjects were able to distinguish the stimuli and the carrier frequency of over 1 kHz easier than the carrier frequency of less than 1 kHz. The results indicated that a higher carrier frequency shows a lower JND, which means more sensitive. This is, however, contrary to our assumption that lower carrier frequency, which has a lower threshold, is more sensitive.

## 2.6 Limitation of the study

Investigating the JND of time constant has several limitations:

1. We were unable to generate very small time constants of collision vibration, which would have been closer to the real collision vibrations [33]. Our results also showed that when the time constant is small, a large JND with a wide distribution may occur. This may lead to a significant difference from the JND of a large time constant range.

2. The stimuli in our experiment were assumed to have the same amplitude as in the voltage of the piezo signal, which reflects the same acceleration. However, the maximum amplitude measured by the acceleration sensor was not constant, as shown in Figure 2.11. In addition, the intensity of high-frequency vibration is feeble. In [50], their results showed that when the amplitude is closer to its threshold, the JNDs value become bigger. Therefore, in our experiment, the same acceleration peak of stimuli may lead to a different intensity sensation. When the frequency is

high, e.g., 1,000 Hz, the intensity of stimuli is much smaller than that of the low-frequency stimuli, and higher JNDs or larger range distributions by subjects may occur as revealed by the results. A scale of amplitude used to adjust the intensity of stimuli is needed to investigate the JNDs of time constant in future studies. For investigating the envelope and carrier discrimination of the AM vibration, a similar intensity difference shall be considered in future studies. However, even with the generated amplitude of the stimuli, we could find a significant difference caused by the carrier frequency at the upper JNDs.

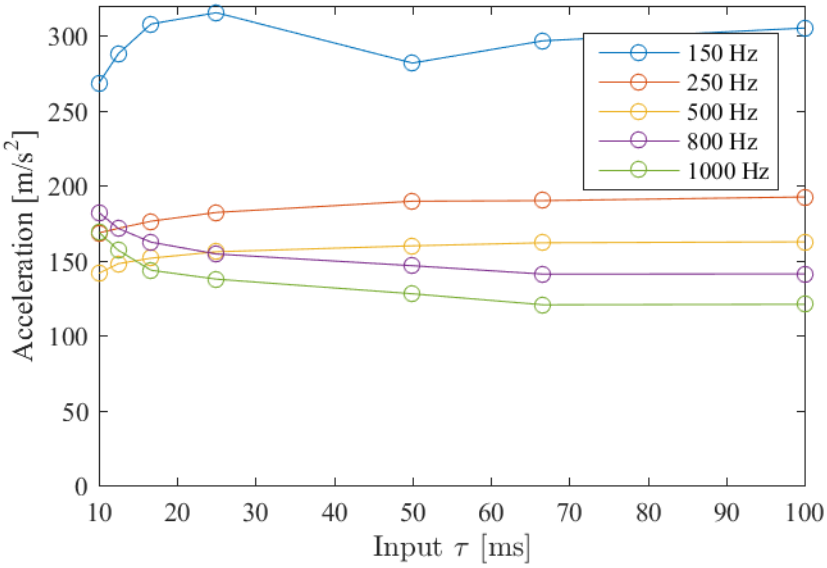


Figure 2.11: Maximum amplitude of the generated stimuli at different frequencies along with the time constant.

## 2.7 Summary

Humans can perceive the envelope of an AM vibration even when the carrier frequency is higher than the perceivable frequency range [31, 32]. Concerning continuous high-frequency vibrations, the perceptual characteristics of the envelope and carrier of a vibration have been investigated in several previous studies [31, 32]; however, those characteristics for one-impulse high-frequency vibrations such as the collision vibration have not yet been investigated.

Our experimental results suggest that humans can perceive the envelope of a vibration, especially for the single-pulse vibrations such as collision vibrations. The experimental results of measuring the JNDs of time constant revealed significant differences caused by the reference for the upper JNDs. The mean upper JND of the reference time constant, 10.8 ms, is 60 % while that of the reference time constant, 50 ms, is 23 %. This suggests

that humans are more sensitive to the changes in a long time constant. The experimental results of measuring the JNDs of time constant did not reveal significant differences caused by the carrier frequency for the upper JNDs. This suggests that the carrier frequency did not strongly affect the discrimination of the envelope. This means that the carrier frequency of the high-frequency vibration can be changed without changing the perception of the envelope. Therefore, we can shift the carrier frequency and still maintain the envelope sensation by the modulation. A lower carrier frequency could reduce the difficulties of generating high-frequency vibrations and reduce through modulation the sound of the vibration when using a lower frequency carrier.

In addition, we also conducted a preliminary experiment to investigate the envelope and carrier discrimination of the AM vibration. Amplitude-modulated vibrations have different carrier frequencies with frequencies less than 1 kHz in the humanly perceivable frequency, and frequencies higher than 1 kHz beyond the humanly perceivable frequency range. Our results showed that subjects could detect 20 % of the change in envelope frequency on both 1,680 Hz and 500 Hz carrier frequencies. In addition, subjects could distinguish the stimuli easier when the carrier frequency was over 1 kHz than they could when the carrier frequency was less than 1 kHz. The results indicated that a higher carrier frequency shows a lower JND, which is more sensitive. The results are contrary to our assumption that lower carrier frequency, which has a lower threshold, is more sensitive.

# Chapter 3

# Introduction of time-domain segment to intensity-based perception model of high-frequency vibration

## 3.1 Introduction

High-frequency vibrations induced by scratching or tapping on surfaces were reported as the cues for roughness or hardness perception [33, 22, 19, 54]. Thus, transmitting high-frequency vibrations has been attempted for supporting telerobotic surgery [55] and delivering realistic textures [56, 57]. In practical applications, the tactile stimuli must be transmitted in real-time; therefore, a perceptual model that can interpret the sensation of the high-frequency vibrations with time-variant patterns is needed.

The intensity of high-frequency vibrations ($>$ 100 Hz), which is generally defined as the integral of a stimulus wave over time or spectral power summed across all frequencies, is the primary cue to convey tactile information perceived by the Pacinian system [28, 29, 30, 4]. Makous et al. [28] found that the intensity model, which is a function of spectral power divided by the threshold power, constitutes a measure of the ability to excite a Pacinian system. Bensmaia et al. improved the intensity model with the spectral characteristics based on the psychophysical and neurophysiological findings [30]. Bensmaia et al. also applied this spectral model to finely textured stimuli to predict the perceptual dissimilarity [4]. The limitation of the conventional model is that it cannot interpret the sensation of the envelope.

A missing argument concerning the intensity-based model is the determination of sufficient time duration to integrate the intensity of stimulus, to account for the vibrations with a relatively slow time-variant envelope. For instance, Figure 3.1 shows an example of an equivalent energy-based waveform reproduction process for emulating the stimulus with two different integral segment sizes (broken blue lines), i.e., (a) long-term and (b) short-term segment cases. Here, the original stimulus was an AM high-frequency vibration

($>$ 100 Hz) with a low-frequency envelope ($<$ 50 Hz). In the long-term segment case (a), for the duration of long segment size, the intensity on each segment constitutes a flat line of the same level. Thus, we could reproduce an intensity-equivalent waveform with a sinusoidal wave of the constant amplitude. In the short-term segment size case (b), however, the time segment duration was shorter than the envelope period of the original stimulus, such that the original stimulus was divided into several segments and the intensities of each segment changed in a step-wise manner. Thus, the reproduced sinusoidal waveform by the modulation could also have step-wise changes on the envelope. These two cases demonstrated that a reproduced waveform concerning the intensity-model depends on the segment sizes.

If the intensity-equivalent waveforms with different segment size are different sensation, the intensity-based model would require a suitable segment size. The low-frequency components occurring in the envelope of the high-frequency vibrations are should efficiently differentiate the tactile perception. Several researchers reported that a human could detect the low-frequency envelope of a high-frequency modulated vibration [31, 32, 39]. Therefore, we need to find that whether there is an appropriate time segment size related to segmented intensity modulation. Besides, Bensmaia et al. also found that the high-frequency stimuli of the equal intensity were found difficult to discriminate in their experiment, especially when the function of the rapidly adapting (RA) channel was minimized with the low-frequency adapting stimulus [29]; thus, we need to consider the activities of the RA system.

The present study introduced a time-domain segment into the intensity-based perception model. In particular, we investigated the discrimination ability of the reproduced time-segmented wave that had the same intensity as that of the original vibration on each segment, as a pilot study to determine the proper segment size for the intensity-based modulation. This study targets the AM high-frequency vibrations (carrier frequency $f_c =$ 300 or 600 Hz) that have relatively low envelope frequencies ($f_e =$15, 30, or 45 Hz). These select low envelope frequencies together were considered as the frequency range, assumed to be perceived by Meissners corpuscles.

To simplify the experimental conditions and discussions in this chapter, we incorporated several assumptions:

1. The original stimuli and reproduced vibrations stimuli by the modulation should have the same carrier frequency

2. The stimulus intensity is the general integral power of vibration displacement in the time domain.

Assumption (1) avoids the frequency dependence of the Pacinian system on the intensity models, which were incorporated with the human detection threshold [28] and

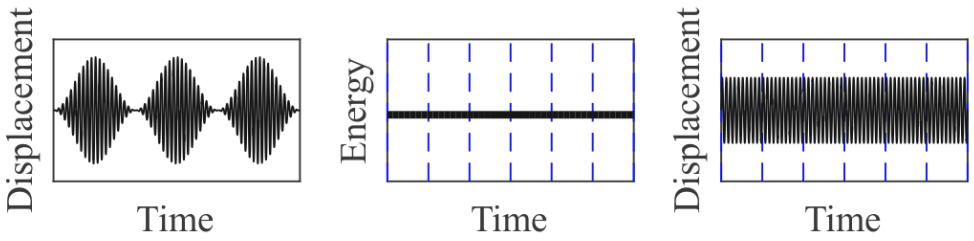


(a) Long-term segment case (left: original wave, middle: long-term segment energy, right: reproduced wave)

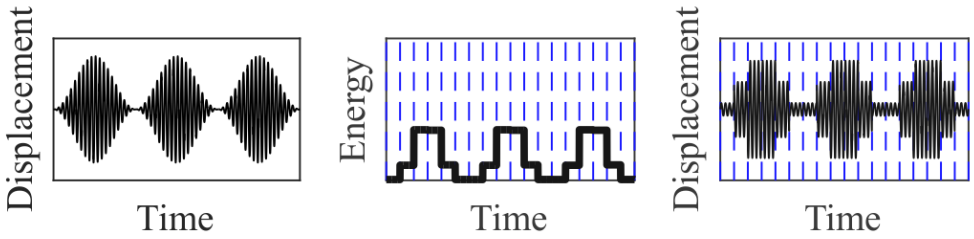


(a) Short-term segment case (left: original wave, middle: short-term segment energy, right: reproduced wave)

Figure 3.1: Waveforms of the same segmental energy for different segment cases

the spectral characteristics [30]. Thus, we use the integral intensity assumed in (2). Besides, we also avoid the phase effects of segmentation by carefully selecting the segment to be synchronized with the original waveform, in order not to generate other periodic vibrations.

We investigated the relationships between the time segment size and the discrimination performance through the psychophysical experiments. In the experiment, participants compared the reproduced stimuli using different segment sizes modulated from the original stimuli of different carrier and envelope frequencies. We also confirmed the effect of the carrier and envelope frequencies on the ability to discriminate the high-frequency vibrations. The work in this chapter was published in [58].

## 3.2 Objectives of the chapter

In this chapter, we introduced the time-domain segment in the intensity-based perception model. First, we verify whether the segmented intensity model could emulate the perceptual vibrations modulated from the original waves. Second, we investigate the discrimination ability of the reproduced time-segmented waveform that has the same intensity as that of the original vibration on each segment, as a pilot study to investigate the suitable segment size for the intensity-based modulation.

## 3.3 Significance of the Study

The intensity of a high-frequency vibration (> 100 Hz) plays an important in forming the texture and collide sensation. A modified vibration is also used to model different types of tactile sensations. A time-segment intensity model can combine the intensity and vibration patterns to design the vibration rendering parameters. Besides, in the practical applications, we need to transmit the tactile stimuli in real-time; therefore, the segmented intensity model can be used to modulate the high-frequency vibrations that have a low-frequency envelope. If we know the proper segment size concerning the segmented intensity model, we will know the possible delay of this modulation.

## 3.4 Proposed Model

In this chapter, we incorporated the time-domain segment into the intensity model to represent the intensity changes of high-frequency vibrations in the time domain. By using our model, we reproduced a perceptually similar stimulus from the original vibration and investigated the relationships between the time segment sizes and the discrimination performance of stimuli of several carrier and envelope frequencies.

The original wave $v(t)$ is divided into time segments $t_p$ as shown in Figure 3.2(a). The dashed lines are the segment boundaries. Figure 3.2(b) shows that the intensity of the original signal $P(n)$ of each segment calculated by integrating the displacements of the wave as follows:

$$P(n) = \int_{nt_p}^{(n+1)t_p} v(t)^2 dt. \tag{3.1}$$

As shown in Figure 3.2(c), based on the calculated energy of the original signal, the amplitude of perceptually similar vibration, $A_p(n)$, on each segment is calculated as follows:

$$P'(n) = \int_{nt_p}^{(n+1)t_p} \left(A_p(n)\sin(2\pi f_c t + b(n))\right)^2 dt, \tag{3.2}$$

where $f_c$ and $b(n)$ are the carrier frequency of the original signals and the initial phase of the wave in each segment, respectively; and the intensity of the perceptually similar signal, $P'(n)$, was the same as that of the original wave $P(n)$. Finally, as shown in Figure 3.2(d), the perceptually similar vibration $v'(t)$ is determined by

$$\begin{aligned} v'(t) = A_p(n)\sin(2\pi f_c t + b(n)) \\ (nt_p < t < (n+1)t_p). \end{aligned} \tag{3.3}$$

In this chapter, we adopt the AM vibrations as the original high-frequency vibration, $v(t)$, which is represented as

$$v(t) = v_e(t)v_c(t), \tag{3.4}$$

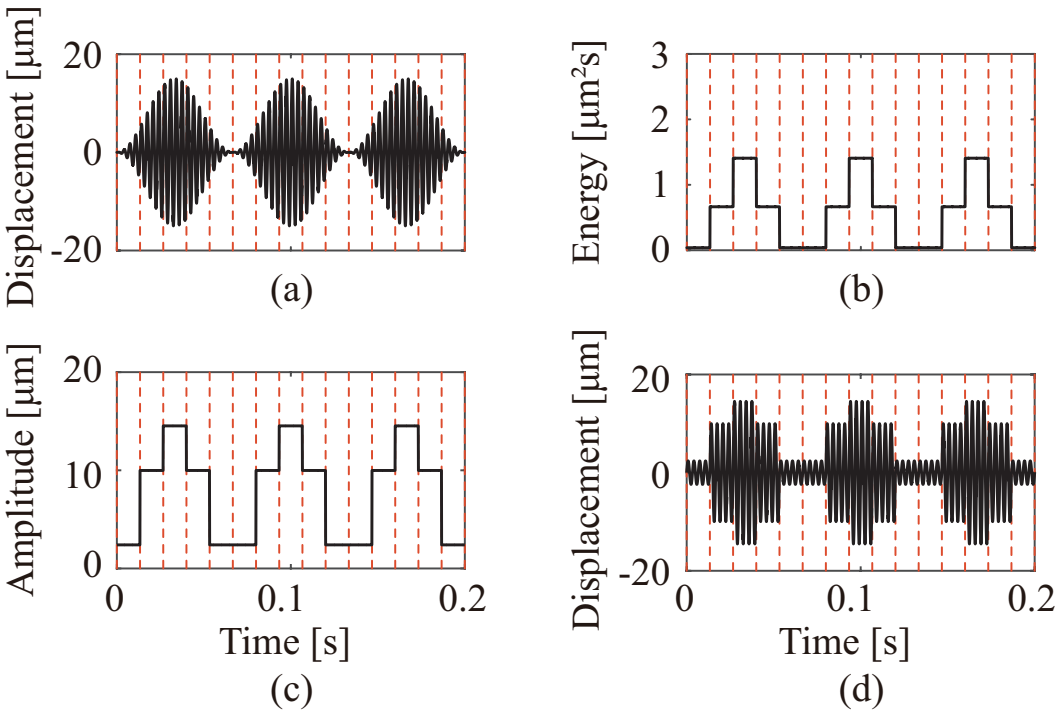


Figure 3.2: Method processes: (a) The original vibration signal is segmented into small pieces of time sets using time segment size $t_p$ in the time domain; (b) The intensity of each segment is calculated by Eq. 3.1; (c) The amplitudes of each segment are calculated based on the energy in the original data using Eq. 3.2; and (d) The stimuli are reproduced using Eq. 3.3.

$$v_e(t) = 1 + \sin(2\pi f_e t + \phi), \tag{3.5}$$

$$v_c(t) = \sin(2\pi f_c t), \tag{3.6}$$

where $f_e$ and $f_c$ is the envelope and carrier frequencies of the AM vibration, respectively, and $\phi$ is the envelope phase.

## 3.5 Method

We conducted psychophysical experiments to investigate the relationships between the smoothness (the temporal resolution) of energy change of a vibration and the discrimination ability of vibration. In the experiment, participants compared the stimuli reproduced by the proposed model with the original wave under different time segment sizes. Besides, comparisons were drawn among different carrier and envelope frequencies to investigate the effect of carrier and envelope frequencies on the relationships between the time segment size and the discrimination performance.

### 3.5.1 Materials

The reproduced vibrations were modulated from the original AM wave using five types of segment sizes. To avoid reproducing perturbed stimuli, we selected the time segment

sizes, $t_p$, which evenly divide the envelope period $t_e$. We defined a segment ratio $r_s = t_p/t_e$; thus, five types of time segment sizes $t_p$ were described as $r_s = 1/6, 1/5, 1/4, 1/3$, and $1/2$.

Six combinations of carrier frequencies and envelope frequencies were adopted as the original AM vibrations. The carrier frequencies ($f_c$) of 300 Hz and 600 Hz are used for the AM stimuli. In addition, we also adopted three envelope frequencies: $f_c = 15, 30$, and 45 Hz. These envelope frequencies were assumed to be the frequency range mainly perceived by Meissners receptors, while the high carrier frequencies of the stimuli should be in the frequency range sensitively activated by Pacinian corpuscles.

We selected various stimuli, i.e., six original AM waves ($(fc, fe) = (300, 15)$, $(300, 30)$, $(300, 45)$, $(600, 15)$, $(600, 30)$, and $(600, 45)$), and a total of 30 reproduced vibrations (six original AM vibration $\times$ five segment number $r_s = 1/6, 1/5, 1/4, 1/3$, and $1/2$), with a total number of 36 stimuli. The stimulus had an 800-ms duration time. In our experiments, 30 stimuli pairs were used, and each pair of stimuli had an original AM vibration and a reproduced wave modulated from the original wave with segment number $r_s$, using the segmented intensity model.

To verify the displacement profiles of the 36 stimuli, we measured the displacements of a piezoelectric vibrator tip using a laser displacement sensor (LK-H025, KEYENCE CORPORATION) as shown in Figure 3.3. The displacements were measured without a finger pressing the top of the actuator. The actuator had strong push and pull forces (800 N and 50 N, respectively), the modulated waves and the original waves had the same carrier frequency, and the constant force was constant during the experiment. Therefore, we assumed that the change in waves induced by the pressing force of 0.5 N did not significantly affect the perceptual difference between the original stimuli and the modulated stimuli.

### 3.5.2 Participants

The participants were two female subjects and seven male subjects (age groups 20–28 years, all right-handed). All participants had no motor or sensory limitations according to their self-reports. Informed consent was obtained; however, the participants were not aware of the purpose of the experiment. They were informed to discriminate the stimuli in the experiments.

### 3.5.3 Apparatus

The experimental apparatus is shown in Figure 4.4. A tactile high-frequency vibration was generated by a piezo actuator (PZ12-112, Matsusada Precision) and its push and pull forces were 800 N and 50 N, respectively. The subjects finger contacted the actuator through an 8-mm diameter hole in the plate; the diameter of the contact part is 6 mm, as shown in Figure 3.5. The actuator was connected to a load cell (LUR-A-100NSA1, Kyowa Electronic Instruments) to measure the contact force, which is 0.5 N between the actuator and a participants finger pad. The load cell was connected to a lab jack, which

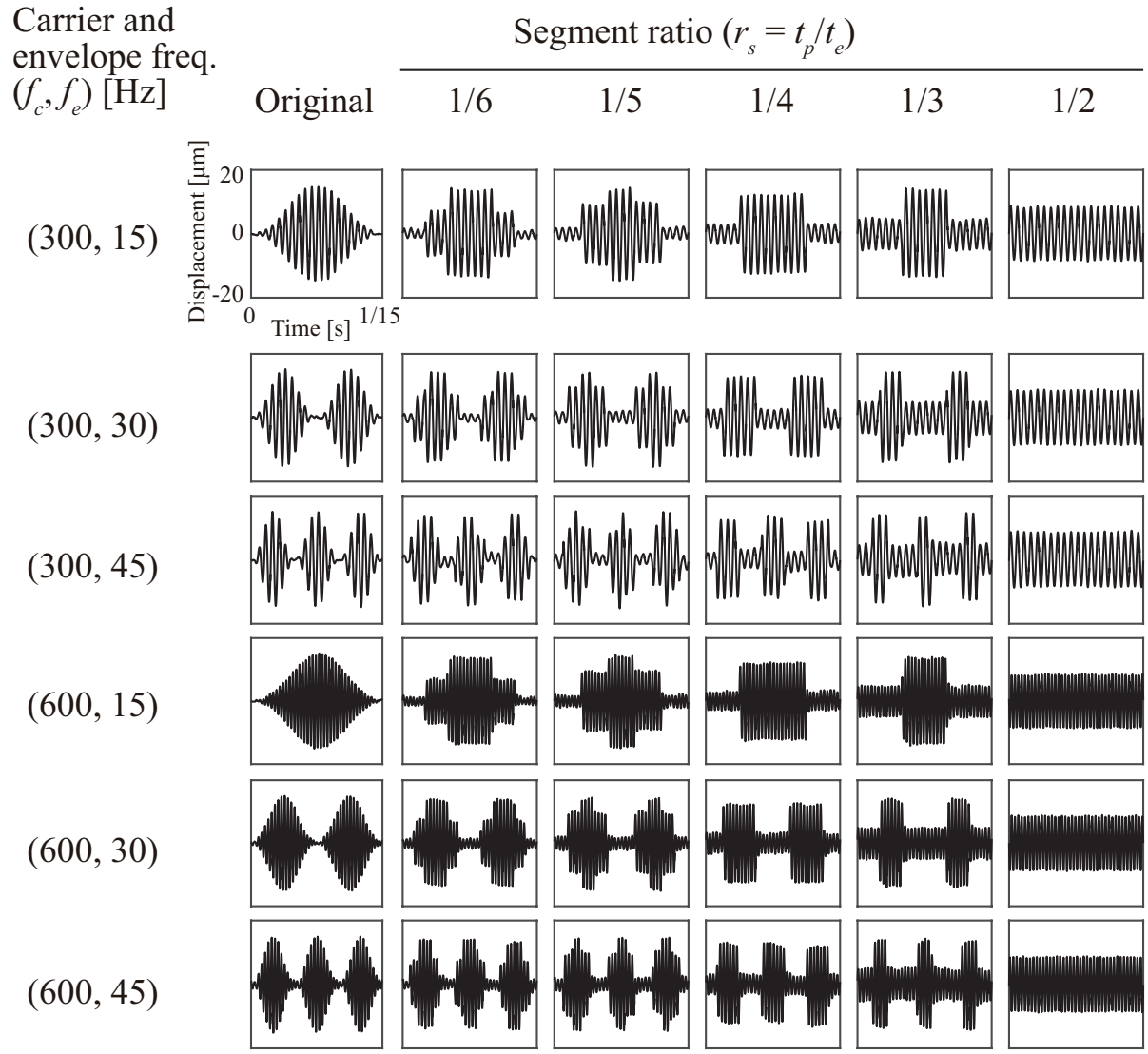


Figure 3.3: Measured displacement profile of stimuli

was used to change the height of the actuator for adjusting the contact force between the actuator contact surface and a subjects finger. A computer generated and fed the input signal to the actuator through a USB audio interface (UR22mkII, Steinberg) and a piezo driver (PZJRP6A, Matsusada Precision).

### 3.5.4 Tasks and procedures

Three alternative forced-choice paradigms were used for measuring the discrimination ratio between the original and reproduced vibrations. We adopted 30 conditions (six original AM vibrations × five segment numbers) and 20 trials for each of the stimuli pair. Therefore, each participant conducted a total of 600 trials.

At each trial, the participant received three stimuli. The time interval between the stimuli is 0.8 s. The order of the stimuli was randomized. Two stimuli were the same as the original stimuli, while the other one was a reproduced stimulus. After receiving the three stimuli, the participants would identify those stimuli that were different from the

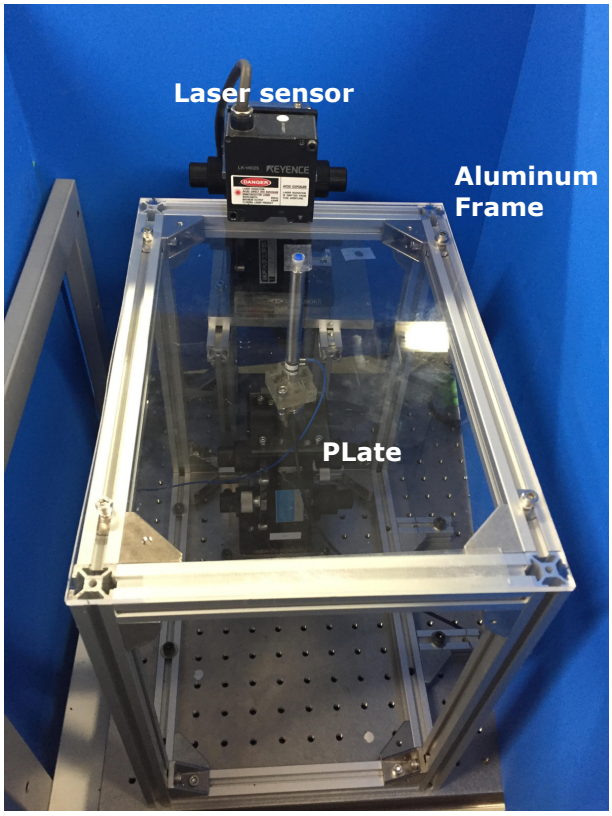


Figure 3.4: Experimental apparatus: A participant presses their index finger pad on the contact part of the actuator and rests their hand on the plate to stabilize the contact with the actuator.

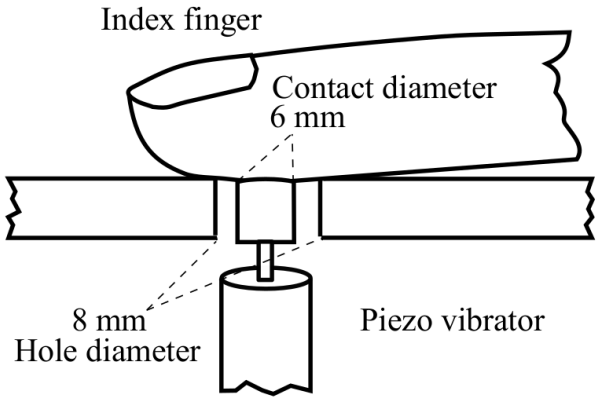


Figure 3.5: Contact part between the index finger pad and the piezo vibrator

others. After every 100 trials, the participants rested for five to ten minutes.

Before the experiment, a double-sided adhesive was applied around the hole of the plate. The participants were instructed to press the center of their index finger pad through the hole to bind their finger to it, and then relax their hand on the plate. The lab jack that held the actuator was lifted slowly through the hole on the plate to reach the finger pad. Its height was adjusted until the expected contact force of 0.5 N between the

finger and the actuator was obtained. After every 100 trials, the double-sided adhesive was replaced and the contact force readjusted. Before the experiment, the participants completed 60 trials (two times of the 30 combinations) to familiarize themselves with the experimental procedure.

## 3.6 Results

Each figure from Figure 3.6 to Figure 3.11 shows the correct answer ratio between the original AM vibration and its reproduced vibration under five segment ratios ($r_s$ = 1/6, 1/5, 1/4, 1/3, and 1/2 ). For each type of the original AM vibration, the discrimination ratio appears to be affected by the segment ratio, $r_s$.

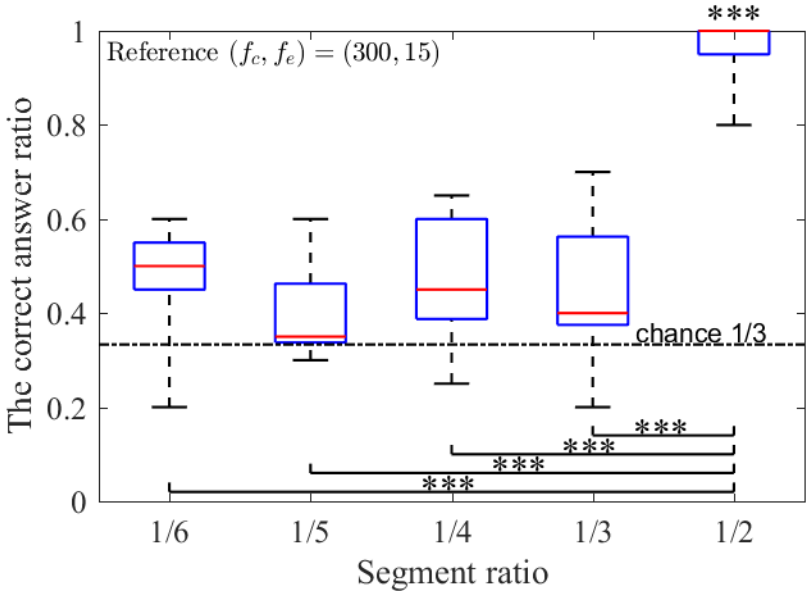


Figure 3.6: Relationships between the discrimination ratio and the segment ratio under different combinations of the carrier and envelope frequencies

We analyzed the differences among the discrimination ratios and chance level 1/3. The Kolmogorov–Smirnov test was applied to 30 conditions (six original AM vibrations × five segment ratios) to test the normality of distribution. The result of the test revealed that all 30 conditions had normal distributions. Therefore, we used the one-way ANOVA and post-hoc analysis (the Tukey–Kramer test) for analyzing data.

Firstly, the results of one-way ANOVA and post-hoc analysis revealed significant differences between the discrimination ratio at the segment ratio ($r_s$ = 1/2) and chance level 1/3, with all six original AM vibrations ($p < 1.0 \times 10^{-7}$). It further showed that the conventional intensity-based model could not represent perceptually similar vibrations for original AM vibrations.

Next, no significant differences were observed between the four segment ratios ($r_s$ = 1/6, 1/5, 1/4, and 1/3) and chance level ($p > 0.05$), except the condition (($f_c$, $f_e$, $r_s$) = (300, 30, 1/4)) and the condition (($f_c$, $f_e$, $r_s$) = (600, 15, 1/3)), and the p-values are

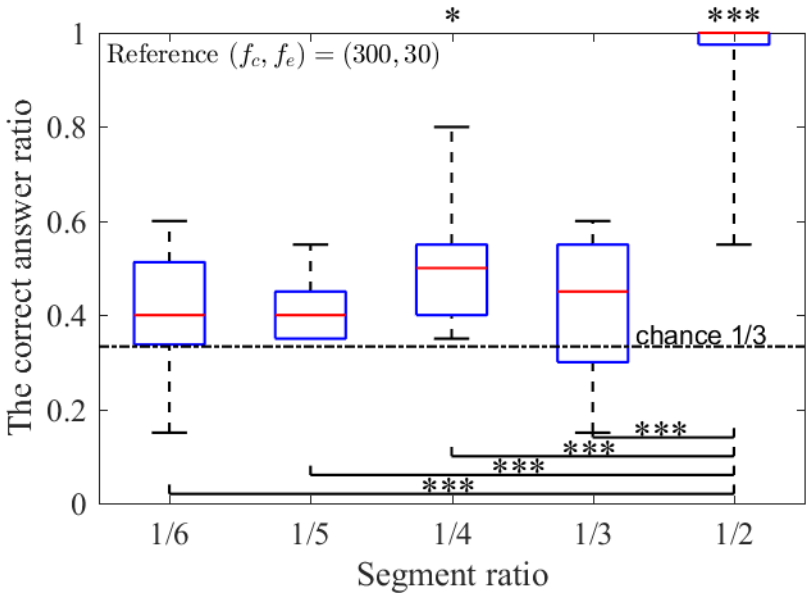


Figure 3.7: Relationships between the discrimination ratio and the segment ratio under different combinations of carrier and envelope frequencies

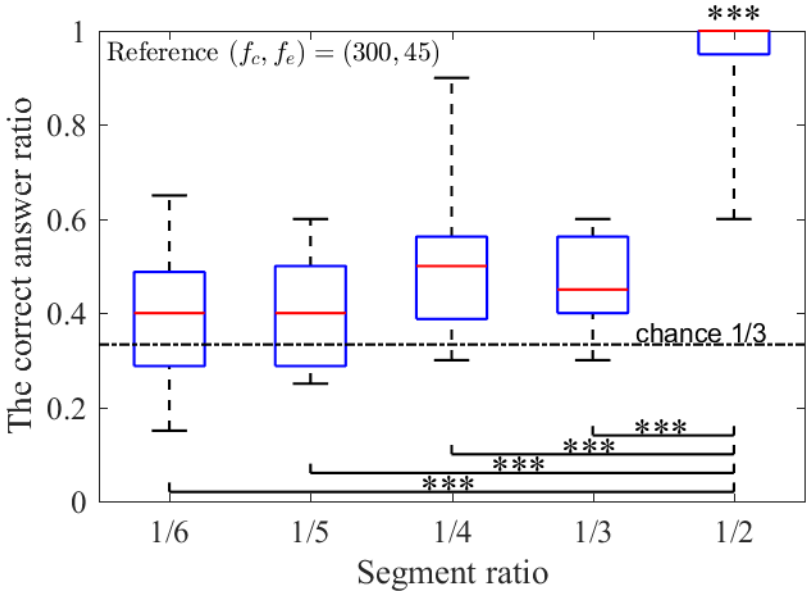


Figure 3.8: Relationships between the discrimination ratio and the segment ratio under different combinations of carrier and envelope frequencies

0.0381 and 0.0004, respectively. In addition, the discrimination ratios at the four segment ratios ($r_s = 1/6, 1/5, 1/4$, and $1/3$) are significantly smaller than that at $r_s = 1/2$, in all original AM vibrations ($p < 1.0 \times 10^{-6}$). The participants mostly had low discrimination ratios, which were near the chance level, in the segment conditions except $r_s = 1/2$. While the high-resolution envelope step ($r_s = 1/6$) demonstrated the highest degree of similarity among the six segment ratios, the lower-resolution ($r_s = 1/3$) could deliver the sensation that was relatively similar to the sensation of the original AM vibration.

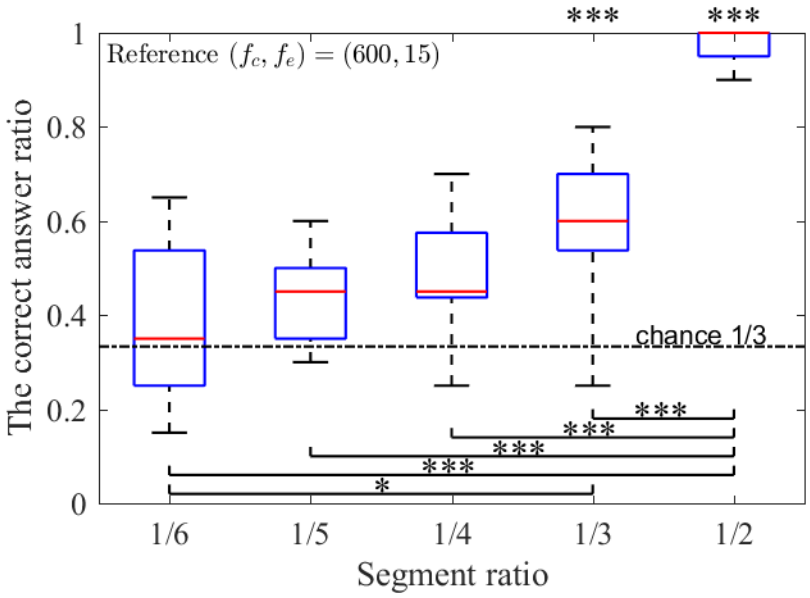


Figure 3.9: Relationships between the discrimination ratio and the segment ratio under different combinations of carrier and envelope frequencies

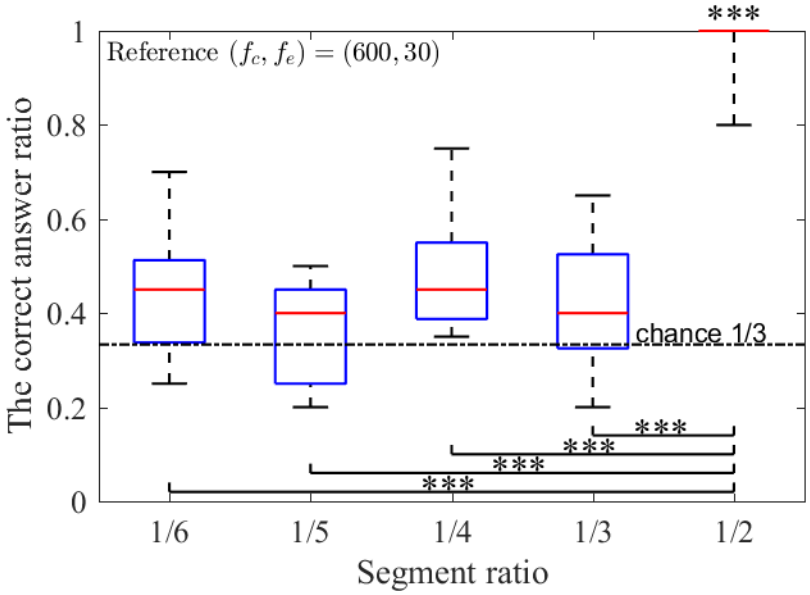


Figure 3.10: Relationships between the discrimination ratio and the segment ratio under different combinations of carrier and envelope frequencies

The results suggest that the time-segmented, intensity-based model could reproduce perceptually similar vibrations for the AM vibrations, when compared with the conventional intensity-based model. Furthermore, it was found that a small segment number of the envelope period ($r_s = 1/3$) could reproduce a similar perception of the AM vibration.

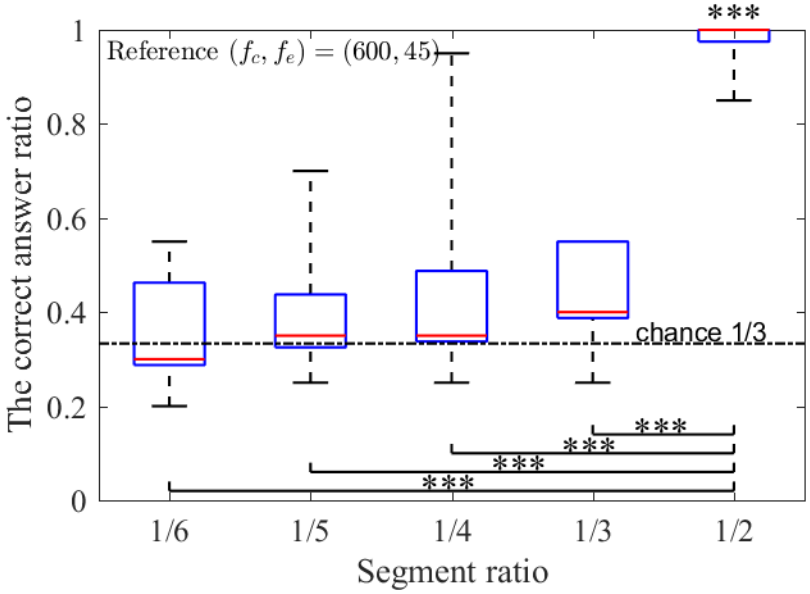


Figure 3.11: Relationships between the discrimination ratio and the segment ratio under different combinations of carrier and envelope frequencies

## 3.7 Discussion

The first finding detailed of the study in this chapter was the participants could discriminate easily between the flat sinusoidal vibration ($r_s = 1/2$) and the original AM vibration, even if the energy of the two vibrations were constant. The mean discrimination rates for the $r_s = 1/2$ case on each condition of the six types of original vibrations were higher than 0.9. On the other hand, other segment ratios ($r_s = 1/3, 1/4, 1/5$, and $1/6$) had a relatively low mean of the discrimination ratios ($< 0.51$), except for the condition of ($f_c$, $f_e$, $r_s$) = (600, 15, 1/3) whose mean ratio is 0.59. These suggest that the time-segmented, intensity-based modulation could possibly reproduce similar stimuli at the segment ratios ($r_s = 1/3, 1/4, 1/5$, and $1/6$). These results were not unexpected because several researchers have already reported that humans can detect the envelopes of the high-frequency vibrations modulated by a low frequency envelope [31, 32, 39]. However, the present study confirmed experimentally that the conventional intensity-based model could not explain the slow varying envelope sensation of high-frequency vibrations, and proposed the time-segment analysis as a potential solution.

It should be noted that our motivation was not to critique the conventional models. These models avoided the effects of low-frequency components for a good reason to assess the Pacinian system [30], and several studies have already addressed the possible relationship between the envelope detection and the RA system [29, 59, 32].

The second interesting finding was that the segment size did not strongly affect the discrimination ratio between the original waves and the reproduced waves. We expected a trend where the discrimination rates would increase when the segment ratios increase (seg-

ment duration decreases). However, the experimental results did not reveal any such tendency. Surprisingly, even a single-step vibration ($r_s = 1/3$) could reproduce the similar perception to some degree, except for the ($f_c$, $f_e$) = (600, 15) condition. The intensity of high-frequency vibration was maintained in this experiment, and the results suggested that the envelope property of AM vibrations might be perceived with simpler features, such as the number of peaks in the envelope, rather than the high resolution of time segmentation. A possible implication of this simple feature detection is the function of the RA system, which is activated corresponding to the onset and offset of skin deformation. If the time-segmented, step-wise vibration could generate similar skin deformation, the RA system could detect similar information.

An exception to the condition of ($f_c$, $f_e$, $r_s$) = (600, 15, 1/3) requires further investigations of the effects of segment durations. This condition had a relatively high mean discrimination ratio (0.59). Figure 3.9 shows that there is a marginal increase in the correct answer ratio as the segments ratio increase. There is also a significant difference between the correct ratios at segment ratios $r_s = 1/6$ and $r_s = 1/3$, respectively. In [5], Lim et al. found that low-frequency envelope detection threshold increased with the carrier frequency. Our results demonstrated the same trend when comparing the conditions ($f_c$, $f_e$) = (300, 15, 1/3) and ($f_c$, $f_e$) = (600, 15, 1/3). As shown in Figure 3.3, both the $r_s = 1/3$ and $r_s = 1/4$ conditions have a similar single-step waveform but different durations. We need to investigate if the differences could be explained by the Pacinian or Meissner representations in future studies.

## 3.8 Limitation of the study

One of the limitations of this study is the application of a simple intensity-model that did not consider the frequency effect on the sensation of the Pacinian system [28, 30, 4]. In this chapter, such a dependency has been shown to not have a significant impact on the results because the same carrier frequency combinations for the discrimination tests were used. For applying the time-segment, intensity-based model for general waveforms, the effects of carrier frequency on human perception should be considered. Another limitation was the measurement of the waves of the stimuli without the finger exerting a force, because the actual waves may change when the subject exerts a force on the actuator. The changes of the waves may lead to different sensations. The displacements of the sinusoidal waves before and after the exertion of force by the finger was measured using an accelerometer, as shown in Figure 3.12. Figure 3.13 shows the different ratios of amplitude of the sinusoidal waves of the carrier frequency from 200–700 Hz. The results showed a different ratio (600 Hz) larger than the one at 300 Hz. In our experiment, we adopted the carrier frequencies of 300 Hz and 600 Hz. The results did not show a significant difference between the results at a carrier frequency of 300 Hz and those at a carrier frequency of 600 Hz in all the conditions using the one-way ANOVA analysis.

An example is shown in Figure 3.14, comparing the results at the condition ($f_c$, $f_e$, $r_s$) = (300, 15, 1/6) and those at ($f_c$, $f_e$, $r_s$) = (600, 15, 1/6)—no significant difference was detected. The results indicate that even the waves were changed by the pressing force, the effect of the carrier frequency on sensations were only marginal, and we could neglect the difference.

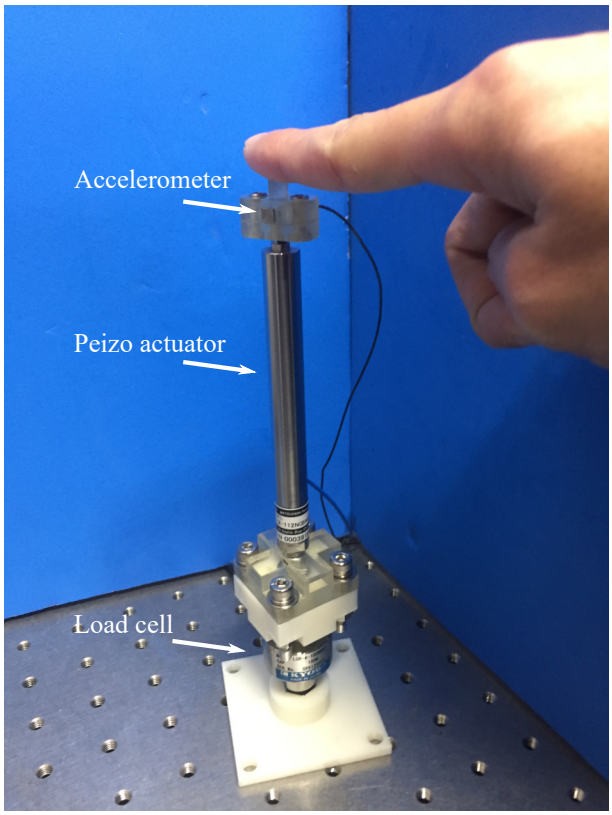


Figure 3.12: Measurement of the wave of stimuli by the accelerometer when the actuator was pressed with a constant force of 0.5 N

## 3.9 Summary

The intensity of the high-frequency vibration (> 100 Hz), which is generally regarded as the integration of stimulus intensity over time or spectral power summed across all frequencies, has been focused as a primary cue to convey the vibrotactile information perceived by the Pacinian Corpuscle. Several researchers have reported that humans could detect the low-frequency envelope of a high-frequency vibration modulated at low frequencies. A missing argument for the intensity-based model is the determination of the adequate time duration to integrate the intensity of the stimulus, to account for the relatively slow time-variant vibration patterns. We introduced a time-domain segment to the intensity-based perception model. In particular, we investigated the ability of a person to discriminate the reproduced time-segmented waveform, which has the same intensity as that of the original vibration on each segment, as a pilot study to determine the suitable segment size for the intensity-based modulation. This study targets the

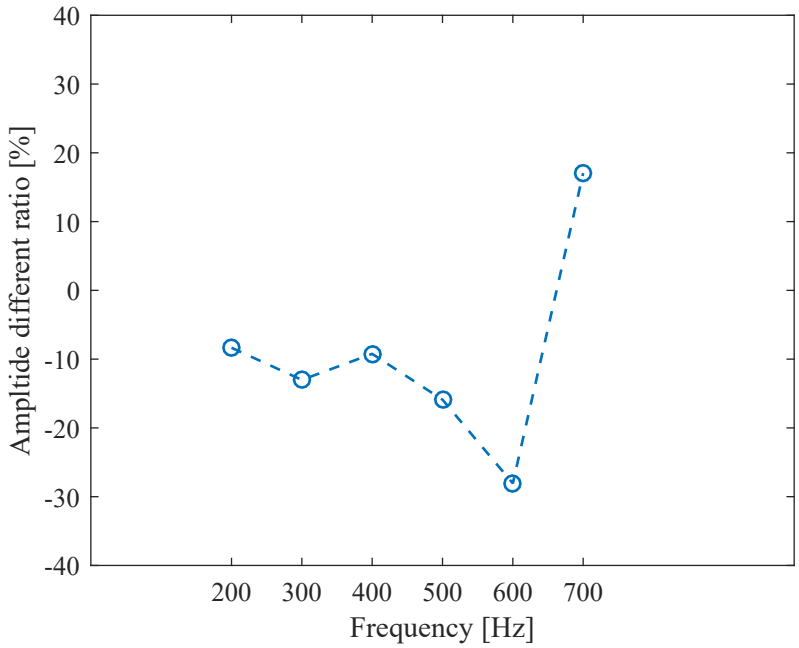


Figure 3.13: Different ratios of the amplitude of waves were measured with the accelerometer when the finger was pressing on the actuator compared to the generated wave without contact force

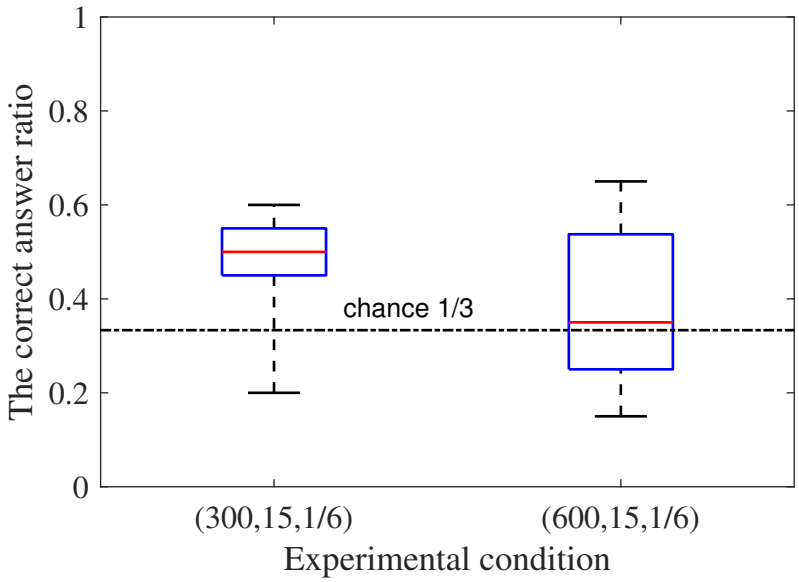


Figure 3.14: Compared results between the conditions ($f_c$, $f_e$, $r_s$) = (300, 15, 1/6) and ($f_c$, $f_e$, $r_s$) = (600, 15, 1/6). No significant difference was observed.

amplitude-modulated (AM) high-frequency vibrations (carrier frequency $f_c$ = 300 or 600 Hz) that have relatively low envelope frequencies ($f_e$ =15, 30, or 45 Hz).

The results suggested that the time-segmented intensity-based model could reproduce perceptually similar waves modulated from the original AM waves. On the contrary, the conventional intensity-based model could not represent perceptually similar vibrations

for AM vibrations of low-frequency envelope. No significant differences could be observed between the four segment ratios ($r_s$ = 1/6, 1/5, 1/4, and 1/3) and chance level ($p > 0.05$), except for the condition (($f_c$, $f_e$, $r_s$) = (300, 30, 1/4)), and the condition (($f_c$, $f_e$, $r_s$) = (600, 15, 1/3)), and their p-values are 0.0381 and 0.0004, respectively. In addition, the discrimination ratios of the four segment ratios ($r_s = 1/6, 1/5, 1/4$, and 1/3) were significantly smaller than that of $r_s$ = 1/2, in all the original AM vibrations ($p < 1.0 \times 10^{-6}$). We a small segment ratio ($r_s = 1/3$) could reproduce the perceptually similar stimuli to the original AM vibrations in most of the conditions. The results also suggested that the peaks of the envelope played an important role in maintaining a similar sensation by modulation.

# Chapter 4

# Dependence of Perceptual Discrimination of High-frequency Vibration on Envelope and Intensity Properties of Waveform

## 4.1 Introduction

To provide relevant haptic information to users, it is important to understand which high-frequency vibration factors, such as the frequency, amplitude, or envelope, form the tactile perception, including similarity, roughness, strength, etc., and how. High-frequency vibration induced by scratching or tapping surfaces has been reported as a cue for roughness or hardness perception [33, 22, 19, 54]. Thus, the transmission of high-frequency vibrations has been attempted in support of telerobotic surgery [55] and delivering realistic textures [56, 57]. To render tactile vibrations, many applications have employed AM and/or frequency-modulated (FM) vibrations are used in many applications, and the authors in [34] had leveraged the modulated vibration to render texture to a contact surface. In addition, image-based tactile vibration using modulated vibration to render different contact surfaces on a flat tablet [35] is another example of such successful efforts. Vibration patterns can be used to present various notifications [60]. For example, decaying sinusoidal waves applied to the skin have been used to indict the roughness or collisions in a virtual environment [24, 33]. Vibration patterns are widely used for tactile generation in VR environments [34] to support the teleoperation of robots [36, 37]. Takenouchi et al., [21] extracted the envelope of a high-frequency vibration, for which the carrier frequency was above the range of human perception.

The intensity of a high-frequency vibration (i.e., above 100 Hz), which is generally defined as the integral of stimulus intensity over time or the spectral power summed across all frequencies, has been identified as a primary cue in the perception of vibrotactile infor-

mation perceived by the Pacinian system [28, 29, 30, 4]. Makous et al. [28] found that the intensity model, which is a function of the spectral power divided by the threshold power, constitutes a measure of the ability to excite a Pacinian system. Bensmaia et al. [30] developed a spectral model that improved on the intensity model by adding spectral characteristics based on psychophysical and neurophysiological findings. In addition, they also applied the spectral model to finely textured stimuli to infer perceptual dissimilarities [4].

However, these intensity models are insufficient when interpreting the perception of the envelope of high-frequency vibrations. For example, in the above model, two sinusoidal waves with slightly different frequencies will be perceived almost identically. If two vibrations are simultaneously generated at the same point, a subject could perceive the beats frequency and even count the number of beats when the new superimposed waveform has a very slow envelope frequency. Lim et al. [5] found that humans can perceive beats in the envelope frequencies from 2.5 to 10 Hz, and the ratio between the beats detection threshold $AT_B(f)$ and amplitude thresholds $AT(f)$ decreases from 20 to 1.25 as the carrier frequency increases from 63.1 Hz to 398 Hz. The results indict the beats can be perceived for very low envelope frequencies and tend to move closer to the $AT$ value as $f_c$ increases. Humans can perceive an AM sinusoidal vibration even when the carrier frequency is above the range they can perceive [31, 32], which suggests that humans may perceive the low-frequency envelope of high-frequency vibrations. Park et al.[39] found that AM vibrations at a very high envelope frequency are similar to sinusoidal vibration ($f_e = 0$), which suggests that when the envelope frequency is high, the beats cannot be perceived and the waveform is therefore perceptually similar to the vibrations without an envelope frequency. Once these results were obtained, Park et al. did not investigate the boundary and intensity effects. Humans have different types of receptors, in which Meissner corpuscles and Pacinian corpuscles are sensitive to the vibrations. Meissner corpuscles are sensitive to the low-frequency vibrations while Pacinian corpuscles are sensitive to the high-frequency vibrations. Meissner or Pacinian exhibit a crossing band near 40 Hz. This thesis poses the question of whether a human can still perceive the envelope when its frequency is high.

The intensity and envelope of a waveform affect the ability of humans to discriminate the high-frequency vibration. However, the associated mechanism describing how envelope perception and intensity are related has not yet been elucidated. It is anticipated that an improved understanding of their effects will assist in the designing of vibration devices for haptic applications in vibration rendering and communications.

The objectives of this study were to identify the possible boundary of perception of the envelope and intensity, and to assess how the two parameters affect the ability of humans to discriminate high-frequency vibrations. By knowing the range of the boundary, we could just maintain the perceivable envelope whose frequency is less than the boundarys, while the carrier frequency could be reduced to maintain the envelope shape. A lower

carrier frequency could reduce the difficulties of generating the high-frequency vibration and reduce the sound of the vibration when using a lower frequency carrier by modulation. To accomplish these objectives, we conducted psychophysical experiments using AM vibrations of different frequencies and intensities. By comparing AM vibrations with sinusoidal vibrations at different intensities, we identified the similarity and differences between them, and by comparing the vibrations of same and different envelopes with one another, we evaluated the effect of the envelope on perception. Then, by comparing stimuli at different intensities, we investigated the effect of intensity on perception. In addition, we examined the effects of carrier frequency on the ability to discriminate.

## 4.2 Objectives of the Chapter

The objectives of this study were to identify the possible boundary of perception of the envelope and intensity, and investigate the carrier frequency and intensity effects on the ability of humans to discriminate high-frequency vibrations. To accomplish this, we conducted psychophysical experiment using the AM vibration of different envelope frequencies and intensities. By comparing the AM vibration with the sinusoidal vibration at different intensity conditions, we will find how the similarity will vary. By comparing the vibrations of same and different envelopes with one another, we will investigate the envelope effect on the perception.

## 4.3 Significance of the Study

In the teleoperation of a construction machine [21], one of the modulation procedures is to extract the envelope. However, we do not know which envelope frequency range is suitable for maintaining. By knowing the perceivable envelope frequency range, the envelope whose frequency is lower than the boundary could be preserved and a relatively lower carrier could be used for the modulation. A lower frequency carrier could be used to maintain the envelope sensation as shown in Figure 1.11. It may contribute to reducing the difficulties of generating the high-frequency vibrations and reducing the sound of the vibration.

## 4.4 Beats and Envelope Perception

A human can perceive the envelope of high-frequency vibrations. Two sinusoidal waves with slightly different frequencies will have undistinguished perception. However, if the two vibrations are generated at the same point simultaneously, it induces the beats phenomenon, and a subject can perceive the beats and even count the number of beats when the waveform has a very slow envelope frequency. In [5], Lim et al. found that a human can perceive the beat for an envelope frequency from 2.5 Hz to 10 Hz (higher envelope frequency was not investigated). The ratio between the beats detection threshold, $AT_B(f)$, and an amplitude threshold, $AT(f)$, is from 20 to 1.25 with the carrier frequency

Table 4.1: Coefficients of the Psychophysical Intensity Model [6]

| Coefficient index (i) | 0 | 1 | 2 | 3 | 4 |
|---|---|---|---|---|---|
| $\alpha_i$ | -0.8592 | 1.9688 | -1.5739 | 0.5419 | -0.0682 |
| $\beta_i$ | 39.6979 | -90.4316 | 75.0109 | -27.0254 | 3.5759 |

increasing from 63.1 Hz to 398 Hz. The results showed that the beats could be perceived even with a very low envelope frequency and become closer to the $AT$ value as the $f_c$ increases. In [39], Park et al., found that AM vibrations of high envelope frequencies are close to sinusoidal vibrations ($f_e == 0$). The results suggest that the when the envelope frequency is high, the beat perception is not clear and is perceptually similar to the vibration without an envelope frequency.

## 4.5 Related Intensity Models

### 4.5.1 Power Intensity Model

The relation between physical stimuli and sensation is often expressed by Stevens power law [61]. We show the power intensity model [62] of the vibration.

$$I\left(f\right) = k[\phi]^{\beta(f)} \tag{4.1}$$

where $\phi$ is the objective magnitude of the waveform, $\phi = 20\log_{10}(A)$, the unit of amplitude, $A$, is 1 $\mu m$, $I(f)$ is the perceived intensity or subjective magnitude of the sinusoidal wave of frequency, $f$. $a(f)$ is the exponent parameter, which is a scale of the intensity related to frequency $f$.

This power law may also be expressed by the following function,

$$I\left(f\right) = k[\phi - \phi_0]^{\beta(f)}, \tag{4.2}$$

where $\phi_0$ representing the $AT$ of the wave, $\phi_0 = 20\log_{10}(AT(f))$, where $AT(f)$ is the amplitude threshold of the sinusoidal wave of frequency $f$.

### 4.5.2 Mobile Intensity Model

In [6]the intensity model of the vibration on mobile devices is shown as following function,

$$\log I(f) = 20\log_{10}\left(\frac{A}{AT(f)}\right)\sum_{i=0}^{4}\alpha_i\left(\log_{10}F\right)^i + \sum_{i=0}^{4}\beta_i\left(\log_{10}F\right)^i \tag{4.3}$$

where $A$ is the amplitude of the waveform, $f$ is the frequency, $AT(f)$ is the amplitude threshold, which is related to frequency $f$, and $\alpha_i$ and $\beta_i$ are the fitting parameters. The best-fit $\alpha_i$ and $\beta_i$ are given in Table 4.1.

### 4.5.3 Spectral Intensity Model

In [30]the intensity model of vibration with one to three frequency components on the finger is represented by following function,

$$I = \left[ \left( \frac{A}{AT(f)} \right)^2 \right]^{a(f)}, \tag{4.4}$$

where $A$ is the amplitude of the waveform, $f$ is the frequency, $AT(f)$ is the amplitude threshold, which is related to frequency $f$, and $a(f)$ is exponent parameter, which is a scale of the intensity related to frequency $f$.

In [30]Bensmaia et al. developed the spectral intensity model to a spectral mini-channel model. This mini-channel model has a lot of mini-channels based on the frequency. Each response of the mini-channel is characterized by Gaussian filter with the center frequency, $f_c$, and standard deviation, $\alpha f_c$. The intensity of a single channel (center frequency $f_c$) is described by the following function,

$$Z_s(f_c) = \sum_f I(f) e^{-\frac{(f-f_c)^2}{2(\alpha f_c)^2}}. \tag{4.5}$$

## 4.6 Methods

### 4.6.1 Amplitude-modulated vibration

In this study, we employed the AM vibrations to investigate the effects of intensity and envelope on human perception. The following equation was used to describe the AM vibrations,

$$q(t) = env(t) * \cos(2\pi f_c t), \tag{4.6}$$

where $env(t)$ is an envelope waveform and $f_c$ is the carrier frequency.

The following equation is used to express one type of AM vibration:

$$q(t) = A\left(0.5 + 0.5sin(2\pi f_e t - \frac{\pi}{2})\right) sin(2\pi f_c t) \tag{4.7}$$

where $A$ is the amplitude, $f_e$ is the envelope frequency, and $f_c$ is the carrier frequency.

This waveform can also be presented as:

$$\begin{aligned} q(t) =& 0.5A\sin(2\pi f_c t) + 0.25A\sin\left(2\pi\left(f_e - f_c\right)t\right) \\ & - 0.25A\sin\left(2\pi\left(f_e + f_c\right)t\right) \end{aligned} \tag{4.8}$$

From Eq. 4.7, the vibration is made up of an envelope signal, a carrier signal, and three sinusoidal waves.

Table 4.2: Amplitude thresholds and exponents of the sinusoidal waves for the different frequencies

| $f$ [Hz] | $AT(f)$ [$\mu$m] | Exponent $a(f)$[4] |
|---|---|---|
| 100 | 0.25 | 0.65 |
| 150 | 0.17 | 0.6 |
| 200 | 0.18 | 0.51 |
| 300 | 0.18 | 0.52 |
| 400 | 0.20 | 0.34 |

### 4.6.2 Stimuli

In this experiment, the stimuli are defined by Eq. 4.7 and each consists of a combination of three parameters, namely, the amplitude $A$, carrier frequency $f_c$, and envelope frequency $f_e$. The related intensity parameters, which consist of the frequency $f$, amplitude threshold $AT(f)$, and exponent $a(f)$ of the sinusoidal waves, are shown in Table 4.2. The amplitude threshold (AT) of the sinusoidal waves was measured via psychophysical experiments, which applied the 1-up 2-down staircase method as per the three-interval forced-choice procedure. The experiment involved five subjects, and the mean values of the results are shown in Table 4.2.

For the $AT(f)$, values of $AT(f)$ were fit using the following equation based on the ATs in Table 4.2,

$$\log(AT(f)) = a + be^{-\frac{(f+c)^2}{d}}, \tag{4.9}$$

The AT(f) values after fitting are shown in Figure 4.1.

The values of $a(f)$ were fit using the following equation based on the values of $a(f)$ listed in Table 4.2:

$$a(f) = kf + c, \tag{4.10}$$

where $a(f)$ is the exponent parameter with a unit response (1 dB). The $a(f)$ after fitting are shown in the Figure 4.2.

Using these parameters, the spectral intensity model was applied to evaluate the intensity of the vibration. Tables 4.3 to 4.5 list the parameters of the stimuli, including carrier frequency $f_c$, envelope frequency $f_e$, and intensity $I$. The intensity, $I$, was calculated as follows,

$$I = I(f_c) + I(f_c - f_e) + I(f_c + f_e). \tag{4.11}$$

Table 4.3: Stimuli parameters: Pairs of stimuli comparing different intensities of sinusoidal and AM waveforms, when $I_1 = I_2$

| Num | $I_1$ | $f_{c1}$ | $f_{e1}$ | $I_2$ | $f_{c2}$ | $f_{e2}$ |
|---|---|---|---|---|---|---|
| 1 | 25 | 300 | 0 | 25 | 300 | 12 |
| 2 | 25 | 300 | 0 | 25 | 300 | 20 |
| 3 | 25 | 300 | 0 | 25 | 300 | 32 |
| 4 | 25 | 300 | 0 | 25 | 300 | 50 |
| 5 | 25 | 300 | 0 | 25 | 300 | 80 |
| 6 | 25 | 300 | 0 | 25 | 300 | 125 |
| 7 | 50 | 300 | 0 | 50 | 300 | 12 |
| 8 | 50 | 300 | 0 | 50 | 300 | 20 |
| 9 | 50 | 300 | 0 | 50 | 300 | 32 |
| 10 | 50 | 300 | 0 | 50 | 300 | 50 |
| 11 | 50 | 300 | 0 | 50 | 300 | 80 |
| 12 | 50 | 300 | 0 | 50 | 300 | 125 |
| 13 | 75 | 300 | 0 | 75 | 300 | 12 |
| 14 | 75 | 300 | 0 | 75 | 300 | 20 |
| 15 | 75 | 300 | 0 | 75 | 300 | 32 |
| 16 | 75 | 300 | 0 | 75 | 300 | 50 |
| 17 | 75 | 300 | 0 | 75 | 300 | 80 |
| 18 | 75 | 300 | 0 | 75 | 300 | 125 |

Table 4.4: Stimuli parameters: Stimuli pairs comparing sinusoidal and AM waves of different carrier frequencies $f_{c1} \neq f_{c2}$

| Num | $I_1$ | $f_{c1}$ | $f_{e1}$ | $I_2$ | $f_{c2}$ | $f_{e2}$ |
|---|---|---|---|---|---|---|
| 19 | 50 | 300 | 0 | 50 | 400 | 12 |
| 20 | 50 | 300 | 0 | 50 | 400 | 20 |
| 21 | 50 | 300 | 0 | 50 | 400 | 32 |
| 22 | 50 | 300 | 0 | 50 | 400 | 50 |
| 23 | 50 | 300 | 0 | 50 | 400 | 80 |
| 24 | 50 | 300 | 0 | 50 | 400 | 125 |
| 25 | 50 | 400 | 0 | 50 | 400 | 12 |
| 26 | 50 | 400 | 0 | 50 | 400 | 20 |
| 27 | 50 | 400 | 0 | 50 | 400 | 32 |
| 28 | 50 | 400 | 0 | 50 | 400 | 50 |
| 29 | 50 | 400 | 0 | 50 | 400 | 80 |
| 30 | 50 | 400 | 0 | 50 | 400 | 125 |

Table 4.5: Stimuli parameters: stimuli pairs comparing AM waves with different carrier frequencies $f_{c1} \neq f_{c2}$ and different intensity levels.

| Num | $I_1$ | $f_{c1}$ | $f_{e1}$ | $I_2$ | $f_{c2}$ | $f_{e2}$ |
|---|---|---|---|---|---|---|
| 31 | 25 | 300 | 12 | 25 | 400 | 12 |
| 32 | 25 | 300 | 20 | 25 | 400 | 20 |
| 33 | 25 | 300 | 32 | 25 | 400 | 32 |
| 34 | 25 | 300 | 50 | 25 | 400 | 50 |
| 35 | 25 | 300 | 80 | 25 | 400 | 80 |
| 36 | 25 | 300 | 125 | 25 | 400 | 125 |
| 37 | 50 | 300 | 12 | 50 | 400 | 12 |
| 38 | 50 | 300 | 20 | 50 | 400 | 20 |
| 39 | 50 | 300 | 32 | 50 | 400 | 32 |
| 40 | 50 | 300 | 50 | 50 | 400 | 50 |
| 41 | 50 | 300 | 80 | 50 | 400 | 80 |
| 42 | 50 | 300 | 125 | 50 | 400 | 125 |
| 43 | 75 | 300 | 12 | 75 | 400 | 12 |
| 44 | 75 | 300 | 20 | 75 | 400 | 20 |
| 45 | 75 | 300 | 32 | 75 | 400 | 32 |
| 46 | 75 | 300 | 50 | 75 | 400 | 50 |
| 47 | 75 | 300 | 80 | 75 | 400 | 80 |
| 48 | 75 | 300 | 125 | 75 | 400 | 125 |

Table 4.6: Stimuli parameters: Stimuli pairs comparing AM waves with same envelope frequencies, $f_{e1} = f_{e2}$, and different intensities, $I_1 \neq I_2$.

| Num | $I_1$ | $f_{c1}$ | $f_{e1}$ | $I_2$ | $f_{c2}$ | $f_{e2}$ |
|---|---|---|---|---|---|---|
| 49 | 50 | 300 | 12 | 25 | 300 | 12 |
| 50 | 50 | 300 | 20 | 25 | 300 | 20 |
| 51 | 50 | 300 | 32 | 25 | 300 | 32 |
| 52 | 50 | 300 | 50 | 25 | 300 | 50 |
| 53 | 50 | 300 | 80 | 25 | 300 | 80 |
| 54 | 50 | 300 | 125 | 25 | 300 | 125 |
| 55 | 50 | 300 | 12 | 75 | 300 | 12 |
| 56 | 50 | 300 | 20 | 75 | 300 | 20 |
| 57 | 50 | 300 | 32 | 75 | 300 | 32 |
| 58 | 50 | 300 | 50 | 75 | 300 | 50 |
| 59 | 50 | 300 | 80 | 75 | 300 | 80 |
| 60 | 50 | 300 | 125 | 75 | 300 | 125 |

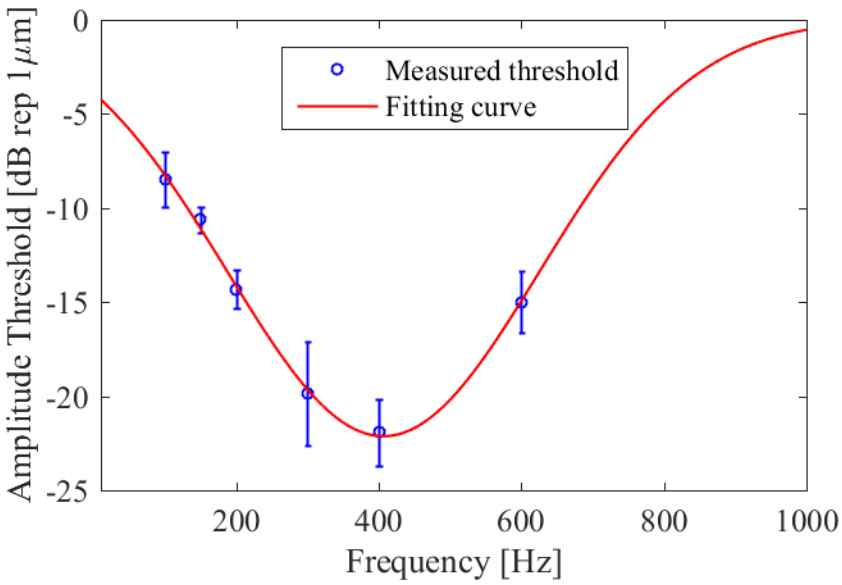


Figure 4.1: Interpolated amplitude threshold ($AT$) based on experimental measurements of the five subjects listed in Table 4.2. The results are denoted by the blue circles with a standard error of mean (SEM). The interpolated curve is described by $\log(AT(f)) = a + be^{-\frac{(f+c)^2}{d}}$, in which $a, b, c$ and $d$ were the fitting parameters.

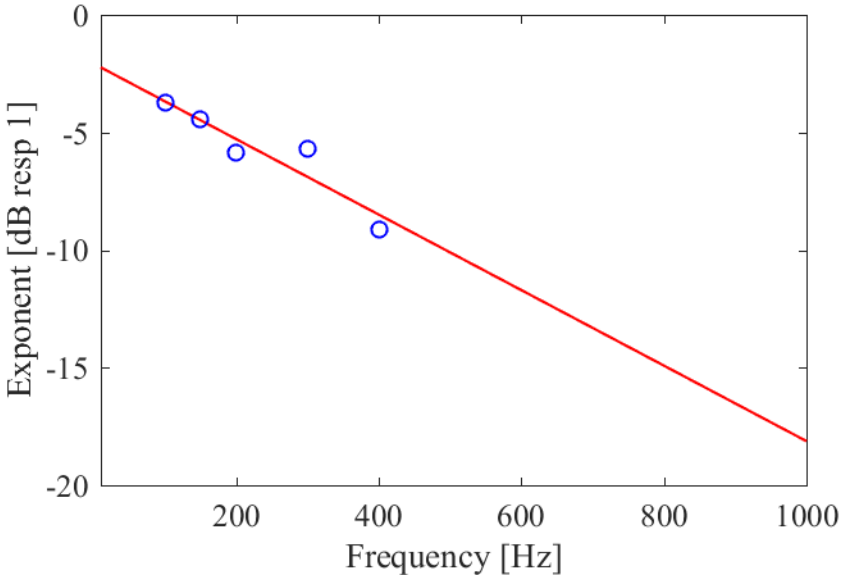


Figure 4.2: Exponent $a(f)$ [4] fitted using values listed in Table 4.2. The results are indicated by the blue circles. The fitting curve was based on the equation, $a(f) = kf + c$, in which $k$ and $c$ were the fitting parameters.

The experiment was based on three levels of intensities: $I = 25$, 50, and 75. To determine the displacement profiles of the stimuli, the displacement of the piezoelectric vibrator tip was measured using a laser displacement sensor (LK-H025, KEYENCE Corporation). The displacement was measured without a finger on the actuator. Some examples of the stimuli are shown in Figure 4.3. Because of the large push and pull forces (800 N and 50 N,

respectively) of the actuator, it was assumed that the vibratory waveform did not change significantly between the preliminary measurements, in which there was no contact force and the experiment during which the participants press their fingers on the actuator to exert a force of 0.5 N as instructed.

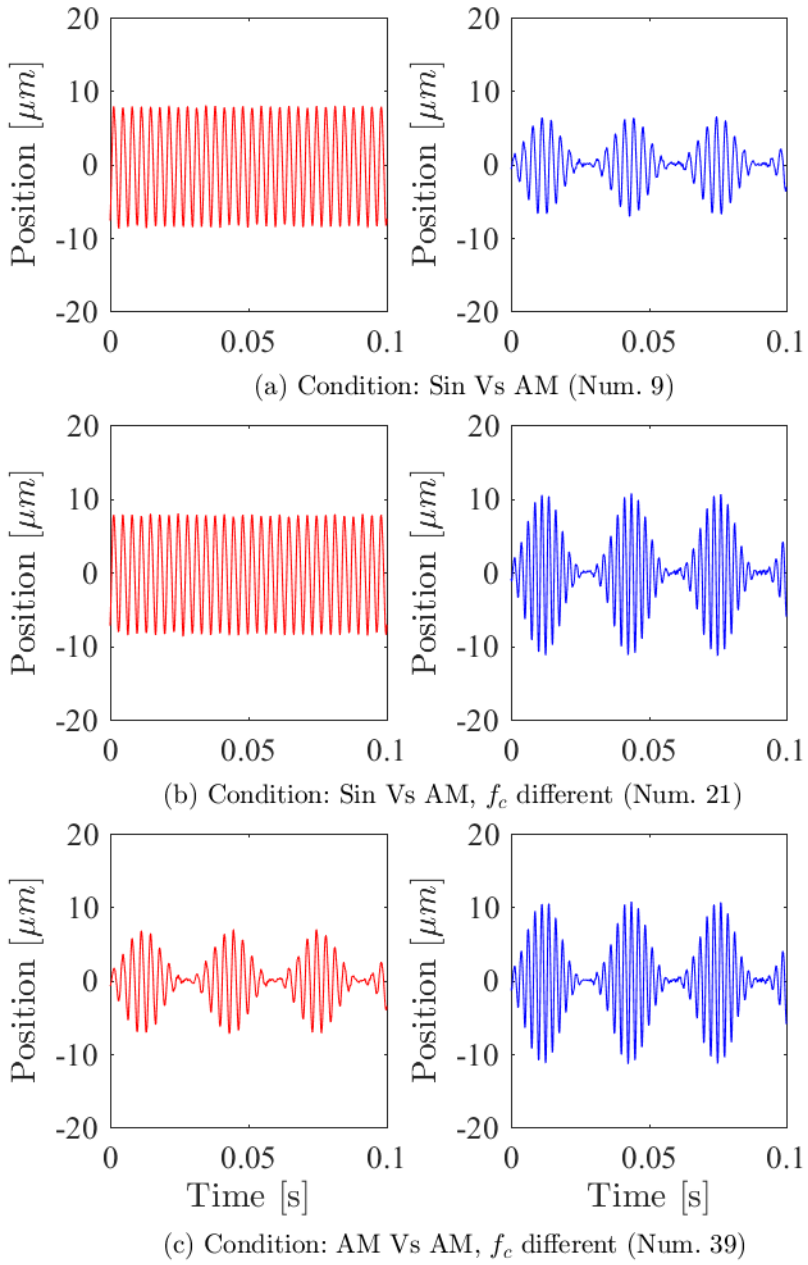


(a) Condition: Sin Vs AM (Num. 9)

(b) Condition: Sin Vs AM, $f_c$ different (Num. 21)

(c) Condition: AM Vs AM, $f_c$ different (Num. 39)

Figure 4.3: Examples of stimuli waves measured by the laser sensors. (a) Stimuli pair number 9 on the Table 4.3; (a) Stimuli pair number 21 on the Table 4.4; (c) Stimuli pair number 39 on the Table 4.5;

### 4.6.3 Apparatus

The experimental apparatus is shown in Figure 4.4, in which a tactile high-frequency vibration is generated by a piezo actuator (PZ12-112, Matsusada Precision) with push and pull forces of 800 N and 50 N, respectively. The subjects finger contacts the actuator through a 9-mm diameter hole in the plate. The diameter of the point of contact is 6 mm. The actuator is connected to a load cell (LUR-A-100NSA1, Kyowa Electronic Instruments) to measure the contact force, which is typically 0.5 N, between the actuator and a finger pad of a participant. The load cell is connected to a lab jack that is used to change the height of the actuator to adjust the contact force between the actuator and finger pad. A computer generates the input signal to the actuator through a USB audio interface (UR22mkII, Steinberg) and a piezo driver (PZJRP6A, Matsusada Precision).

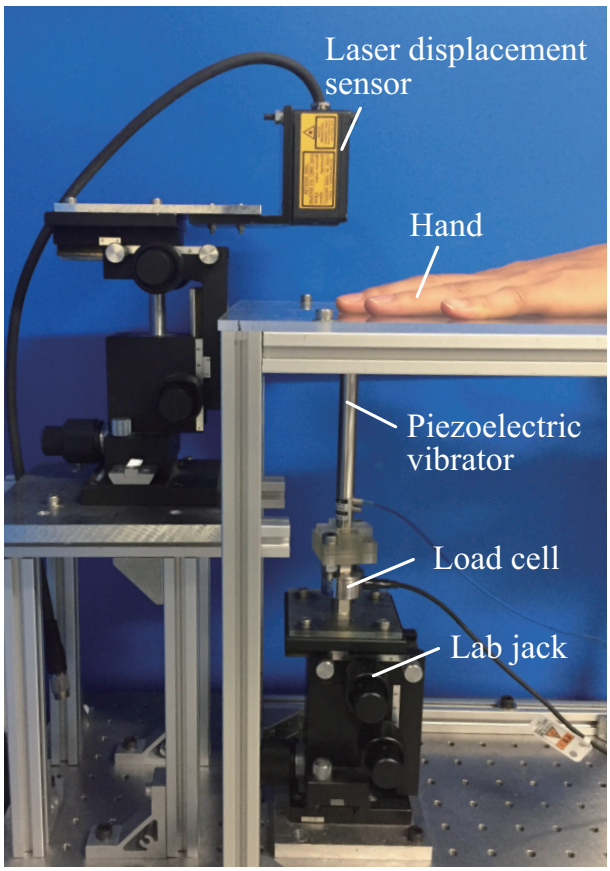


Figure 4.4: Subjects place their hand on the plate and contact the actuator with their finger

### 4.6.4 Participants

The participants consisted of ten female and five male subjects in the age groups of 20–28 years. A total of 14 subjects were right-handed and one of them was left handed. Based on their self-reports, no participants had any motor or sensory limitations. While informed consent was obtained, the participants were unaware of the purpose of the experiment that was to found the perceivable boundary of the envelope frequency. They

were informed to discriminate the stimuli in the experiments.

### 4.6.5 Tasks and procedures

Three alternative forced-choice paradigms were selected to measure the discrimination ratio between the comparative vibrations. Sixty conditions listed in Tables 4.3 to 4.6 were adopted with ten trials adopted for each condition. A total of 600 trials were conducted on each participant.

In each trial, the participant received three stimuli in an arbitrary order at 1-s intervals. Two of the stimuli are the same as stimulus one while the other one is stimulus two. After all the three stimuli were induced, the participants were asked to identify which stimulus was different from the others. After every 48 trials, the participants rested for five to ten minutes.

Prior to the experiment, a piece of double-sided adhesive tape was affixed around the hole in the plate. The participants were instructed to press the center part of their index finger pad on the hole and then relax their hand on the plate. The lab jack holding the actuator was slowly raised through the hole on the plate until it came in contact with the finger pad. Its height was adjusted until the expected contact force of 0.5 N was achieved between the finger and the actuator. After every 48 trials, the double-sided adhesive tape was replaced and the contact force was readjusted. Prior to the actual experiment, the participants completed 48 trials to familiarize themselves with the experimental procedure.

## 4.7 Results

In this section, we derive the sensitivity $d'$ as per a three-alternative, forced-choice procedure to determine the ability to discriminate between the pairs of stimuli. The calculation procedure is based on the one described in [63]. The Kolmogorov–Smirnov test was conducted to confirm that all stimuli pairs had normal distributions and data was analyzed using ANOVA and the post-hoc analysis via a Tukey–Kramer test.

### 4.7.1 Discrimination between sinusoidal and AM vibrations at different intensity levels

Figures 4.5 to 4.7 show the d' as per the signal detection theory that was used to compare the stimuli in Table 4.3. These stimuli have the same intensity (I = 25, 50, or 75) and carrier frequency ($f_c = 300$ Hz), but various envelope frequencies that were equally distributed on a logarithmic scale: $f_{e1} = 0$ and $f_{e2} = 12$, 20, 32, 50, 80, and 125 Hz. Based on the results, significant differences were observed between the envelope frequencies of 12, 20, 32, 50, and 125 Hz. In contrast, no significant differences were observed between the envelope frequencies of 80 and 125 Hz, which suggests that the envelope frequency, $f_e = 80$ Hz, can be a discrimination boundary between the AM vibrations ($f_e \neq 0$ Hz) and sinusoidal wave ($f_e = 0$ Hz). Figure 4.8 shows a comparison of the three intensity

levels. Figure 4.8 shows that there are significant differences between the d' of intensity $I = 25$ and d' of intensity $I = 75$ at envelope frequency $f_e = 80$ Hz, and between the d' of intensity $I = 25$ and d' of intensity $I = 75$ at envelope frequency $f_e = 125$ Hz, respectively. The corresponding p-values were 0.0235 and 0.0012, respectively.

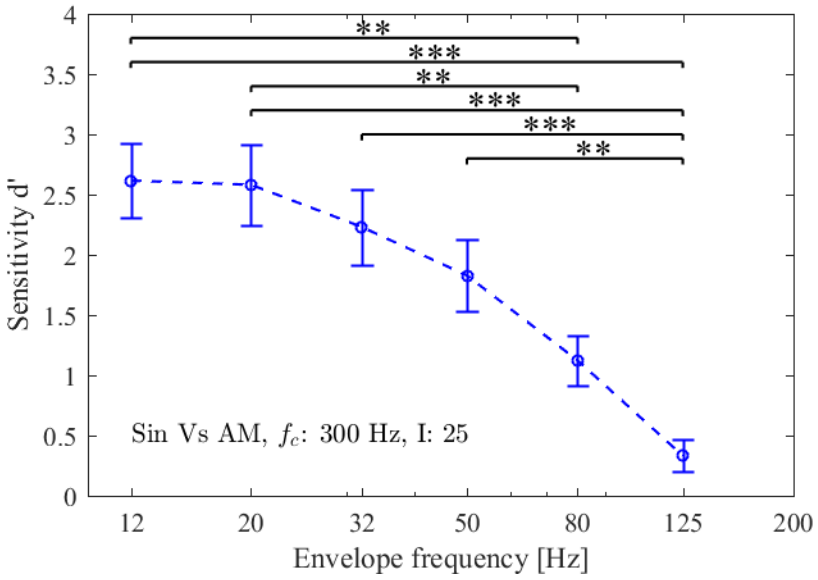


Figure 4.5: Sensitivity $d'$ of a comparison between the stimuli with an envelope frequency $f_{e1} = 0$ Hz and different envelope frequencies $f_{e2}$ from 12–125 Hz at an intensity $I = 25$. Here, $^*p < 0.05$, $^{**}p < 0.01$, $^{***}p < 0.001$, and the error bars represent the standard error of the mean.

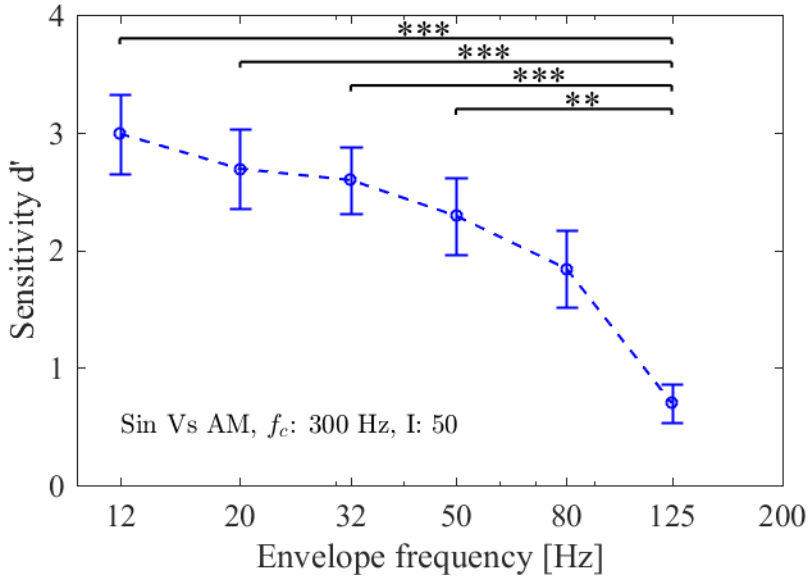


Figure 4.6: Sensitivity $d'$ of a comparison between the stimuli with an envelope frequency $f_{e1} = 0$ Hz and different envelope frequencies $f_{e2}$ from 12–125 Hz at an intensity $I = 50$. Here, $^*p < 0.05$, $^{**}p < 0.01$, $^{***}p < 0.001$, and the error bars represent the standard error of the mean.

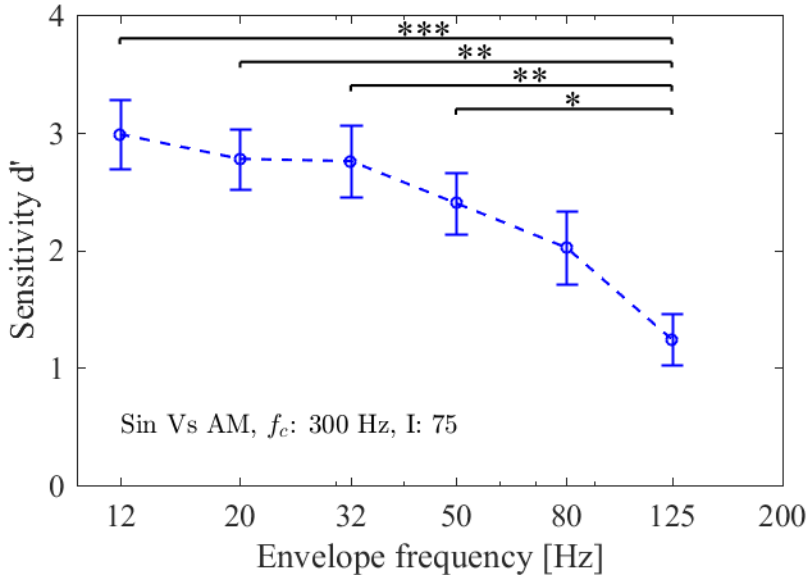


Figure 4.7: Sensitivity $d'$ of a comparison between the stimuli with an envelope frequency $f_{e1} = 0$ Hz and different envelope frequencies $f_{e2}$ from 12–125 Hz at an intensity $I = 75$. Here, $^*p < 0.05$, $^{**}p < 0.01$, $^{***}p < 0.001$, and the error bars represent the standard error of the mean.

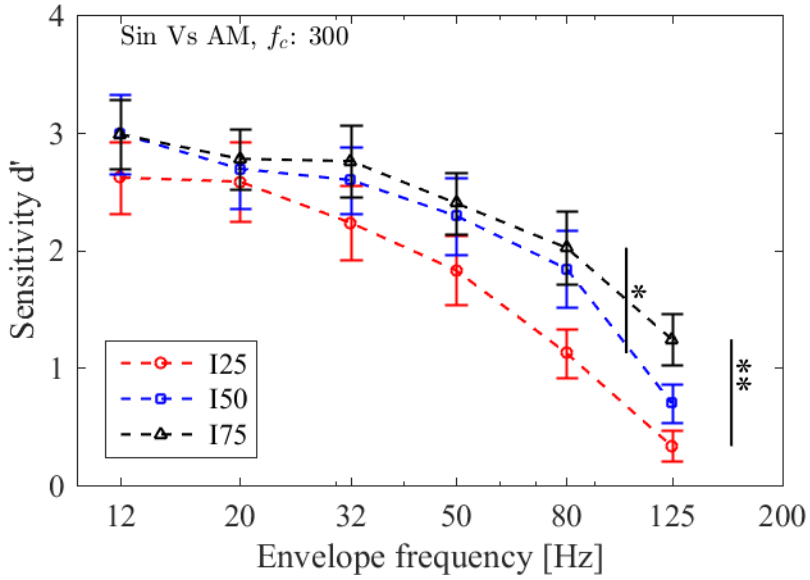


Figure 4.8: Sensitivity $d'$ of a comparison between the stimuli with an envelope frequency $f_{e1} = 0$ Hz and different envelope frequencies $f_{e2}$ from 12 to 125 Hz and the same carrier frequency $f_c = 300$ Hz. The intensity conditions are $I = 25$, 50, and 75. There are significant differences between $I = 25$ and $I = 75$ at $f_e = 80$ Hz, and between $I = 25$ and $I = 75$ at $f_e = 125$ Hz. Here, $^*p < 0.05$, $^{**}p < 0.01$, $^{***}p < 0.001$, and the error bars represent the standard error of the mean.

### 4.7.2 Discrimination between sinusoidal and AM vibrations of different carrier frequencies

As shown in Figure 4.9, the d' from the signal detection theory was used to compare the stimuli in Table 4.4, which had the same intensity (I = 50)different carrier frequencies

($f_{c1}$ = 300 Hz vs $f_{c2}$ = 400 Hz), and different envelope frequencies of $f_{e1}$ = 0 Hz and $f_{e2}$ = 12,20, 32, 50, 80, and 125 Hz. Based on the results, significant differences were noted between the envelope frequencies 12, 20, 32, 50, 80, and 125 Hz while no differences were noted among the envelope frequencies 12, 20, 32, 50, and 80 Hz. Figure 4.10 depicts d' from the signal detection theory used to compare the stimuli in Table 4.4, which had the same intensity (I = 50), different carrier frequencies ($f_{c1}$ = 300 vs $f_{c2}$ = 400), and different envelope frequencies of $f_{e1}$ = 0 Hz and $f_{e2}$ = 12, 20, 32, 50, 80, and 125 Hz, which were equally distributed on a logarithmic scale. The results showed that there were significant differences between the envelope frequencies of 12, 20, 32, 50, and 125 Hz while no differences were noted between the envelope frequencies 12, 20, 32, 50, and 80 Hz or between 80 and 125 Hz. Figure 4.11 shows a comparison among the different carrier frequencies in Figure 4.5, 4.9, and 4.10. Significant differences were observed between $f_{c1}$ = $fc2$ = 300 Hz and $f_{c1}$ =$fc2$ = 400 Hz at an envelope frequency $f_e$ = 125 Hz.

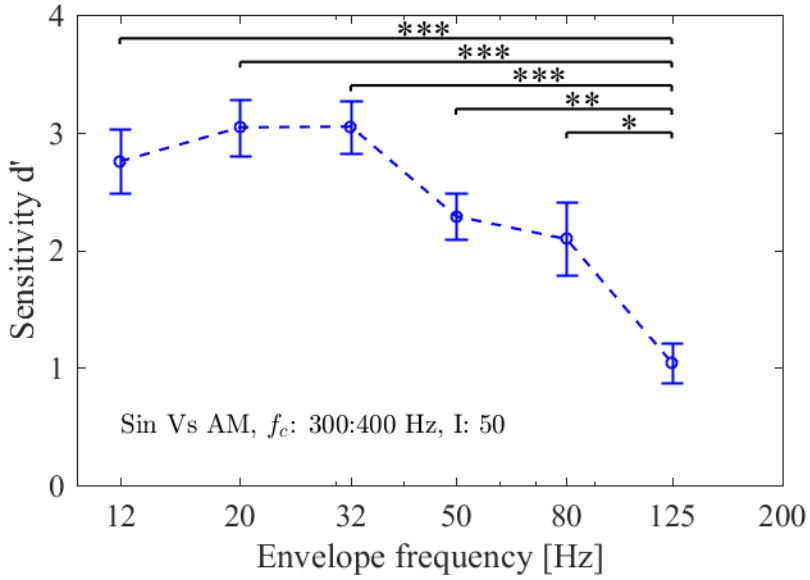


Figure 4.9: Sensitivity d' of the comparison between the stimuli with an envelope frequency $f_{e1}$ = 0 Hz and different envelope frequencies $f_{e2}$ from 12–125 Hz. The carrier frequency condition was $f_{c1}$ = 300 Hz vs $f_{c2}$ = 400 Hz and the intensity was $I$ = 50. Here, $^*p < 0.05$, $^{**}p < 0.01$, $^{***}p < 0.001$, and the error bars represent the standard error of the mean.

### 4.7.3 Discrimination of the AM vibration of different carrier frequencies

Figure 4.12 shows that the d' values from the signal detection theory used to compare the stimuli in Table 4.5 that had the same intensities ($I$ = 25, 50, or 75) and envelope frequencies ($f_{e1}$ = $f_{e2}$), but different carrier frequency ($f_{c1}$ = 300 Hz vs $f_{c2}$ = 400 Hz). No significant difference was noted among the envelope frequencies at each intensity. Figure 4.13 shows a comparison the three intensity levels of Figure 4.12, where significant

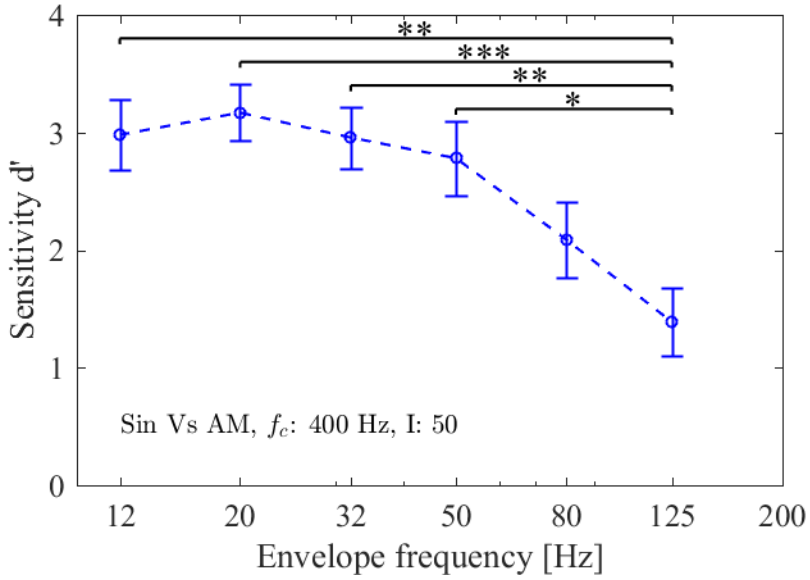


Figure 4.10: Sensitivity $d'$ of a comparison between the stimuli with an envelope frequency $f_{e1} = 0$ Hz and different envelope frequencies $f_{e2}$ from 12–125 Hz. The carrier frequency was $f_c = 400$ Hz and the intensity was $I = 50$. Here, $^*p < 0.05$, $^{**}p < 0.01$, $^{***}p < 0.001$, and the error bars represent the standard error of the mean.

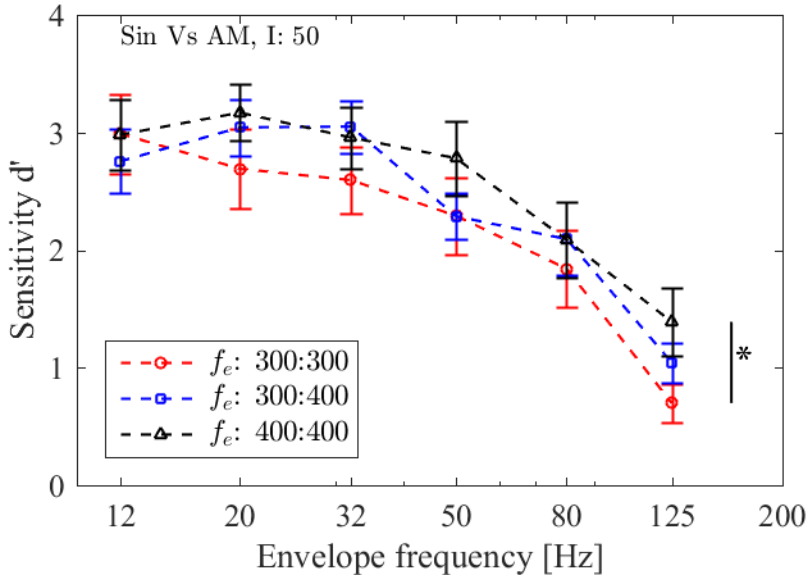


Figure 4.11: Sensitivity $d'$ obtained from comparing the stimuli with an envelope frequency $f_{e1} = 0$ Hz and different envelope frequencies $f_{e2}$ from 12–125 Hz. The carrier frequencies were $f_{c1} = f_{c2} = 300$ Hz, and $f_{c1} = 300$ Hz, $f_{c2} = 400$ Hz, and $f_{c1} = f_{c2} = 400$ Hz, which are represented by the red circles, blue squares, and black triangle, respectively. Significant differences were observed between $f_{c1} = fc2 = 300$ Hz and $f_{c1} = f_{c2} = 400$ Hz at $f_e = 125$ Hz. Here, $^*p < 0.05$, $^{**}p < 0.01$, $^{***}p < 0.001$, and the error bars represent the standard error of the mean.

differences can be observed between the $d'$ at intensity $I = 25$ and d' at intensity $I = 75$, and between the d' at intensity $I$ =50 and d' at intensity $I = 75$. The p-values were

0.0017 and less than 0.0001.

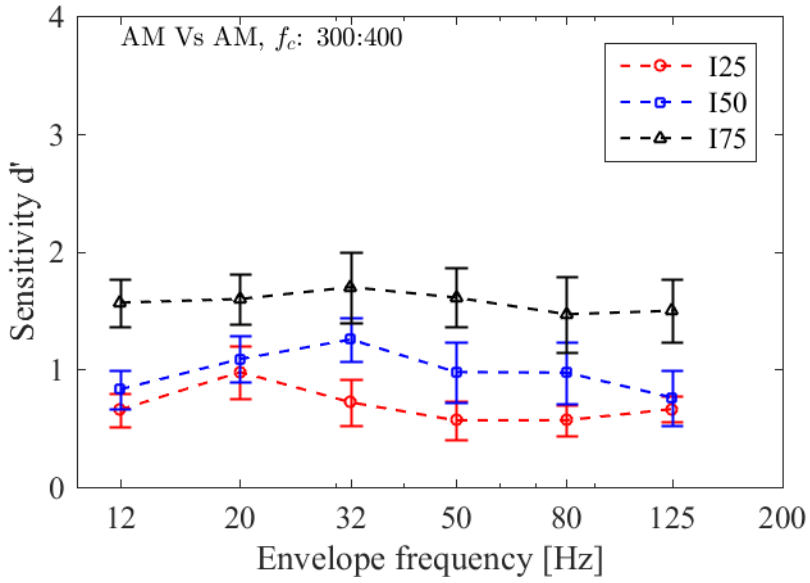


Figure 4.12: Sensitivity $d'$ of the comparing stimuli with the same envelope frequency $f_{e1} = f_{e2}$ from 12–125 Hz and two carrier frequency $f_{c1} = 300$ Hz vs $f_{c2} = 400$ Hz. The intensity conditions are $I = 25$, 50, and 75 shown by the red circle, blue square, and black triangle respectively. $^*p < 0.05$, $^{**}p < 0.01$, $^{***}p < 0.001$. The error bars represent the standard error of the mean

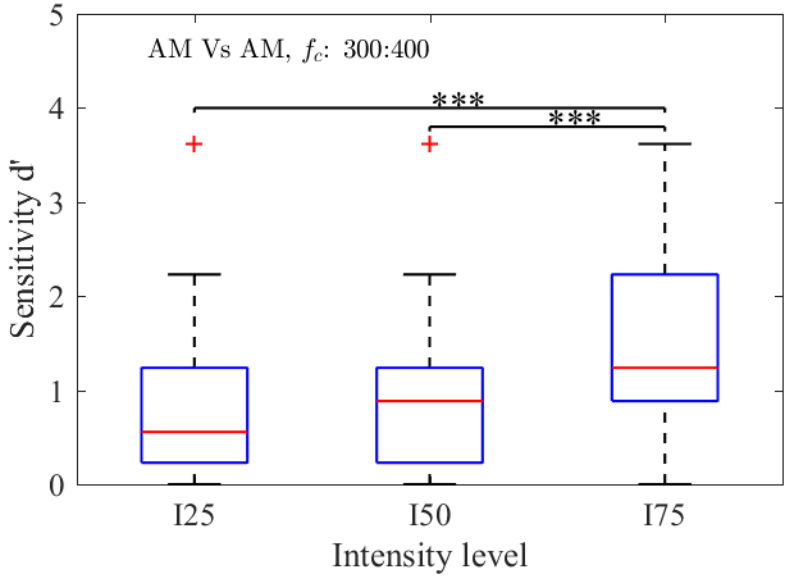


Figure 4.13: Sensitivity $d'$ of a comparison between stimuli with the same envelope frequency $f_{e1} = f_{e2}$ from 12 to 125 Hz and different carrier frequencies $f_{c1} = 300$ Hz vs $f_{c2} = 400$ Hz. The intensity conditions were I = 25, I = 50 and I = 75. Here, $^*p < 0.05$, $^{**}p < 0.01$, $^{***}p < 0.001$.

### 4.7.4 Discrimination of the AM vibration of different intensity

Figure 4.14 shows the d' values from the signal detection theory used to compare the stimuli in Table 4.6, had the same envelope frequencies ($f_{e1} = f_{e2}$), but different intensities ($I_1 = 25$ vs $I_2 = 50$ , $I_1 = I_2 = 50$, and $I_1 = 50$ vs $I_2 = 75$). No significant difference was noted among the envelope frequencies at each intensity condition. Figure 4.15 shows a comparison the three intensity conditions of Figure 4.14, where significant differences can be observed between the $d'$ at intensity $I_1 = 25$ vs $I_2 = 50$ and d' at intensity $I_1 = I_2 = 50$, and between the d' at intensity $I_1 = 25$ vs $I_2 = 50$ and d' at intensity $I_1 = 50$ vs $I_2 = 75$. The p-values in both of these cases were less than 0.001.

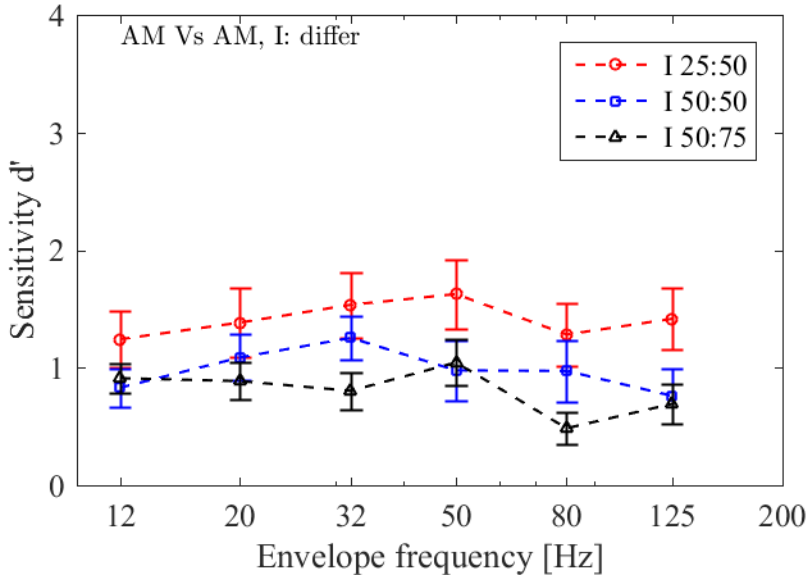


Figure 4.14: Sensitivity $d'$ of the comparative stimuli with the same envelope frequency $f_{e1} = f_{e2}$ from 12– 125 Hz and different intensities I = 35, 50 and 75. The different intensity conditions are $I_1 = 25$ vs $I_2 = 50$ , $I_1 = I_2 = 50$, and $I_1 = 50$ vs $I_2 = 75$ shown as the red circle, blue square, and black triangle respectively. $^*p < 0.05$, $^{**}p < 0.01$, $^{***}p < 0.001$. The error bars represent the standard error of the mean.

### 4.7.5 Comparing the stimuli with different envelopes and stimuli with the same envelope

Figure 4.16 to Figure 4.18 depict the sensitivity $d'$ values obtained from comparing stimuli with the same envelope frequencies, $f_{e1} = f_{e2}$, from 12–125 Hz, and comparing the stimuli with different envelope frequencies, $f_{e1} = 0$ Hz, $f_{e2}$ from 12–125 Hz at the intensity, $I = 25$, 50, and 75, respectively. The cases with different envelope frequency conditions, $f_e$, are denoted using the red circles, while those that were the same are denoted using blue squares. The carrier frequencies were $f_{c1} = f_{c2} = 300$ Hz, and $f_{c1} = 300$ Hz, $f_{c2} = 400$ Hz, respectively. With these three intensity conditions, it was found that there were significant differences for the envelope frequencies of 12, 20, 32, 50, and 80 Hz while no

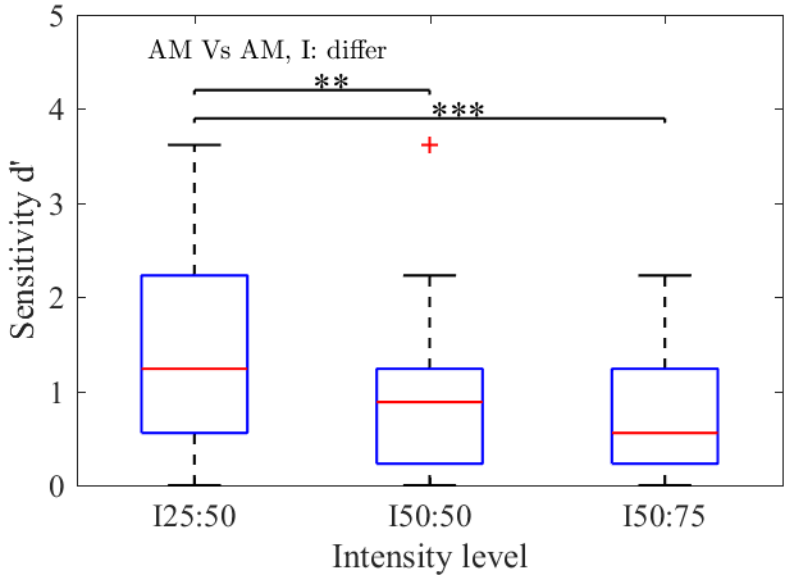


Figure 4.15: Sensitivity $d'$ of comparing all stimuli with the same envelope frequency, $f_{e1} = f_{e2}$, from 12–125 Hz and different intensities I = 35, 50 and 75. The different intensity conditions are $I_1 = 25$ vs $I_2 = 50$ , $I_1 = I_2 = 50$, and $I_1 = 50$ vs $I_2 = 75$. $^*p < 0.05$, $^{**}p < 0.01$, $^{***}p < 0.001$.

significant differences were observed for an envelope frequency of 125 Hz.

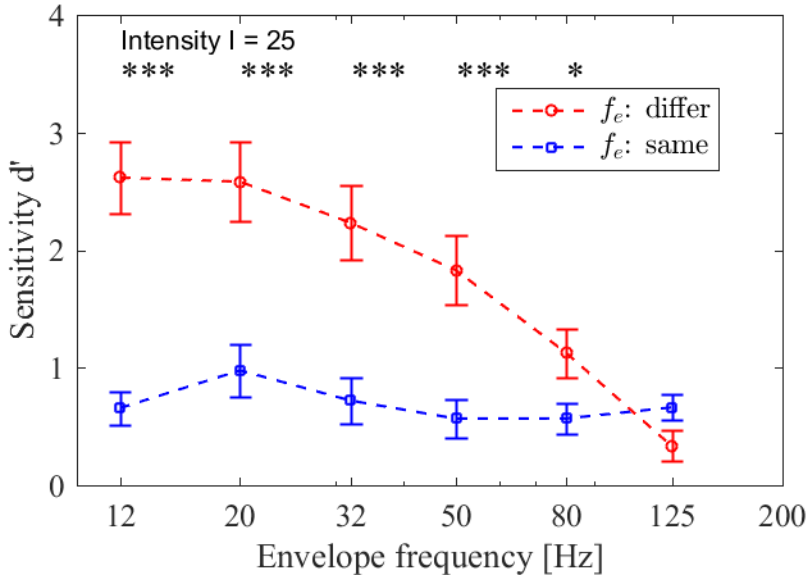


Figure 4.16: Sensitivity $d'$ of a comparison between the stimuli with envelope frequencies, $f_{e1} = f_{e2}$, from 12 to 125 Hz. The cases for different envelope frequency are denoted with red circles while those when the envelope frequencies were the same are denoted with blue squares. The carrier frequencies were $f_{c1} = f_{c2} = 300$ Hz and $f_{c1} = 300$ Hz, $f_{c2} = 400$ Hz, respectively. The intensities were $I = 25$. Here, $^*p < 0.05$, $^{**}p < 0.01$, $^{***}p < 0.001$, and the error bars represent the standard error of the mean.

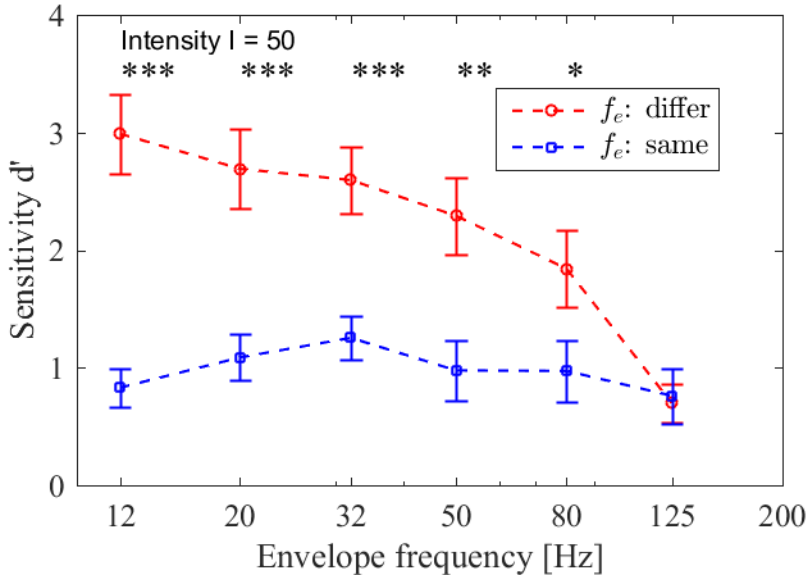


Figure 4.17: Sensitivity $d'$ of a comparison between the stimuli with envelope frequencies $f_{e1} = f_{e2}$ from 12–125 Hz. The cases for different envelope frequencies are denoted with red circles while those when the envelope frequencies were the same are denoted with blue squares. The carrier frequencies were $f_{c1} = f_{c2} = 300$ Hz and $f_{c1} = 300$ Hz, $f_{c2} = 400$ Hz, respectively. The intensities were $I = 50$. Here, $^*p < 0.05$, $^{**}p < 0.01$, $^{***}p < 0.001$, and the error bars represent the standard error of the mean.

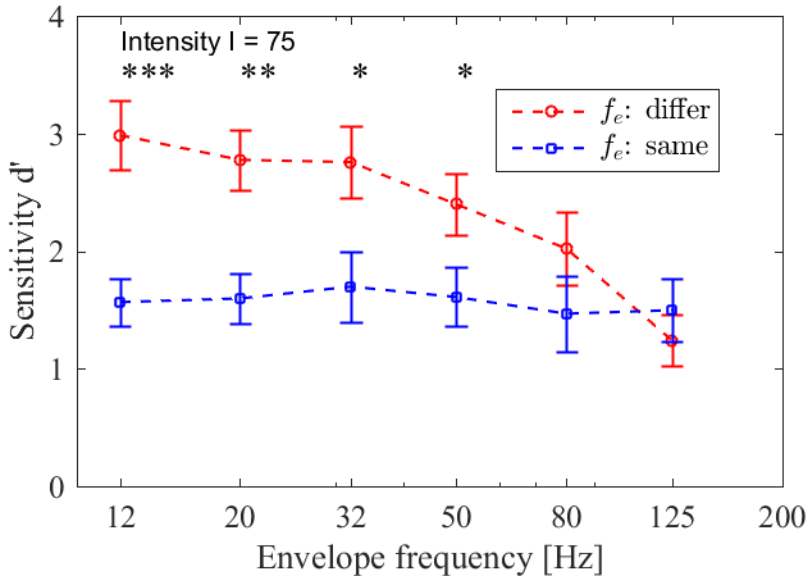


Figure 4.18: Sensitivity $d'$ of a comparison between the stimuli with envelope frequencies $f_{e1} = f_{e2}$ from 12–125 Hz. The cases for different envelope frequencies are denoted with red circles while those when the envelope frequencies were the same are denoted with blue squares. The carrier frequencies were $f_{c1} = f_{c2} = 300$ Hz and $f_{c1} = 300$ Hz, $f_{c2} = 400$ Hz, respectively. The intensities were $I = 75$. Here, $^*p < 0.05$, $^{**}p < 0.01$, $^{***}p < 0.001$, and the error bars represent the standard error of the mean.

## 4.8 Discussion

### 4.8.1 Perception of the envelope frequency

The results of the experiments described earlier indicate that perceptual discrimination of stimuli has an envelope frequency dependence, as shown in Figures. 4.5 to 4.8. As the envelope frequency increased, the sensitivity of the vibration decreased. In [31], the threshold of the AM vibration is just below the threshold of the Meissner corpuscle, and it indicts the activity of Meissner corpuscle. In our results, the sensitivity reduced with envelope frequency increase. In the low envelope frequency region from 12–50 Hz, the sensitivity $d'$ was found to be high, while in the high envelope frequency region from 80–125 Hz, the sensitivity $d'$ was low. These results are similar to those for the active frequency range of the Meissner corpuscle reported in [3]. The threshold of the Meissners corpuscle, which is believed to be sensitive to the peak values of the waveforms, reached its lowest point at approximately 40 Hz but increased as the frequency increased. The threshold of the Pacinian corpuscle, which is thought to be sensitive to the intensity of the wave, is present above 10 Hz and reaches its lowest point at approximately 300 Hz. These two receptors overlap in frequency from 10–100 Hz. Below 40 Hz, the threshold of Meissners corpuscle is low, while above 40 Hz, the amplitude threshold of the Pacinian corpuscle is high. Meissners corpuscles are thought to be sensitive to the peak position, peak velocity, and the maximum of the product of position and velocity below 100 Hz [64, 65, 66, 29], while Pacinian corpuscles may not be sensitive to the position and velocity, but are sensitive to the intensity or power of the stimuli above 100 Hz [28, 29, 54, 30, 4, 67]. These results imply the perception of a lower envelope by the Meissners corpuscle when it is between 12 and 50 Hz. The sensitivity is low, and discrimination is difficult, especially in the case of a very high envelope frequency and low intensity where $d'$ is less than one ($f_e = 125$ Hz, $I = 25$).

### 4.8.2 Perception of intensity

The intensity model works well for a high envelope frequency of 125 Hz, and when the intensity is the same, it is difficult to discriminate the vibrations. Intensity-based modeling [30] of the Pacinian corpuscle is based on the assumption that the same intensity would be perceived as similar. At low envelope frequencies, the discrimination is straightforward, which may be because they fall within the active frequency range of the Meissners corpuscle. From Figure 4.5 to 4.8, it can be seen that there were significant differences between envelope frequencies of 12–50 Hz and 125 Hz. The sensitivity was low at higher envelope frequency ranges where the activities of the Meissners corpuscles are assumed to be weaker. From Figures. 4.16 to 4.18, no significant difference was observed between the vibrations of stimuli with the same envelope and the stimuli with different envelopes, when the envelope frequency, $f_e$, was 125 Hz. The sensitivity d' of

high envelope frequencies were low but not 0, which suggests that subjects were still able to discriminate to some extent. This may be due to the roughness of the intensity model. Figure 4.13 shows that the sensitivity of carrier frequency difference increases with intensity when they have the same envelope frequencies. Figure 4.7 shows that there was a slight increase in sensitivity for comparing the stimuli of sinusoidal and AM vibrations. There are significant differences between $I = 25$ and $I = 75$ at $f_e = 80$ Hz, and between $I = 25$ and $I = 75$ at $f_e = 125$ Hz. It may suggest that the sensitivity of envelope frequency increases with intensity increase. Figure 4.15 shows significant differences between the $d'$ at intensity $I_1 = 25$ vs $I_2 = 50$ and d' at intensity $I_1 = I_2 = 50$, and between the d' at intensity $I_1 = 25$ vs $I_2 = 50$ and the d' at intensity $I_1 = 50$ vs $I_2 = 75$. It also may suggest that the envelope was not strongly perceived when intensity I = 25 was compared to intensities I = 50 and I = 75.

### 4.8.3 Perception of carrier frequency

The carrier frequency was found to have a mild effect as shown in Figure 4.11. The significant differences only arose between $f_{c1} = f_{c2} = 300$ Hz and $f_{c1} = f_{c2} = 400$ Hz at an envelope frequency of $f_e = 125$ Hz. This suggests that the intensity information was not significantly affected by the carrier frequency. In [54, 30, 4, 67], superimposed vibrations or fine texture vibrations were used for discrimination, which did not contain clear envelope perception. The intensity models in these studies could well predict the perceptual dissimilarities based on the intensity differences between the stimuli, and the frequency of the stimuli does not significantly affect the discrimination. In our experiment, the sensitivity exhibited an envelope frequency dependence, while the carrier frequency of the stimuli had a slight effect on the discrimination. These may suggest that the carrier frequency of the vibration has a minimal effect on the perceptual discrimination.

## 4.9 Limitation of the study

One limitation of the current study is that the intensity model we used was a relatively simple Equation 4.4. Other researchers have endeavored to identify more specific models, such as the spectral mini-channel model [30]. Another limitation is that we employed a simple type of AM vibration and did not consider any types of complex vibration. Thus, an area of future research will determine if complex waveforms exhibit tendencies similar to those obtained in this study.

## 4.10 Summary

The intensity of high-frequency vibrations (i.e., vibrations > 100 Hz), which is generally defined as the integral of the intensity of the stimulus over time or the spectral power summed across all frequencies, has been identified as a primary cue with which to convey vibrotactile information as per the Pacinian system. However, the intensity model is insufficient when interpreting the perception of the envelope of high-frequency vibra-

tions. The intensity and envelope together affect the ability of humans to discriminate high-frequency vibrations.

The objectives of the current study are to identify the boundary where the envelope has a strong effect on discriminating vibrations and investigate the effect of the carrier frequency on the discriminate was investigated. We experimented to assess the discrimination ability of subjects exposed to AM and sinusoidal vibrations of different envelope frequencies, carrier frequencies, and intensity levels using the intensity model developed in previous studies. In this way, we investigated the effect of the intensity and envelope on the ability of humans to discriminate high-frequency vibrations. Our results show that the perceptual discrimination of the tested stimuli had an envelope frequency dependence, in which the discrimination ability increased as the envelope frequency increased. For an envelope frequency of an AM vibration in the range of 12–50 Hz, the discrimination ability was higher than that for the sinusoidal vibration, although the intensity did not strongly affect the discrimination ability in this range. When the envelope frequency of an AM vibration was 125 Hz, the discrimination ability was low compared to that of the sinusoidal vibration, and there was no significant dependence on the envelope frequency. Our results showed that perceptual discrimination tended to increase as the intensity increased, which occurred whether or not the stimuli being compared had the same envelope frequency. Although it was difficult to discriminate the vibration when the intensities were the same, the intensity model was found to be accurate for a higher envelope frequency of 125 Hz. No significant differences in the perceptual discrimination were observed between the stimuli with same or different envelopes. In addition, the results suggest that the perceptual discrimination increased as the intensity increased when both the stimuli had the same envelope.

Our study suggested that the boundary for the envelope perception is at an envelope frequency of approximately 80–125 Hz and at low envelope frequencies less than 50 Hz, the envelope perception of the vibration is straightforward. It is found that the carrier frequency had little effect on the discrimination of vibration, and the ability to discriminate the vibration slightly increased as the intensity increase. Therefore, we can shift the carrier frequency but still maintain the envelope sensation by modulating at the low intensity. A lower carrier frequency could reduce the difficulties of generating high-frequency vibrations and reduce the sound of the vibration when using a lower frequency carrier by modulation.

# Chapter 5

# Perceptual Modulation Application: Sound reduction of vibration feedback by perceptually similar modulation

## 5.1 Introduction

The transmission of tactile vibrations is used in many robotic applications, such as in the telerobotic surgery where a contact vibration feedback system is developed and qualitatively evaluated [56, 57]. Some of these vibrations, which have high-frequency components, occur when the surface of the object is scratched or tapped by the users hands or tools. These high-frequency vibrations were reported as cues for roughness or hardness perception [33, 22, 19, 54]. This suggests that high-frequency vibrations play an important role in conveying perceptual phenomena in robotic applications.

However, these high-frequency vibrations also will expend energy in the form of noise that can be heard by operators and non-users alike. The sound levels of vibrations increase as the frequency increases in the range of 300–1,000 Hz, when the amplitude of the waves are a constant [40].

In this study, we intend to develop a methodology for modulating the noisy and high-frequency vibrotactile waves into noise-free and perceptually similar vibrotactile waves. However, if we reduce the carrier frequency of the waves, the perception information may be changed.

In previous studies, researchers found that vibrations of different frequencies could have similar perception characteristics, such as intensity and hardness, when their amplitudes are modulated based on sensation. In [28, 29, 30], the researchers observed that the high-frequency stimuli have equal perceived intensities while the stimuli have different amplitudes. In [68], the author found that if the decaying sinusoidal waves have the same

hardness sensation, the amplitude of the wave will decrease as the frequency increases in the range of 50–350 Hz.

In this study, we focus on modulating the high-frequency collision vibrations that occur when the surface of the object is tapped by hands or tools. In [33], Okamura et al. found that the perception of the collision vibration is modeled after three parameters (amplitude A, frequency $f$, and time constant $\tau$) of their decaying sinusoidal model. It can generate the perception of tapping different materials, such as tapping on wood, metal, or rubber. Therefore, our methodology relies on modulating amplitude A and the frequency, $f$, of the collision vibrations. The time constant, $\tau$, is not modulated because it may change the time duration and the envelope of the stimuli, which have not been fully studied in previous studies. For simplifying the experimental procedures, time constant $\tau$ is kept constant in this study.

Our modulation method for the wave is to use the perceptually similar, low-frequency collision vibrations to represent the high-frequency collision vibrations, and the sound is assumed to be reduced after the modulation. The experimental procedures used in this study are as follows: 1. We conducted a psychophysical experiment by adjusting the amplitude of test low-frequency collision vibrations to produce a sensation as similar to that provided by the original reference high-frequency collision vibrations as possible. 2. We verified whether a human could perceive the perceptual difference between the modulated collision waves obtained and the original waves. 3. We measured the sound pressure levels of the experimental collision vibrations at different frequencies. Using these three experiments, we investigated the perceptual similarity and the sound levels between the original collision vibrations and the modulated vibrations in the frequency range of 300 to 1,012 Hz. The work in this chapter was published in [69, 70].

## 5.2 Objectives of the Chapter

We focus on the modulation of high-frequency collision vibrations that occur when the surface of the object is tapped by hands or tools. The high-frequency waves will induce noise. We aim to reduce this sound generated by the collision vibrations using the haptic modulation method, which uses the perceptually similar low-frequency collision vibrations to represent high-frequency collision vibrations.

## 5.3 Significance of the Study

The modeling of high-frequency vibrations plays an important role for vibration rendering in haptic applications. We aim to model the similar perceptual vibrations with different parameters, e.g., amplitude, frequency, and envelope of the stimuli. This modeling can help us to design the vibration linked to the available actuators for presenting a larger range of touch sensation. One important purpose of this chapter is to describe the method we used to reduce the sound generated by the high-frequency rendering of colli-

sion vibration. A lower frequency stimulus generates a similar sensation while the sound is reduced. This will benefit applications that require low-decibel environment, such as an industrial environment that require silence. Other types of modeling of high-frequency will be developed in future studies.

## 5.4 Experiment One: Investigating the perceptually similar collision vibrations

In this experiment, we identified the amplitudes of the stimuli that produced similar perceptions at different frequencies. The subject adjusted the amplitude of one stimulus to achieve a sensation as close to that of another stimulus as possible, at a different frequency.

### 5.4.1 Stimuli

The collision vibration model used in this study is a decaying sinusoidal waveform[33], where $Q(t)$ is the vibration produced by the contact, $A$ is an attack amplitude, $\tau$ is a time constant, and $f$ is a frequency.

$$Q(t) = Ae^{-\frac{t}{\tau}}\sin(2\pi ft) \tag{1}$$

The perceived intensity of stimulus changes with the frequency. Murray et al., [37] found that the perceived intensity increased as frequency increased from 100–200 Hz, when the sinusoidal vibration occurred on the fingertip. Verrillo et al., [71] measured the perceived intensity of sinusoidal vibrations in the frequency range from 25–700 Hz. The amplitude contours of equally perceived intensity for sinusoidal vibrations were U-shaped curves. The curves decreased in the low-frequency range and achieved a minimum of approximately 200–300 Hz. For frequencies higher than 300 Hz, the curve increased again for an amplitude lower than 10 $\mu m$. It remained constant or slightly decreased if the amplitude was more than 10 $\mu m$. If intensity can represent the perceptual similarity for collision vibrations higher than 300 Hz, it may be possible to replace the frequency of collision vibrations with little or no difference in perception. Previous researches also indicate that the amplitude contours of the perceptually similar collision vibrations may have different characteristics in the high-frequency range depending on low or high amplitude. However, researchers in these studies investigated the perceived intensity of sinusoidal vibration. In our study, we investigate the collision vibration using decaying sinusoidal vibrations.

The perceived hardness changes with the frequency. In [68], the author found that if decaying sinusoidal waves had the same hardness sensation, the amplitude of the waves will decrease as the frequency increased in the range of 50–350 Hz. If the hardness can represent the perceptual similarity for collision vibrations, a high amplitude may be needed for the low-frequency collision vibrations to be perceptually similar to high-frequency collision vibrations.

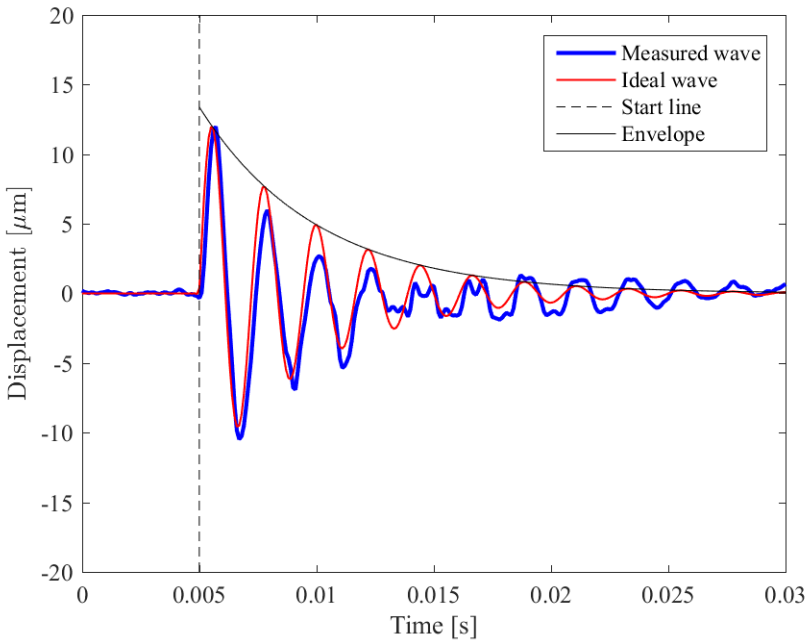


Figure 5.1: Experimental stimulus example: A = 13.4 $\mu m$, $\tau$ = 5 ms, $f$ = 450 Hz

In our experiment, the subject judged the perceptual similarity between a reference stimulus and a test stimulus. We used the collision vibrations represented by the decaying sinusoidal model. For the reference stimuli, we selected several frequencies, each of which was 1.5 times the previous frequency. The difference ratio of 50 % is higher than in the Webers law (20 %) as reported in [44] for sinusoidal waves. The initial frequency is 300 Hz, which is close to the most sensitive frequency for humans. We chose reference amplitudes of $A = 6\ \mu m$ and $A = 12\ \mu m$ for all the frequencies.

The test frequencies were 300 Hz and 450 Hz. The parameters of the reference and test stimuli are shown in Table.5.1. One of the experimental stimuli is shown in Figure 5.1. The difference between measured amplitude A and ideal amplitude A is less than 5 %. The wave was measured without finger contact using the piezo actuator, as shown in Figure 5.2.

Table 5.1: Parameters of the reference stimuli and the test stimuli in experiment 1

| Reference $f$ [Hz] | Reference A [$\mu$m] | Test $f$ [Hz] | Test A [$\mu$m] |
|---|---|---|---|
| 300 | 6, 12 | 300, 450 | |
| 450 | 6, 12 | 300, 450 | |
| 675 | 6, 12 | 300, 450 | Adjust |
| 1012 | 6, 12 | 300, 450 | |

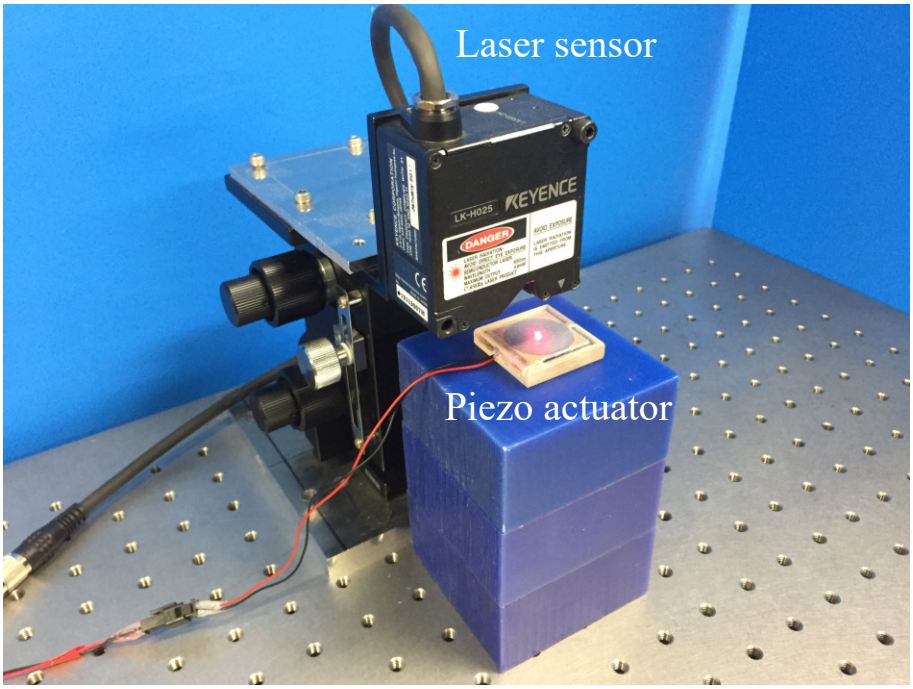


Figure 5.2: Wave of collision vibration measured by a laser sensor

### 5.4.2 Subjects

Six subjects (age group of 21 to 28 years; four male and two female subjects; five right-handed and one left-handed) took part in the study. No subjects have motor or sensory limitations by self-report.

### 5.4.3 Experimental Setup

A piezo actuator (PowerHap 15G - Prototypes) was inserted in a vibrator case. A PC sent the vibration signal to the piezo actuator through a USB audio interface (UR22mkII, Steinberg) and a piezo driver (PZJRP6A, Matsusada Precision).

Figure 5.3 shows the relationship between the amplitude of the input voltage to the piezo actuator, and the measured the amplitude of the stimuli. To adjust the amplitude of the test stimuli, we change the input voltage based on this measured relationship.

### 5.4.4 Tasks and Procedures

The participants sat comfortably in front of a computer. The actuator is fixed on the center of the right-hand palm by using a double-sided tape. The subjects right forearm is rested on a thick foam, and they keep their palm upward during the experiment as shown in Figure 5.4.

The participants adjusted the amplitude of the test stimuli so that the test stimulus perception was most similar to the reference stimulus. They could freely play the stimuli during the adjustment. They were able to increase the amplitude, $A$, by using the Up key and decrease the same by using the Down key. Pressing and holding the key would cause a larger change. They were able to play the presented stimuli by using the Space

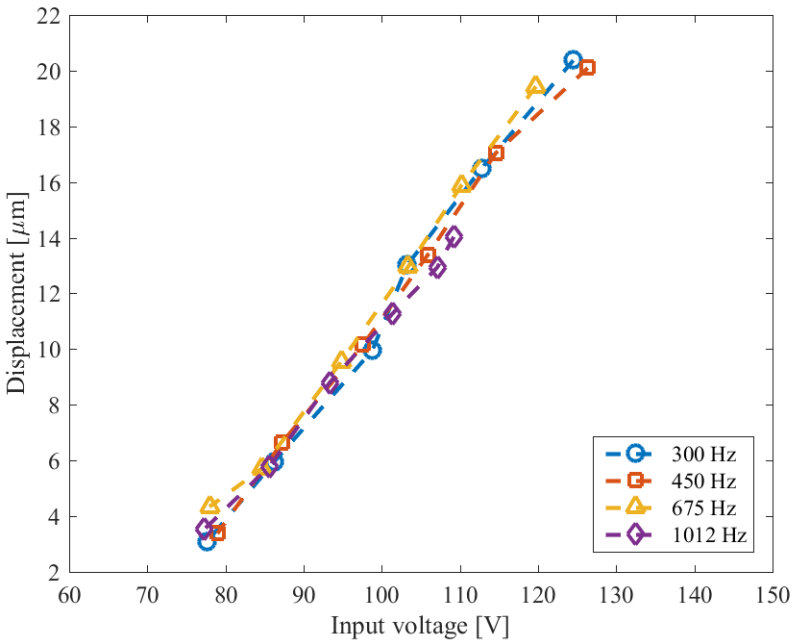


Figure 5.3: Relationship between the input voltage and the maximum amplitude of the measured wave

key and experience each pair as many times as they wanted to. They pressed the Enter key to record the amplitude of the test stimuli; then they could perceive the next pair of stimuli. The intensity (amplitude A = 4 $\mu m$) of the test vibration was initially set to be lower than the reference stimulus.

At the beginning of the experiment, the participant would perceive all 16 stimuli pairs (eight reference stimuli × two test stimuli × three repetitions). Training helped the participant accustomed with the experimental procedure and stimuli. After the training, the subject would continue to perceive a total of 48 stimuli pairs (eight reference stimuli × two test stimuli × three repetitions) in a random order. The participants were asked to wear headphones and were exposed to pink noise during the experiment to block external auditory cues.

### 5.4.5 Results

We calculated each subjects values using the mean values of the three trials, after which we calculated the mean values of all the subjects. Table 5.2 shows the mean values of the amplitudes of all the participating subjects and standard errors in all the conditions. The results show that the standard values of the adjusted amplitudes can be 23 % to 81 % of the mean value for each stimuli pair. These ratios (23 % to 81 %) are greater than those from the Webers law (20 %), which is reported in [44] for sinusoidal waves. It suggests that the subjects were not sensitive to the amplitude difference in the experiment.

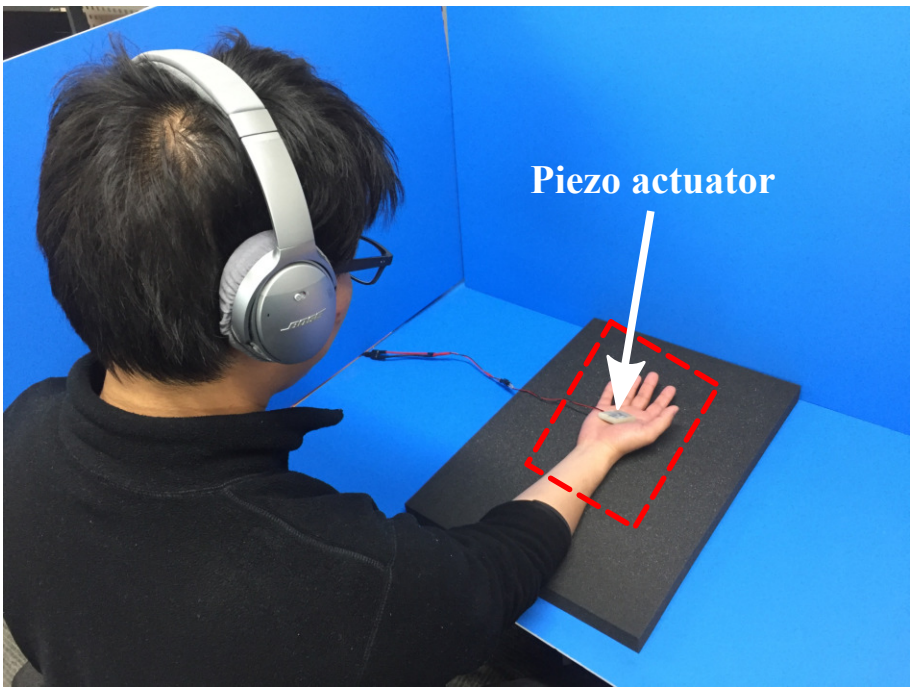


Figure 5.4: Subject resting the arm on a foam with the piezo actuator fixed to the palm

Table 5.2: Amplitudes of the test stimuli exhibiting the most similarity to the reference stimuli

| Test $f$ [Hz] | Test A [$\mu$m] | Reference $f$ [Hz] 300 | 450 | 675 | 1012 |
|---|---|---|---|---|---|
| | | Test A (mean±S.D.) [$\mu$m] | | | |
| 300 | 6 | 6.6±2.5 | 6.6±2.3 | 7.5±4.6 | 7.7±5.7 |
| 300 | 12 | 9.4±3.2 | 10.7±3.7 | 10.5±4.4 | 9.8±5.0 |
| 450 | 6 | 6.7±1.5 | 6.1±2.0 | 6.6±1.9 | 7.3±5.9 |
| 450 | 12 | 9.8±3.0 | 10.3±2.4 | 9.0±4.2 | 10.8±4.9 |

## 5.5 Experiment Two: Comparing the perceptual similarity of the collision vibrations

In this experiment, we compare the perceptual similarity between the reference stimuli and the test stimuli obtained in experiment one.

### 5.5.1 Stimuli

There are eight reference stimuli and eight test stimuli. The reference stimuli are the same vibrations used in the first experiment. The test stimuli are the test stimuli with the amplitudes as shown in Table 5.2.

### 5.5.2 Subjects

Five subjects (age group of 21 to 28 years; four male and one female subjects; all right-handed) took part in the study. No subjects had motor or sensory limitations by self-report.

### 5.5.3 Experiment Setup

Experimental apparatus are the same as the first experiment.

### 5.5.4 Tasks and Procedures

The participants sat comfortably in front of a computer. The actuator consists of a stick to the center of the right-hand palm. The subjects forearm rests on a thick foam, and they keep the palm upward during the experiment.

The participants perceived two groups of stimuli during each trial. One group had two identical reference stimuli while the other group had one reference stimuli and one test stimulus. The subjects task was to judge which group had different stimuli. At the beginning of the experiment, the subject would perceive all 16 stimuli pairs (eight reference stimuli $\times$ two test stimuli). Initial training helped the participant familiarize themselves with the experimental procedure and all the experimental stimuli. Data for the training were not recorded. After the training, the subject would receive 48 stimuli pairs (eight reference stimuli $\times$ two test stimuli *times* three repeat times). The results were recorded for the following analysis.

### 5.5.5 Results

Figure 5.5 to Figure 5.8 shows the correct answer ratio that the subjects judged for identifying the groups with two different stimuli.

The Kolmogorov–Smirnov test was applied to all 16 conditions (eight reference stimuli $\times$ two test stimuli types) for testing the normality of distribution. The result of the test showed that only six out of 16 conditions had normal distributions. Therefore, we used the Kruskal–Wallis test and post-hoc analysis (Fishers least significant difference procedure) for analyzing data.

The results of the Kruskal–Wallis test and the post-hoc analysis revealed significant differences between the reference collision vibration and the test collision vibration, which only occurred at the conditions for the reference stimulus (A = 12 $\mu$m, $f$ = 1012 Hz) and the test stimulus (A = 9.8 $\mu$m, $f$ = 300 Hz). The post-hoc p-value of the comparing stimulus is 0.02. It suggests that the subjects cannot easily distinguish the reference stimuli and the test stimuli. This proves that the stimuli obtained in the first experiment are perceptually similar even though they had different frequencies, except for the pair of reference stimulus (A = 12 $\mu$m, $f$ = 1012 Hz) and the test stimulus (A = 9.8 $\mu$m, $f$ = 300 Hz), where a significant perceptual difference occurred.

The low correct answer ratio may suggest people cannot easily distinguish the reference

collision vibration from the test collision vibration. It may also indicate that the frequency difference is not a distinguishable parameter for the short-time collision vibrations in the high-frequency range of 300 Hz1,012 Hz.

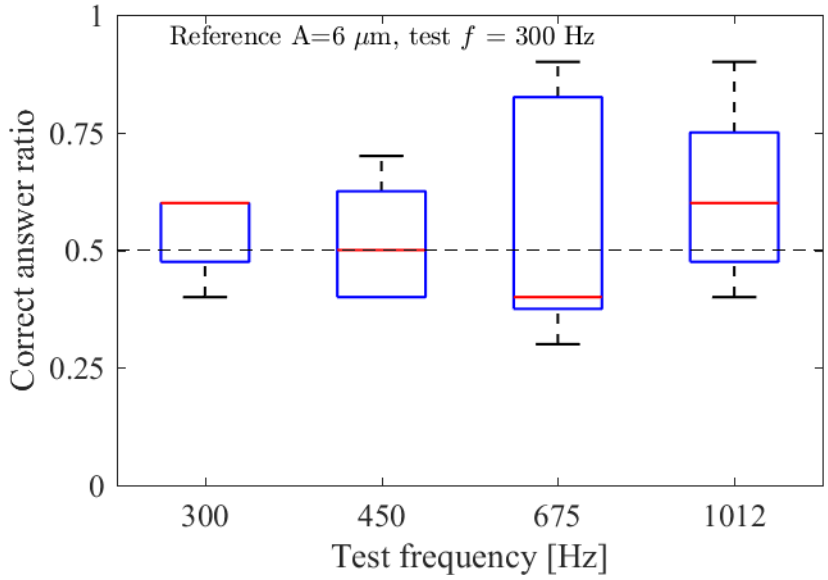


Figure 5.5: Correct answer ratio for subjects judging the comparing reference stimulus 6 $\mu m$ and 300 Hz, and the perceptually similar stimuli of frequency ranging from 300–1,012 Hz.

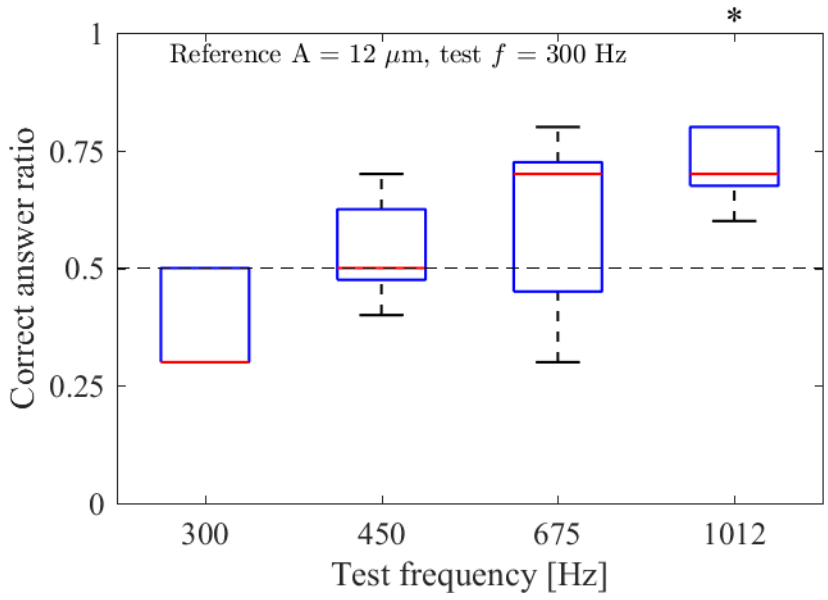


Figure 5.6: Correct answer ratio for subjects judging the comparing reference stimulus 12 $\mu m$ and 300 Hz, and the perceptually similar stimuli of frequency ranging from 300–1,012 Hz. $^*p < 0.05$

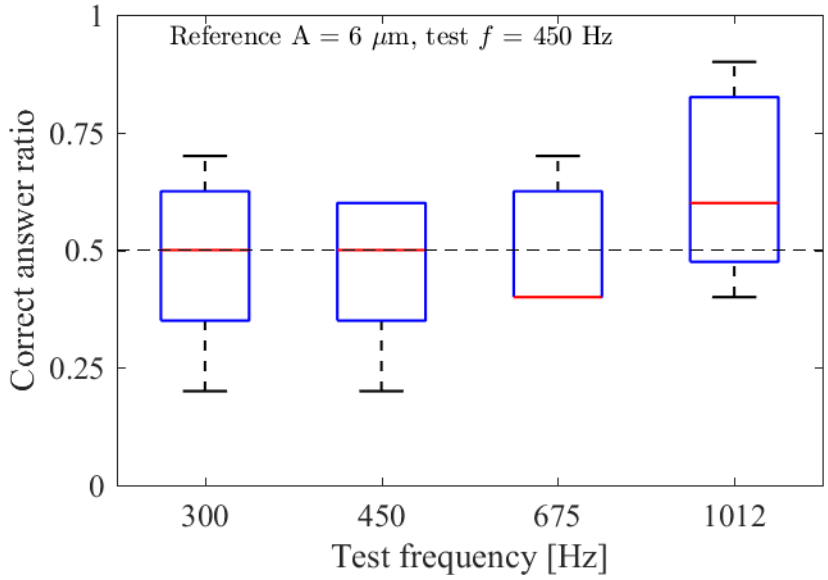


Figure 5.7: Correct answer ratio for subjects judging the comparing reference stimulus 6 $\mu m$ and 450 Hz, and the perceptually similar stimuli of frequency ranging from 300–1,012 Hz.

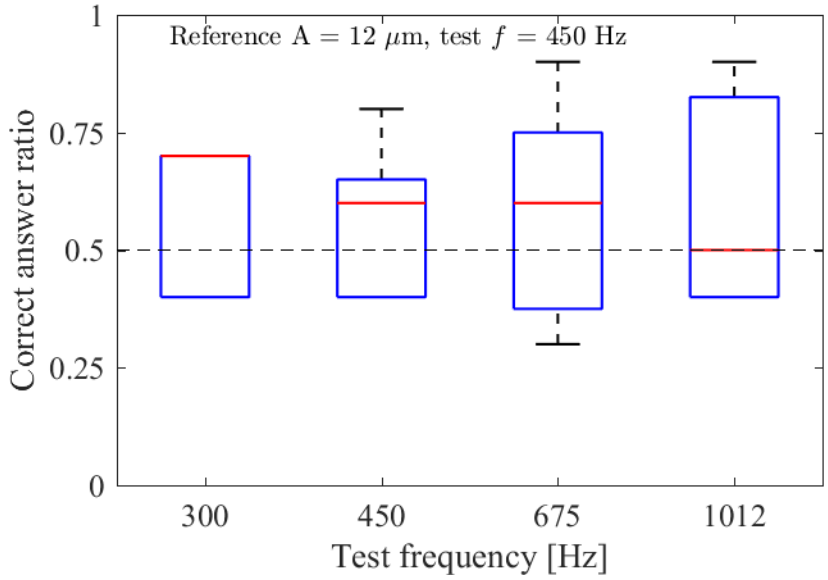


Figure 5.8: Correct answer ratio for subjects judging the comparing reference stimulus 12 $\mu m$ and 450 Hz, and the perceptually similar stimuli of frequency ranging from 300–1,012 Hz.

## 5.6 Experiment Three: Sound measurement of collision vibrations

In the third experiment, we investigated the sound pressure level of the collision vibration obtained in the first experiment.

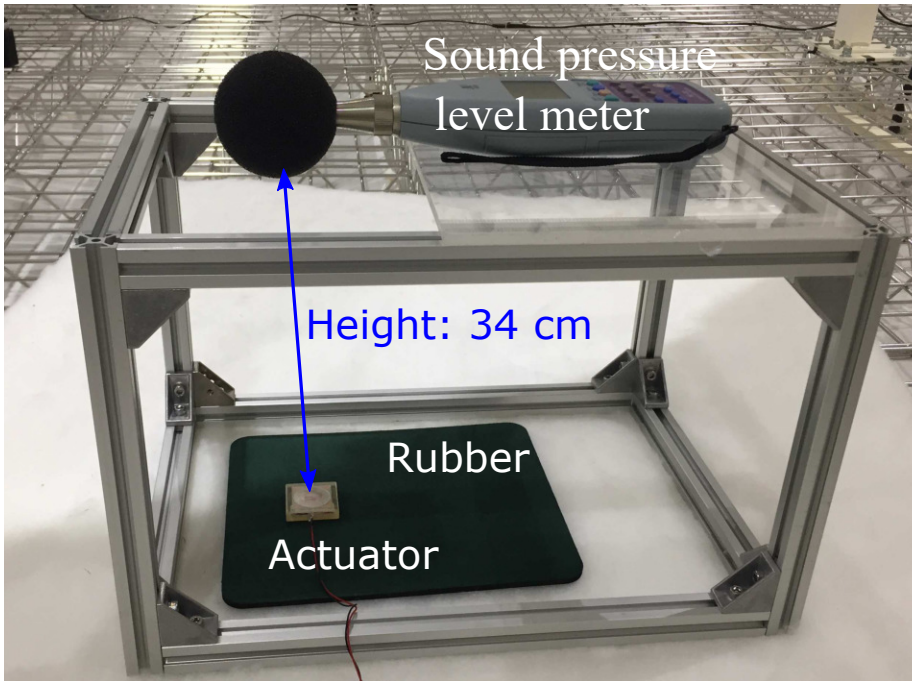


Figure 5.9: The sound pressure meter is on a box at a height of 35 cm from the actuator. The actuator is placed on a rubber plate. The experiment is conducted in an anechoic room.

### 5.6.1 Experiment Setup

The tactile apparatus is the same as in the first experiment. We used a sound pressure meter (RION NL-32) that measures the A-weighted sound pressure level of every collision vibration. The time constant of the sound pressure level meter is selected as Fast. The sound pressure level meter is on top of an aluminum frame, which is 35 cm from the actuator. The measurement was conducted in an anechoic chamber, as shown in Figure 5.9.

### 5.6.2 Results

The actuator continually generates collision vibrations at a rate 20 times per second continuously as we measured the sound pressure. The values of A-weighted sound pressure levels from these experimental collision vibrations are shown from Figure 5.10 to Figure 5.13. The sound pressure level of the reference collision vibrations (A = 12 $\mu m$, $f$ = 675 Hz) is higher than the test collision vibrations (A = 10.5 $\mu m$, $f$ = 300 Hz) and (A = 9.0 $\mu m$, $f$ = 450 Hz). The sound pressure levels of the reference collision vibrations ($f$ = 1012 Hz) are higher than the test collision vibrations ($f$ = 300 Hz and 450 Hz). It suggests that in these conditions, the lower sound level can be found using the test stimuli and comparing it to the reference stimuli.

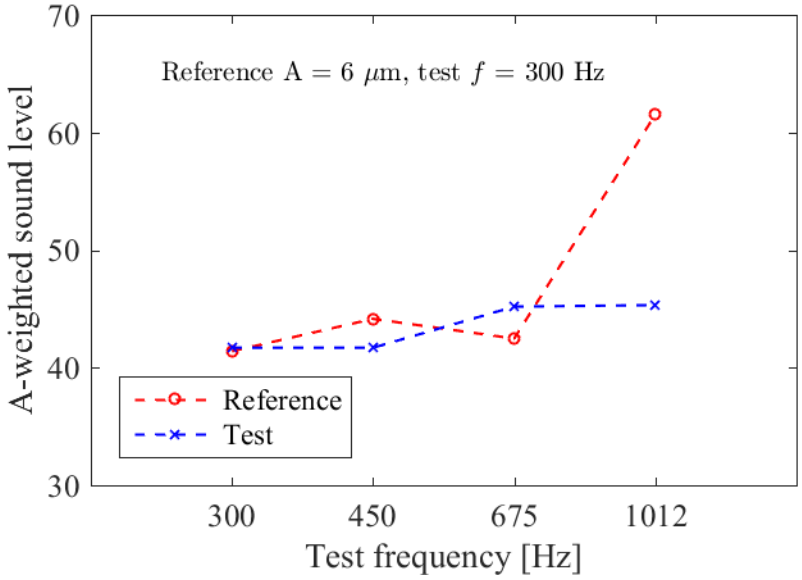


Figure 5.10: A-weighted sound pressure levels of the reference stimulus 6 $\mu m$ and 300 Hz, and the perceptually similar stimuli of frequency ranging from 300–1,012 Hz.

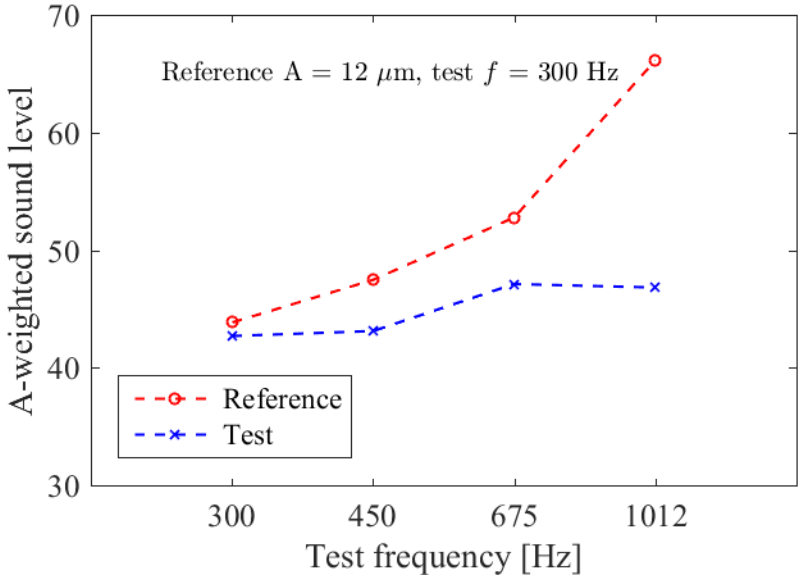


Figure 5.11: A-weighted sound pressure levels of the reference stimulus 12 $\mu m$ and 300 Hz, and the perceptually similar stimuli of frequency 300–1,012 Hz.

## 5.7 Discussion

The first observation of the study is that the stimuli obtained in the first experiment are perceptually similar vibrations, even though they have different frequencies except for the pair of the reference stimulus (A = 12 $\mu$m, $f$ = 1012 Hz) and the test stimulus (A = 9.8 $\mu$m, $f$ = 300 Hz). The perceptual similarities are verified by the results of the second experiment. In the second experiment, the results of the Kruskal–Wallis test and the post-hoc analysis showed significant differences between the reference collision and

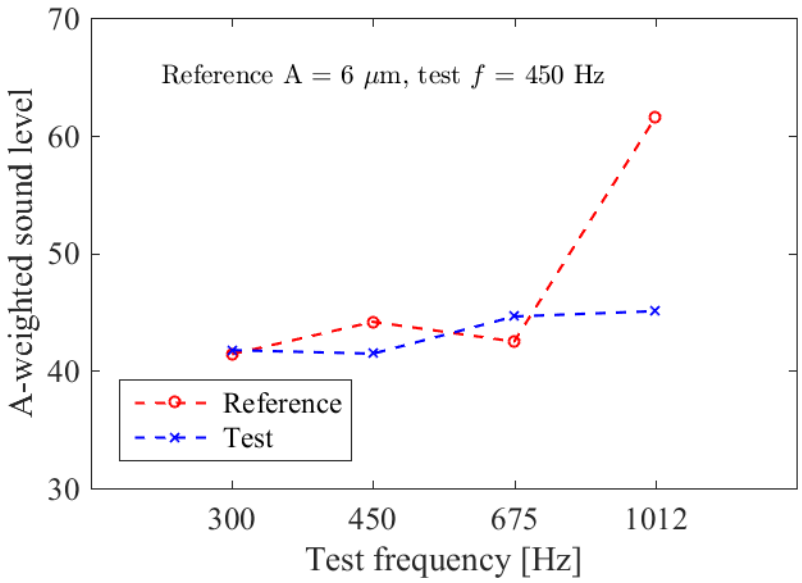


Figure 5.12: A-weighted sound pressure levels of the reference stimulus 6 $\mu m$ and 450 Hz, and the perceptually similar stimuli of frequency 300 Hz–1012 Hz.

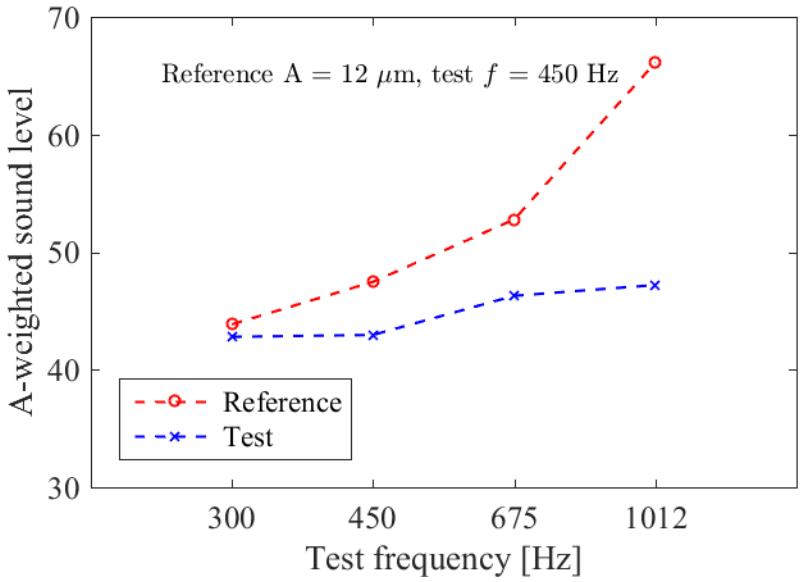


Figure 5.13: A-weighted sound pressure levels of the reference stimulus 12 $\mu m$ and 450 Hz, and the perceptually similar stimuli of frequency 300–1,012 Hz.

test collision vibrations, which only occurred at the condition with a reference stimulus (A = 12 $\mu$m, $f$ = 1012 Hz) and the test stimulus (A = 9.8 $\mu$m, $f$ = 300 Hz), as shown in Figure 5.6. The post-hoc p-value of this comparing stimulus is 0.02.

The perceptually similar stimuli occurred in a relatively large range of the amplitude. We can see that a large standard error occurred at all the conditions. In [72], Hatzfeld et al. found that the Weber fraction of amplitude is not constant when the amplitude reaches near to the threshold, the Weber fraction is higher, when the amplitude is much higher

than the threshold. In [73, 74], the authors found that there is a temporal summation for threshold and a longer duration of the stimulus lead to a lower threshold. In our experiment, a very short duration is used for the collision vibration presented by the time constant $\tau = 5$ ms. A large distribution of amplitude occurred when finding similar perceptual vibrations.

The perceptual similarity stimuli occurred in a relatively large range of frequency. We can see that in most cases, the sensation of the stimuli is similar even when the frequency difference is large, such as 300–1,012 Hz. This is similar to the activities of the Pacinian corpuscle, which can be predicted by the intensity or power of the stimuli over 100 Hz [28, 29, 54, 30, 4, 67]. The stimuli having different frequencies will have a similar sensation if their intensity is the same.

The second finding of this study is that in the third experiment, the sound pressure levels of the reference collision vibrations ($f = 675$ Hz) are higher than the test collision vibrations ($f = 300$ Hz and 450 Hz) at a high reference amplitude (A = 12 $\mu m$). The sound pressure level of reference collision vibrations ($f = 1012$ Hz) are higher than the test collision vibrations ($f = 300$ Hz and 450 Hz) at both low and high reference amplitudes (A = 6 $\mu m$ 12 $\mu m$). Generally, a lower sound pressure level leads to lower noise. This suggests that in these conditions, the frequency of the collision vibrations can be reduced to maintain a similar sensation while also reducing the sound level.

## 5.8 Limitations of the study

1. We could only investigate collision vibrations with a small time constant ($\tau = 5$ ms). The perception characteristics of collision vibrations may change with a longer time constant. Further investigation of collision vibrations with a longer time constant will help us find the limitation of the proposed modulation method.

2. The results revealed a perceptual difference when a high carrier frequency of 1,012 Hz was shifted to the lower carrier frequency of 300 Hz. Further investigation of suitable carrier frequency range shall be investigated in future studies.

## 5.9 Summary

In this chapter, we developed a methodology for modulating noisy and high-frequency vibrotactile signals to noise-free and perceptually similar collision vibrations at a frequency range of 300 Hz to 1,012 Hz. Firstly, we conducted a psychophysical experiment to adjust the amplitude of test low-frequency collision vibrations to produce a sensation as close to that produced by the reference high-frequency collision vibrations as possible. Secondly, we verified whether a human could perceive the difference between the obtained perceptually similar collision vibrations. Thirdly, we measure the sound pressure level of the experimental collision vibrations at different frequencies. Using these three experiments, we attempted to use low-frequency ($f = 300$ Hz or 450 Hz) collision vibrations,

which are perceptually similar to high-frequency collision vibrations ($f$ = 675 Hz or 1,012 Hz).

In addition, the subjects could not easily distinguish these collision vibrations except for the pair of the reference stimulus (A = 12 $\mu$m, $f$ = 1012 Hz) and the test stimulus (A = 9.8 $\mu$m, $f$ = 300 Hz). The sound pressure levels of the reference collision vibrations ($f$ = 675 Hz) are higher than that of the test collision vibrations ($f$ = 300 Hz and 450 Hz) at a high reference amplitude (A = 12 $\mu m$), and the sound pressure level of reference collision vibrations ($f$ = 1012 Hz) are higher than the test collision vibrations ($f$ = 300 Hz and 450 Hz) at both low and high reference amplitudes (A = 6 $\mu m$ and 12 $\mu m$). The results demonstrate that the proposed modulating method has reduced the sound level of the collision vibration while maintaining the perceptual quality.

In addition, we found the perceptually similar stimuli occurred in a relatively large range of the amplitude. We observe the occurrence of a large standard error in all the conditions. In [72], Hatzfeld et al. found that the Weber fraction of amplitude was not constant when the amplitude reached near the threshold, and that the Weber fraction is higher when the amplitude is much higher than the threshold. In our experiment, a very short duration was used for the collision vibration presented by the time constant $\tau$ = 5 ms. The large distribution of amplitude occurred in finding the similar perceptual vibration. We also found that the perceptually similar stimuli occurred in a relatively broad range of the frequency. We can see that in most cases, the sensation of the stimuli is preserved even when the frequency difference is significant, such as 300 Hz and 1,012 Hz. It is similar to the activities of the Pacinian corpuscle, which can be predicted by the intensity or power of the stimuli over 100 Hz [28, 29, 54, 30, 4, 67].

# Chapter 6

# Conclusions

This study aims to investigate the human perception of high-frequency vibrations with respect to haptic modulation. Humans can perceive the envelope of high-frequency vibrations, which contains the information of contact characteristics, such as material properties. The proposed method modulates the envelope of the original vibrotactile signal to enhance the perceptual feeling of the transmitted vibration. The basic concept of the modulation is shown in Figure **??** and applied in [21]. However, conventional studies do not shed light on the perceptual characteristics of the envelope of high-frequency vibrations. Therefore, this study aims to bridge this knowledge gap and focus on investigating the perceptual characteristics of the envelope. We believe these investigations can improve our modulation-based design of teleoperation of construction machines as well as other applications using high-frequency vibration feedback.

Firstly, we investigate envelope perception for one-impulse collision vibrations such as collision vibration. The experimental results of measuring the JNDs of time constant showed significant differences caused by the reference for the upper JNDs. The mean upper JND of reference time constant is 10.8 ms % while the mean upper JND of reference time constant 80 ms is 60 %. It suggests that humans are more sensitive to the change in a long time constant. The experimental results of measuring the JNDs of time constant did not show any significant differences caused by the carrier frequency for the upper JNDs. The results suggest that the carrier frequency did not strongly affect the discrimination of the envelope. Thus, the carrier frequency of the high-frequency vibration can be changed without changing the perception of the envelope. Therefore, we can shift the carrier frequency while preserving the envelope sensation by modulation.

Secondly, we introduced the time-domain segments to the intensity-based perception model. In particular, we investigated the discrimination ability of the reproduced, time-segmented waveform, which has the same intensity as that of the original vibration on each segment, as a pilot study to investigate the suitable segment size for the intensity-based modulation. The results suggested that the time-segmented, intensity-based model could

reproduce perceptually similar waves modulated from the original AM waves. Although we could not find an identical segment size, we were able to find a segment ratio of the envelope period. A small segment ratio ($r_s = 1/3$) could reproduce the perceptually similar stimuli to the original AM vibrations in most conditions. In addition, the results suggest that the peaks of the envelope played an important role in preserving similar sensation upon modulation.

Thirdly, we investigate the perceptual property of the envelope and the intensity that affects the ability of humans to discriminate high-frequency vibrations, and the effect of carrier frequency on the discrimination. Our results proved the envelope frequency dependence of the stimulis perceptual discrimination when the ability to discriminate increases with the envelope frequency when comparing the AM vibration with the sinusoidal vibration. Our results also suggest that the boundary for the envelope perception should be at an envelope frequency at approximately 80 to 125 Hz and the envelope perception of vibration at envelope frequencies less than 50 Hz is straightforward. It is found that the carrier frequency had little effect on the discrimination of vibration, and the ability to discriminate the vibration slightly increased with intensity. Therefore, we can shift the carrier frequency while preserving the envelope sensation by the modulation at a low intensity.

Finally, we developed a methodology for modulating noisy, high-frequency vibrotactile signals to noise-free, perceptually similar collision vibrations at a frequency range of 300–1,012 Hz. The results proved that the proposed modulating method has reduced the sound level of collision vibration while maintaining perceptual similarity, especially for the high frequency of 1,012 Hz.

# Investigating the envelope discrimination ability of high-frequency vibration

Humans can perceive the envelope of AM vibrations even when the carrier frequency is higher than the human somatosensory frequency range [31, 32]. With respect to continuous high-frequency vibrations, the perceptual characteristics of the envelope and carrier of vibrations have been investigated in several previous studies [31, 32]; however, those characteristics for one-impulse high-frequency vibrations such as collision vibration have not yet been investigated.

Our experimental results suggest that humans can perceive the envelope of vibrations, especially for the single-pulse vibration such as collision vibration. The experimental results of measuring the JNDs of time constant demonstrated significant differences caused by the reference for the upper JNDs. The mean upper JND of reference time constant 10.8 ms is 60 % while the mean upper JND of reference time constant 50 ms is 23 %. It suggests that humans are more sensitive to the change in a long time constant. The

experimental results of measuring the JNDs of time constant did not show any significant differences caused by the carrier frequency for the upper JNDs. It suggested that the carrier frequency did not strongly affect the discrimination of the envelope. Thus, the carrier frequency of the high-frequency vibration can be changed without changing the perception of the envelope. Therefore, we can shift the carrier frequency while preserving the envelope sensation by modulation. A lower carrier frequency could reduce the difficulties of generating high-frequency vibrations and reduce the sound of the vibration when using a lower frequency carrier by modulation.

In addition, we also conducted preliminary experiments to investigate the envelope and carrier discrimination of the AM vibration. The AM vibrations have different carrier frequencies with frequencies less than 1 kHz, which should be in the humanly perceivable frequency, and a frequency higher than 1 kHz, which should be beyond the humanly perceivable range. Our results showed that subjects could detect 20 % of the change in envelope frequency on both 1,680 Hz and 500 Hz carrier frequencies. In addition, subjects were able to distinguish the stimuli when the carrier frequencies were over 1 kHz easier than they could when the carrier frequency were less than 1 kHz. The results indicated that the latter shows a lower JND, and is more sensitive. The results are contrary to our assumption that a lower carrier frequency of 500 Hz, which has a lower threshold, is more sensitive. The perceptual characteristics of the envelope of high-frequency vibrations will be investigated further.

## Introduction of Time-domain Segment to Intensity-based Perception Model of High-frequency Vibration

The intensity of high-frequency vibrations ($>$ 100 Hz), which is generally defined as the integral of stimulus energy over time or spectral power summed across all frequencies, is a primary cue to convey vibrotactile information perceived by the Pacinian system. Several researchers reported that humans can detect the envelope of a high-frequency vibration modulated at low frequencies. A missing argument for the intensity-based model is the determination of adequate duration to integrate the energy of the stimulus to account for the relatively slow time-variant vibration patterns. We introduce a time-domain segment to the intensity-based perception model. In particular, we investigate the discrimination ability of the reproduced, time-segmented waveform that has the same intensity as that of the original vibration on each segment, as a pilot study to investigate the suitable segment size for the intensity-based modulation. This study targets the AM high-frequency vibrations (carrier frequency $f_c = 300$ or 600 Hz) that have relatively low envelope frequencies ($f_e$ =15, 30, or 45 Hz).

The results suggest that the time-segmented, intensity-based model could reproduce perceptually similar vibrations for the AM vibrations when compared to the conven-

tional intensity-based model. Furthermore, we found that a small segment number of the envelope period ($r_s = 1/3$) could emulate the perception of the AM vibration in most conditions. Our experimental also results showed that the conventional intensity-based model could not represent perceptually similar vibrations for AM vibrations of a low-frequency envelope. No significant difference appeared between the four segment ratios ($r_s = 1/6$, $1/5$, $1/4$, and $1/3$) and chance level ($p > 0.05$) except the condition (($f_c$, $f_e$, $r_s$) = (300, 30, 1/4)) the condition (($f_c$, $f_e$, $r_s$) = (600, 15, 1/3)), and the p-values are 0.0381 and 0.0004, respectively. In addition, the discrimination ratios at the four segment ratios ($r_s = 1/6, 1/5, 1/4$, and $1/3$) are significantly smaller than that at $r_s = 1/2$ in all original AM vibrations ($p < 1.0 \times 10^{-6}$).

# Perceptual Discrimination of High-frequency Vibration Depends on Envelope and Intensity Properties of Waveform

The intensity of high-frequency vibrations (> 100 Hz), which is generally defined as the integral of stimulus intensity over time or spectral power summed across all frequencies, has been focused as a primary cue to convey vibrotactile information perceived by the Pacinian system. However, the intensity model cannot interpret the perception of the envelope of high-frequency vibrations. Intensity and envelope are supposed to work together to affect the ability of humans to discriminate high-frequency vibrations. In this study, we aim to find the boundary for the perception of the envelope and the intensity that affect this discrimination ability, and also investigate the effect of carrier frequency on the discrimination. In our experiment, we conducted the discrimination experiment on the AM vibrations and sinusoidal vibrations of different envelope frequencies, carrier frequencies, and intensity levels valued by the intensity model of the previous study to investigate the intensity and envelope effect on the human perceptual discrimination of high-frequency vibrations.

The boundary for the perception of the envelope and the intensity is based on the envelope frequency of approximately 80–125 Hz. This range is near the crossing band of human receptors, Meissner corpuscles and Pacinian corpuscles, and it indicates that the envelope sensation is linked to the activities of the two types of receptors. Comparing the AM waves with the sinusoidal waves, our results showed that the perceptual discrimination ability of the stimuli has an envelope frequency dependence, where the discrimination ability decreases with an increase in the envelope frequency. For the envelope frequency of an AM vibration range of 12–50 Hz, a high degree of discrimination occurred compared to the sinusoidal vibration, and the intensity did not have a strong effect on the discrimination ability in this range. When the envelope frequency of the AM vibration was 125 Hz, low discrimination occurred compared to the sinusoidal waves. Discrimination did

not show any significant dependence on envelope frequency. In addition, we also found that the carrier frequency had little effect on the discrimination while sensitivity tends to increase with intensity.

Therefore, we can shift the carrier frequency based on the perceivable envelope frequency boundary at approximately 80–125 Hz while preserving the envelope sensation by modulation at low intensity. A lower carrier frequency should reduce the difficulties of generating the high-frequency vibration and reduce the sound of vibrations when using a lower frequency carrier by modulation.

## Perceptually Modulation Application: Sound reduction of vibration feedback by perceptually similar modulation

In this chapter, we developed a methodology for modulating noisy, high-frequency vibrotactile signals to noise-free, perceptually similar collision vibrations at a frequency range of 300–1,012 Hz. Firstly, we conducted a psychophysical experiment to adjust the amplitude of test low-frequency collision vibrations to produce a sensation as close to that produced by the reference high-frequency collision vibrations as possible. Secondly, we verified whether a human could perceive the difference between the perceptually similar collision vibrations obtained. Thirdly, we measured the sound pressure level of the experimental collision vibrations at different frequencies. Through these three experiments, we attempted to use lower-frequency ($f$ = 300 Hz or 450 Hz) collision vibrations, which are perceptually similar to high-frequency collision vibrations ($f$ = 675 Hz or 1,012 Hz).

Our results showed that the subjects could not easily distinguish between these collision vibrations, except for the pair of the reference stimulus (A = 12 $\mu$m, $f$ = 1012 Hz) and the test stimulus (A = 9.8 $\mu$m, $f$ = 300 Hz). The sound pressure levels of the reference collision vibrations ($f$ = 675 Hz) are higher than those of the test collision vibrations ($f$ = 300 Hz and 450 Hz) at a high reference amplitude (A = 12 $\mu m$), and the sound pressure level of reference collision vibrations ($f$ = 1012 Hz) are higher than the test collision vibrations ($f$ = 300 Hz and 450 Hz) at both low and high reference amplitudes (A = 6 $\mu m$ and 12 $\mu m$). Our results suggest that our modulating method is able to reduce the sound level of the collision vibration while maintaining the perceptual quality.

In addition, we found that the perceptually similar stimuli occurred in a relatively large range of the amplitude. It can be seen that a large standard error occurred in all conditions. In [72], Hatzfeld et al. found that the Weber fraction of amplitude is not constant when the amplitude reaches near its threshold, and the Weber fraction is higher when the amplitude is much higher than the threshold. In our experiment, a very short duration is used for the collision vibration presented by the time constant $\tau$ = 5 ms. The

large distribution of amplitude occurred in identifying the perceptually similar vibration. We also found that the perceptually similar stimuli occurred in a relatively large range of the frequency. In most cases, we can see that the sensation of stimuli remains largely unchanged even when the frequency difference is large, such as 300–1,012 Hz. This is similar to the activities of the Pacinian corpuscle, which can be predicted by the intensity or power of the stimuli over 100 Hz [28, 29, 54, 30, 4, 67].

# List of Publications and Awards

## Peer-reviewed Publications

[**Cao, WorldHaptics, 2017**] Cao, N., Nagano, H., Konyo, M., Okamoto, S., Tadokoro, S., "Envelope effect study on collision vibration perception through investigating just noticeable difference of time constant," *Proceedings of In World Haptics Conference (WHC), 2017,* pp. 528-533, 2017.

[**Cao, SII, 2017**] Takenouchi, H., Cao, N., Nagano, H., Konyo, M., Okamoto, S., Tadokoro, S., "Extracting haptic information from high-frequency vibratory signals measured on a remote robot to transmit collisions with environments," *in Proceedings of IEEE/SICE International Symposium on System Integration (SII), 2017,* pp. 968-973, 2017.

[**Cao, EuroHaptics, 2018**] Cao, N., Nagano, H., Konyo, M., Okamoto, S., Tadokoro, S., "A Pilot Study: Introduction of Time-Domain Segment to Intensity-Based Perception Model of High-Frequency Vibration," *in Proceedings of Human Haptic Sensing and Touch Enabled Computer Applications,* pp. 321-332, 2018.

[**Cao, RO-MAN, 2018**] Cao, N., Nagano, H., Konyo, M., Tadokoro, S., "Sound Reduction of Vibration Feedback by Perceptually Similar Modulation," *in Proceedings of Robot and Human Interactive Communication (RO-MAN), 2018,* pp. 934-939, 2018.

[**Cao, IEEE Access, 2018**] Cao, N., Konyo, M., Nagano, H., Tadokoro, S., "Dependence of the Perceptual Discrimination of High-Frequency Vibrations on the Envelope and Intensity of Waveforms," *in Multidisciplinary Open Access Journal. (Accepted)*

# Non-peer-reviewed Publications

- Cao, N., Nagano, H., Konyo, M., Tadokoro, S., "Time Constant Discrimination of Collision Vibration," In The Proceedings of JSME annual Conference on Robotics and Mechatronics (Robomec) 2017 (pp. 1P1-N05). The Japan Society of Mechanical Engineers.

- Cao, N., Nagano, H., Konyo, M., Tadokoro, S., "Reducing sound of tactile display for high-frequency collision vibrations," In The Proceedings of JSME annual Conference on Robotics and Mechatronics (Robomec) 2018 (pp. 1P1-K16). The Japan Society of Mechanical Engineers.

# Awards and Honours

- *Best PosterAward* in Eurohaptics 2018, for the paper titled "A Pilot Study: Introduction of Time-domain Segment to Intensity-based Perception Model of High-frequency Vibration".

# Bibliography


[1] S. J. Lederman, "Skin and touch," *Encyclopedia of human biology*, vol. 7, pp. 51–63, 1991.

[2] R. S. Dahiya, G. Metta, M. Valle, and G. Sandini, "Tactile sensing?from humans to humanoids," *IEEE Transactions on Robotics*, vol. 26, no. 1, pp. 1–20, 2010.

[3] S. J. Bolanowski Jr, G. A. Gescheider, R. T. Verrillo, and C. M. Checkosky, "Four channels mediate the mechanical aspects of touch," *The Journal of the Acoustical society of America*, vol. 84, no. 5, pp. 1680–1694, 1988.

[4] S. Bensmaïa and M. Hollins, "Pacinian representations of fine surface texture," *Perception & psychophysics*, vol. 67, no. 5, pp. 842–854, 2005.

[5] S.-C. Lim, K.-U. Kyung, and D.-S. Kwon, "Effect of frequency difference on sensitivity of beats perception," *Experimental brain research*, vol. 216, no. 1, pp. 11–19, 2012.

[6] J. Ryu, J. Jung, G. Park, and S. Choi, "Psychophysical model for vibrotactile rendering in mobile devices," *Presence: Teleoperators and Virtual Environments*, vol. 19, no. 4, pp. 364–387, 2010.

[7] A. M. Okamura, "Methods for haptic feedback in teleoperated robot-assisted surgery," *Industrial Robot: An International Journal*, vol. 31, no. 6, pp. 499–508, 2004.

[8] O. A. Van der Meijden and M. P. Schijven, "The value of haptic feedback in conventional and robot-assisted minimal invasive surgery and virtual reality training: a current review," *Surgical endoscopy*, vol. 23, no. 6, pp. 1180–1190, 2009.

[9] J. J. Abbott, P. Marayong, and A. M. Okamura, "Haptic virtual fixtures for robot-assisted manipulation," in *Robotics research*. Springer, 2007, pp. 49–64.

[10] N. Diolaiti and C. Melchiorri, "Teleoperation of a mobile robot through haptic feedback," in *Haptic Virtual Environments and Their Applications, IEEE International Workshop 2002 HAVE*. IEEE, 2002, pp. 67–72.

[11] C. Colwell, H. Petrie, D. Kornbrot, A. Hardwick, and S. Furner, "Haptic virtual reality for blind computer users," in *Proceedings of the third international ACM conference on Assistive technologies*. ACM, 1998, pp. 92–99.

[12] C. Tarr, J. K. Salisbury Jr, T. H. Massie, and W. A. Aviles, "Method and apparatus for generating and interfacing with a haptic virtual reality environment," Jul. 4 2000, uS Patent 6,084,587.

[13] C. Tarr, "Method and apparatus for generating and interfacing with rigid and deformable surfaces in a haptic virtual reality environment," Feb. 20 2001, uS Patent 6,191,796.

[14] G. C. Burdea, "Force and touch feedback for virtual reality," 1996.

[15] L. Shih, W. A. Aviles, T. H. Massie, and C. M. Tarr, "Systems and methods for interacting with virtual objects in a haptic virtual reality environment," Jul. 16 2002, uS Patent 6,421,048.

[16] R. C. Goertz, "Fundamentals of general-purpose remote manipulators," *Nucleonics*, vol. 10, no. 11, pp. 36–42, 1952.

[17] A. K. Bejczy, "Toward advanced teleoperation in space," *Progress in Astronautics and Aeronautics*, vol. 161, pp. 107–107, 1994.

[18] K. J. Kuchenbecker, J. Gewirtz, W. McMahan, D. Standish, P. Martin, J. Bohren, P. J. Mendoza, and D. I. Lee, "Verrotouch: High-frequency acceleration feedback for telerobotic surgery," in *International Conference on Human Haptic Sensing and Touch Enabled Computer Applications*. Springer, 2010, pp. 189–196.

[19] K. J. Kuchenbecker, J. Fiene, and G. Niemeyer, "Improving contact realism through event-based haptic feedback," *IEEE transactions on visualization and computer graphics*, vol. 12, no. 2, pp. 219–230, 2006.

[20] K. Higashi, S. Okamoto, Y. Yamada, H. Nagano, and M. Konyo, "Hardness perception through tapping: Peak and impulse of the reaction force reflect the subjective hardness," in *International Conference on Human Haptic Sensing and Touch Enabled Computer Applications*. Springer, 2018, pp. 366–375.

[21] H. Takenouchi, N. Cao, H. Nagano, M. Konyo, and S. Tadokoro, "Extracting haptic information from high-frequency vibratory signals measured on a remote robot to transmit collisions with environments," in *System Integration (SII), 2017 IEEE/SICE International Symposium on*. IEEE, 2017, pp. 968–973.

[22] K. Higashi, S. Okamoto, and Y. Yamada, "What is the hardness perceived by tapping?" in *International Conference on Human Haptic Sensing and Touch Enabled Computer Applications*. Springer, 2016, pp. 3–12.

[23] K. Higashi, S. Okamoto, Y. Yamada, H. Nagano, and M. Konyo, "Hardness perception by tapping: Effect of dynamic stiffness of objects," in *World Haptics Conference (WHC), 2017 IEEE*. IEEE, 2017, pp. 37–41.

[24] M. Konyo, H. Yamada, S. Okamoto, and S. Tadokoro, "Alternative display of friction represented by tactile stimulation without tangential force," in *International Conference on Human Haptic Sensing and Touch Enabled Computer Applications*. Springer, 2008, pp. 619–629.

[25] E. H. Weber, *EH Weber: The sense of touch*. Academic Pr, 1978.

[26] P. Hinterseer, S. Hirche, S. Chaudhuri, E. Steinbach, and M. Buss, "Perception-based data reduction and transmission of haptic data in telepresence and teleaction systems," *IEEE Transactions on Signal Processing*, vol. 56, no. 2, pp. 588–597, 2008.

[27] S. Okamoto and Y. Yamada, "Perceptual properties of vibrotactile material texture: Effects of amplitude changes and stimuli beneath detection thresholds," in *System Integration (SII), 2010 IEEE/SICE International Symposium on*. IEEE, 2010, pp. 384–389.

[28] J. C. Makous, R. M. Friedman, and C. J. Vierck, "A critical band filter in touch," *Journal of Neuroscience*, vol. 15, no. 4, pp. 2808–2818, 1995.

[29] S. J. Bensmaıa and M. Hollins, "Complex tactile waveform discrimination," *The Journal of the Acoustical Society of America*, vol. 108, no. 3, pp. 1236–1245, 2000.

[30] S. Bensmaïa, M. Hollins, and J. Yau, "Vibrotactile intensity and frequency information in the pacinian system: A psychophysical model," *Attention, Perception, & Psychophysics*, vol. 67, no. 5, pp. 828–841, 2005.

[31] P. Lamore, H. Muijser, and C. Keemink, "Envelope detection of amplitude-modulated high-frequency sinusoidal signals by skin mechanoreceptors," *The Journal of the Acoustical Society of America*, vol. 79, no. 4, pp. 1082–1085, 1986.

[32] Y. Makino, T. Maeno, and H. Shinoda, "Perceptual characteristic of multi-spectral vibrations beyond the human perceivable frequency range," in *World Haptics Conference (WHC), 2011 IEEE*. IEEE, 2011, pp. 439–443.

[33] A. M. Okamura, M. R. Cutkosky, and J. T. Dennerlein, "Reality-based models for vibration feedback in virtual environments," *IEEE/ASME Transactions on Mechatronics*, vol. 6, no. 3, pp. 245–252, 2001.

[34] T. Ahmaniemi, J. Marila, and V. Lantz, "Design of dynamic vibrotactile textures," *IEEE Transactions on Haptics*, vol. 3, no. 4, pp. 245–256, 2010.

[35] S. Wu, X. Sun, Q. Wang, and J. Chen, "Tactile modeling and rendering image-textures based on electrovibration," *The Visual Computer*, vol. 33, no. 5, pp. 637–646, 2017.

[36] T. Ahmaniemi, "Effect of dynamic vibrotactile feedback on the control of isometric finger force," *IEEE transactions on haptics*, vol. 6, no. 3, pp. 376–380, 2013.

[37] A. M. Murray, R. L. Klatzky, and P. K. Khosla, "Psychophysical characterization and testbed validation of a wearable vibrotactile glove for telemanipulation," *Presence: Teleoperators & Virtual Environments*, vol. 12, no. 2, pp. 156–182, 2003.

[38] A. M. Okamura, J. T. Dennerlein, and R. D. Howe, "Vibration feedback models for virtual environments," in *Robotics and Automation, 1998. Proceedings. 1998 IEEE International Conference on*, vol. 1. IEEE, 1998, pp. 674–679.

[39] G. Park and S. Choi, "Perceptual space of amplitude-modulated vibrotactile stimuli," in *World Haptics Conference (WHC), 2011 IEEE*. IEEE, 2011, pp. 59–64.

[40] Y. Suzuki and H. Takeshima, "Equal-loudness-level contours for pure tones," *The Journal of the Acoustical Society of America*, vol. 116, no. 2, pp. 918–933, 2004.

[41] A. K. Goble and M. Hollins, "Vibrotactile adaptation enhances amplitude discrimination," *The Journal of the Acoustical Society of America*, vol. 93, no. 1, pp. 418–424, 1993.

[42] A. Israr, H. Z. Tan, and C. M. Reed, "Frequency and amplitude discrimination along the kinesthetic-cutaneous continuum in the presence of masking stimuli," *The Journal of the Acoustical society of America*, vol. 120, no. 5, pp. 2789–2800, 2006.

[43] D. A. Mahns, N. Perkins, V. Sahai, L. Robinson, and M. Rowe, "Vibrotactile frequency discrimination in human hairy skin," *Journal of neurophysiology*, vol. 95, no. 3, pp. 1442–1450, 2006.

[44] H. Pongrac, "Vibrotactile perception: Differential effects of frequency, amplitude, and acceleration," in *Haptic Audio Visual Environments and their Applications, 2006. HAVE 2006. IEEE International Workshop on*. IEEE, 2006, pp. 54–59.

[45] A. Israr, S. Choi, and H. Z. Tan, "Mechanical impedance of the hand holding a spherical tool at threshold and suprathreshold stimulation levels," in *EuroHaptics Conference, 2007 and Symposium on Haptic Interfaces for Virtual Environment and Teleoperator Systems. World Haptics 2007. Second Joint*. IEEE, 2007, pp. 56–60.

[46] K. Higashi, S. Okamoto, H. Nagano, and Y. Yamada, "Effects of mechanical parameters on hardness experienced by damped natural vibration stimulation," in *Systems, Man, and Cybernetics (SMC), 2015 IEEE International Conference on*. IEEE, 2015, pp. 1539–1544.

[47] N. Cao, H. Nagano, M. Konyo, S. Okamoto, and S. Tadokoro, "Envelope effect study on collision vibration perception through investigating just noticeable difference of time constant," in *World Haptics Conference (WHC), 2017 IEEE*. IEEE, 2017, pp. 528–533.

[48] N. CAO, H. NAGANO, M. KONYO, and S. TADOKORO, "Time constant discrimination of collision vibration," in *The Proceedings of JSME annual Conference on Robotics and Mechatronics (Robomec) 2017*. The Japan Society of Mechanical Engineers, 2017, pp. 1P1–N05.

[49] H. Levitt, "Transformed up-down methods in psychoacoustics," *The Journal of the Acoustical society of America*, vol. 49, no. 2B, pp. 467–477, 1971.

[50] C. Hatzfeld and R. Werthschützky, "Just noticeable differences of low-intensity vibrotactile forces at the fingertip," in *International Conference on Human Haptic Sensing and Touch Enabled Computer Applications*. Springer, 2012, pp. 43–48.

[51] C. Hatzfeld and R. Werthschützky, "Mechanical impedance as coupling parameter of force and deflection perception: experimental evaluation," in *International Conference on Human Haptic Sensing and Touch Enabled Computer Applications*. Springer, 2012, pp. 193–204.

[52] A. Brisben, S. Hsiao, and K. Johnson, "Detection of vibration transmitted through an object grasped in the hand," *Journal of Neurophysiology*, vol. 81, no. 4, pp. 1548–1558, 1999.

[53] L. Wyse, S. Nanayakkara, P. Seekings, S. Ong, and E. Taylor, "Perception of vibrotactile stimuli above 1 khz by the hearing-impaired," *NIME12*, 2012.

[54] S. J. Bensmaïa and M. Hollins, "The vibrations of texture," *Somatosensory & motor research*, vol. 20, no. 1, pp. 33–43, 2003.

[55] W. McMahan, J. Gewirtz, D. Standish, P. Martin, J. A. Kunkel, M. Lilavois, A. Wedmid, D. I. Lee, and K. J. Kuchenbecker, "Tool contact acceleration feedback for telerobotic surgery," *IEEE Transactions on Haptics*, vol. 4, no. 3, pp. 210–220, 2011.

[56] J. M. Romano and K. J. Kuchenbecker, "Creating realistic virtual textures from contact acceleration data," *IEEE Transactions on Haptics*, vol. 5, no. 2, pp. 109–119, 2012.

[57] W. McMahan, J. M. Romano, A. M. A. Rahuman, and K. J. Kuchenbecker, "High frequency acceleration feedback significantly increases the realism of haptically rendered textured surfaces," in *Haptics Symposium, 2010 IEEE*. IEEE, 2010, pp. 141–148.

[58] N. Cao, H. Nagano, M. Konyo, S. Okamoto, and S. Tadokoro, "A pilot study: Introduction of time-domain segment to intensity-based perception model of high-frequency vibration," in *International Conference on Human Haptic Sensing and Touch Enabled Computer Applications*. Springer, 2018, pp. 321–332.

[59] M. Hollins, K. Delemos, and A. Goble, "Vibrotactile adaptation of the ra system: a psychophysical analysis," *Somesthesis and the Neurobiology of the Somatosensory Cortex*, pp. 101–111, 1996.

[60] B.-A. J. Menelas and M. J.-D. Otis, "Design of a serious game for learning vibrotactile messages," in *Haptic Audio Visual Environments and Games (HAVE), 2012 IEEE International Workshop on*. IEEE, 2012, pp. 124–129.

[61] S. S. Stevens, *Psychophysics: Introduction to its perceptual, neural and social prospects*. Routledge, 2017.

[62] O. Franzén, "The dependence of vibrotactile threshold and magnitude functions on stimulation frequency and signal level: A perceptual and neural comparison," *Scandinavian journal of psychology*, vol. 10, no. 1, pp. 289–298, 1969.

[63] L. T. DeCarlo, "On a signal detection approach to m-alternative forced choice with bias, with maximum likelihood and bayesian approaches to estimation," *Journal of Mathematical Psychology*, vol. 56, no. 3, pp. 196–207, 2012.

[64] F. Looft, "Response of monkey glabrous skin mechanoreceptors to random-noise sequences: I. temporal response characteristics," *Somatosensory & motor research*, vol. 11, no. 4, pp. 327–344, 1994.

[65] F. J. Looft, "Response of monkey glabrous skin mechanoreceptors to random noise sequences: Ii. dynamic stimulus state analysis," *Somatosensory & motor research*, vol. 13, no. 1, pp. 11–28, 1996.

[66] F. Looft, "Response of monkey glabrous skin mechanoreceptors to random noise sequences: Iii. spectral analysis," *Somatosensory & motor research*, vol. 13, no. 3-4, pp. 235–244, 1996.

[67] T. Yoshioka, S. J. Bensmaia, J. C. Craig, and S. S. Hsiao, "Texture perception through direct and indirect touch: An analysis of perceptual space for tactile textures

in two modes of exploration," *Somatosensory & motor research*, vol. 24, no. 1-2, pp. 53–70, 2007.

[68] K. Higashi, S. Okamoto, H. Nagano, M. Konyo, and Y. Yamada, "Vibration-based rendering of virtual hardness: Frequency characteristics of perception," in *Consumer Electronics (GCCE), 2017 IEEE 6th Global Conference on*. IEEE, 2017, pp. 1–2.

[69] N. Cao, H. Nagano, M. Konyo, and S. Tadokoro, "Sound reduction of vibration feedback by perceptually similar modulation," in *2018 27th IEEE International Symposium on Robot and Human Interactive Communication (RO-MAN)*. IEEE, 2018, pp. 934–939.

[70] N. CAO, H. NAGANO, M. KONYO, and S. TADOKORO, "Reducing sound of tactile display for high-frequency collision vibrations," in *The Proceedings of JSME annual Conference on Robotics and Mechatronics (Robomec) 2018*. The Japan Society of Mechanical Engineers, 2018, pp. 1P1–K16.

[71] R. T. Verrillo, A. J. Fraioli, and R. L. Smith, "Sensation magnitude of vibrotactile stimuli," *Perception & Psychophysics*, vol. 6, no. 6, pp. 366–372, 1969.

[72] C. Hatzfeld, S. Cao, M. Kupnik, and R. Werthschützky, "Vibrotactile force perception–absolute and differential thresholds and external influences," *IEEE transactions on haptics*, vol. 9, no. 4, pp. 586–597, 2016.

[73] G. A. Gescheider and J. M. Joelson, "Vibrotactile temporal summation for threshold and suprathreshold levels of stimulation," *Perception & Psychophysics*, vol. 33, no. 2, pp. 156–162, 1983.

[74] G. A. Gescheider, M. E. Berryhill, R. T. Verrillo, and S. J. Bolanowski, "Vibrotactile temporal summation: probability summation or neural integration?" *Somatosensory & motor research*, vol. 16, no. 3, pp. 229–242, 1999.

# Copyright Notice

This dissertation contains reprints from the athor's original publications as follows:

1. Chapter 2, contains reprint from [47]. Copyright 2017 IEEE. Reprinted, with permission, from Cao, N., Nagano, H., Konyo, M., Okamoto, S., Tadokoro, S.,"Envelope effect study on collision vibration perception through investigating just noticeable difference of time constant," *Proceedings of In World Haptics Conference (WHC), 2017*, pp. 528-533, 2017.
   DOI: 10.1109/WHC.2017.7989957

2. Chapter 3, contains reprint from [58]. Copyright Springer International Publishing AG, part of Springer Nature 2018. Reprinted, with permission, from Cao, N., Nagano, H., Konyo, M., Okamoto, S., Tadokoro, S., "A Pilot Study: Introduction of Time-Domain Segment to Intensity-Based Perception Model of High-Frequency Vibration," *in Proceedings of Human Haptic Sensing and Touch Enabled Computer Applications,* pp. 321-332, 2018.
   DOI: https://doi.org/10.1007/978-3-319-93445-7_28
   License Number: 4515130226144

3. Chapter 5, contains reprint from [69]. Copyright 2018 IEEE. Reprinted, with permission, from Cao, N., Nagano, H., Konyo, M., Tadokoro, S., "Sound Reduction of Vibration Feedback by Perceptually Similar Modulation," *in Proceedings of Robot and Human Interactive Communication (RO-MAN), 2018,* pp. 934-939, 2018.
   DOI: 10.1109/ROMAN.2018.8525571

# Acknowledgements

The author wishes to acknowledge the Japanese Government (MEXT) Scholarship Program. The grant has provided the author a major support for the entire duration of the study. Thanks to such program for making this research possible. The author wishes to acknowledge the committee involved in the selection process up to the arrival in Japan. The author also acknowledges Prof. Satoshi Tadokoro for granting acceptance to work in his laboratory.

I express my very great appreciation to my supervisor Assoc. Prof. Masashi Konyo. He is a great mentor for this research and has contributed theoretical insights in countless hours of discussion and guidance throughout this research. I thank him for his patience, encouragement, useful critiques as well as keeping my progress on schedule. I can confidently say that I learned how to conduct and publish academic research of high quality from him. I would also like to thank Asst. Prof. Hikaru Nagano for his generous support and additional guidance for this study. He has particularly provided advice on the development of experimental setups and statistical analysis of experimental data.

The valuable feedback provided by the committee members; Prof. Koichi Hashimoto, Prof. Yasuhisa Hirata, and Prof. Satoshi Tadokoro had greatly improved the material in this research. I wish to thank them for examining this work.

I am grateful for the support of the secretaries Ms. Yuki Saijo, Ms. Mitsuru Takahashi, Ms. Azuma Keiko, Ms. Chiaki Ohno and Ms. Takako Kase. Their efforts on document processing, travel transactions had saved me from these tasks that require effective Japanese communication.

I would like to thank, Denneis Babus, Daniel Gongora, Wenchao Gu, Ren Sugimoto, Arata Horie, Yoichiro Takahashi, Kaoru Saito, Shinya Saito for helping me with different aspects of research life in the lab. I would like to thank the past and present Haptics team members and to the rest of the students in Tadokoro laboratory.

I would like to acknowledge the support provided by my church through their prayers. Special thanks to my pastor Takahiro Ami, his wife Frances Ami. I would have never achieved anything without their support and encouragement.

I would like to thank my friends Dr. Shichao Hu, Dr. Qiang Gang, Dr. Diyi Liu. and my beloved girlfriend Shuang E.

And above all, great thanks to Almighty God through Jesus Christ for bestowing me with this opportunity and strengthening me through my past years.

January 29, 2019
Nan CAO